SHEARING RATE EFFECTS ON DRAINED SHEAR STRENGTH OF FLUE GAS DESULFURIZATION (FGD) BYPRODUCT

A Thesis presented to

the Faculty of the Graduate School

at the University of Missouri – Columbia

In Partial Fulfillment

of the Requirements for the Degree

Master of Science

---

by

TASNEEM A. KHAN

Dr. John Bowders, Thesis Supervisor

MAY 2014

The undersigned, appointed by the dean of the Graduate School, have examined the thesis entitled

"SHEARING RATE EFFECTS ON DRAINED SHEAR STRENGTH OF FLUE GAS DESULFURIZATION (FGD) BYPRODUCT"

presented by Tasneem Khan

a candidate for the degree of Master of Science in Civil Engineering,

and hereby certify that, in their opinion, it is worthy of acceptance.

Dr. John Bowders, P.E., Supervising Professor

Dr. Brent Rosenblad, Committee Member

Dr. Allen Thompson, P.E., Committee Member

DEDICATION

First and foremost, praises and thanks to God, the Almighty, for whatever I have achieved as one of the many blessings from Him in my life.

I dedicate this thesis to my loving husband, Dr Aslam Ali Khan, who supported me in everything I did throughout my time in the MU College of Engineering Civil and Environmental Engineering department's geotechnical program. Without his help, it would have been extremely difficult to concentrate on studies with our one-year-old son, Mohammad Anwar.

ACKNOWLEDGMENTS

The success of this research required guidance and assistance from many people, and I would like to thank all of them for their continuous support.

My sincere thanks go to my adviser, Dr. John Bowders, for giving me an opportunity to do this interesting study. I am especially grateful for his encouragement to pursue independent critical thinking towards solving engineering problems, which has helped me to grow professionally as well as personally. Dr. Bowders always provided me with the full guidance I required, even during his busy schedule. I would also like to thank Dr. Brent Rosenblad, Dr. Erik Loehr and Dr. Bill Likos for their valuable academic guidance throughout my master's program.

I am grateful to Dr. Brent Rosenblad and Dr. Allen Thompson for participating on my committee and helping me grow by sharing their knowledge and expertise. I also appreciate Dr. Russell Dresbach in the MU Soil Characterization Laboratory for his valuable assistance.

I am thankful to Tayler Day, a CEE doctoral candidate who provided all the help needed to complete my experiments in the soil laboratory. I am grateful to all my MUGeo family members Minh Uong, Dan Ding, Ahmed Abu El Ela, Gouzhen Zhang and Joe Gilliam who were always ready to help. A special thanks goes to Caitlin Schnitzer for helping me with the excel plots.

This project was made possible by the interest and support of Ms. Elisabeth Freeman, PE, Burns and McDonnell Engineers, Kansas City, Missouri.

My acknowledgements would be incomplete without thanking Mr. Mahmood Nawar, a doctoral candidate in MU's structural engineering program, and his wife, Nagla, for their continuous support right from the beginning of my studies. I thank my elder sister, Nusrat, for encouraging me to pursue graduate studies. I will never forget the continuous efforts of my parents to provide guidance not only towards my studies but also in all other aspects of my life. I thank them both from the bottom of my heart.

TABLE OF CONTENTS

LIST OF NOTATIONS

ENS - Effective normal stress

NDR - Nominal deformation rate

NDRI - Nominal deformation rate increase

NDRD - Nominal deformation rate decrease

LIST OF TABLES

LIST OF FIGURES

SHEARING RATE EFFECTS ON DRAINED SHEAR STRENGTH OF FLUE GAS DESULFURIZATION (FGD) BYPRODUCT

Tasneem Khan

Dr. John Bowders, Thesis Supervisor

ABSTRACT

Flue gas desulfurization (FGD) sludge (calcium sulfite, $CaSO_3$) is a byproduct produced during cleanup of the flue gas from the burning of coal for electricity generation. About four percent of the total 24 million tons of FGD produced each year is used in beneficial applications, mainly agricultural amendments or manufacture of gypsum wall board. The remainder is typically disposed in embankment landfills. Shear strength of the compacted FGD sludge must be adequately characterized for the safe design of the embankments and analyses of other geotechnical applications. A material's shear strength is a function of the deformation rate used to measure the strength. The effect of deformation rate on the drained shear strength of compacted FGD by-product is considered in this thesis.

Compacted FGD specimens were prepared using standard Proctor method and drained direct shear tests were performed at four different effective normal stresses (500, 1000, 2000, and 3000 psf) using three different deformation rates (0.002, 0.0002 and 0.00002 inches per minute). Effective stress cohesion intercepts were assumed to be zero. Failure envelopes were developed for each deformation rate as follows: ϕ' of 37° (0.002 in/min), ϕ' of 46° (0.0002 in/min), and ϕ' of 57° (0.00002 in/min). The

results indicate shear strength dependence on the deformation rate with slower rates yielding higher strength. If the specimens were fully drained during shear testing, one would not expect a dependence on the deformation rate. Analyses were performed using two different approaches for calculating the time to failure of the shearing specimen. Deformation rates from measured hydraulic conductivity exceeded the rates used in the present study from consolidation data. Based on the shear rates from calculated hydraulic conductivity, the deformation rates used in this study, should yield similar effective stress failure envelopes (ϕ') for all shearing rates. Other possible mechanisms for deformation rate-dependence of the shear strength were considered including: pozzolanic behavior and creep (deformation under constant load). Based on the results of hydraulic conductivity and consolidation testing, these mechanisms are not impacting the shear strength of the compacted FGD.

Re-examination of the time-settlement curves for each consolidation load on the direct shear specimens indicate that the times to reach end of primary consolidation may be much longer than originally assumed. Four specimens out of the 17 show a substantial flattening of the time-settlement curve after more than 900 to 2500 minutes under a given consolidation stress. Using only these four test results yield deformation rates of 4E-5 to 2E-6 inches/minute for fully drained behavior, which further suggests that only the slowest deformation rate (2E-5 inches/minute) used in this thesis yielded fully drained behavior of the compacted FGD sludge. For now, it is recommended that designers use the lowest shear strength parameters (obtained from the direct shear

tests with the highest deformation rates), for design of FGD disposal embankments; i.e., internal friction angle of 37 degrees with zero cohesion.

Additional investigation is recommended including an 'aging-effect' on strength study, measurements of excess pore water pressure dissipation under constant load, parallel shear strength studies on compacted FGD using drained triaxial tests (CD), undrained triaxial tests with pore water pressure measurements ($\overline{CU}$) and direct simple shear tests using the constant volume procedure (DSS-CV) and an extensive constituent analysis of the FGD material.

CHAPTER 1: INTRODUCTION

1.1 Background

According to a United States Geological Survey (USGS) report published in 2001, more than one-half of the nation's electricity is generated by burning coal. In the process of generating electricity, these facilities generate flue gasses containing oxides of sulphur (SOx) and nitrogen (NOx), and particulate trace elements, such as mercury, which in turn lead to air pollution, acid rain, soil acidification, forest degradation and in addition leave behind tons of industrial solid waste. Environmental control technologies have been adopted by power plants to reduce SO_x emissions. Scrubber units, which can absorb 90-95% of SO_x prior to discharge into the atmosphere, have been employed to reduce SO_x emissions. While scrubber units reduce atmospheric emissions, they produce a large quantity of byproducts known as coal combustion products (CCPs). The byproducts include fly ash, boiler slag, bottom ash and flue gas desulfurization (FGD) sludge. The latter creates solid sulfur compounds which can be used for beneficial purposes or stockpiled. FGD sludge is primarily used in Gypsum panel products (wall board), waste stabilization and agricultural amendments. However, most (about 95 percent of the 24 million tons produced annually) FGD sludge is disposed of in embankment fills and impoundments.

The effective stress (drained) shear strength behavior (rapid dissipation of excess pore water pressures generated due to shearing) represents the long-term effective stress strength performance of FGD sludge. As an engineered material, FGD sludge can

be applied in beneficial uses while helping to conserve natural resources provided the engineering properties, in the present case, effective stress shear strength, are adequately known and understood.

1.2. Research Objectives

Effective stress (drained) shear strength parameters can be obtained when the rate at which failure loads are applied are slow compared to the rate at which pore fluids in the material being sheared can drain, and therefore, no excess pore pressure is built up during the shearing process. A 2013 report (Bowders and Day, 2013) on drained direct shear testing of compacted FGD specimens reported that a deformation rate of 0.0002 inches per minute was sufficient to result in measurement of the effective stress (drained) shear strength parameters (c', ϕ') based on Gibson and Henkel (1954) approach.

The primary objective of the research presented herein is to quantify the shear strength behavior (c', ϕ') of compacted FGD when sheared at different deformation rates in drained direct shear tests. More specifically, determine if a deformation rate of 0.0002 inches per minute results in fully drained behavior of the FGD during shear and if not, suggest a deformation rate that will yield effective stress (drained) shear strength parameters (c',ϕ').

1.3 Scope of the research program

Sixteen drained direct shear tests were conducted on specimens of compacted FGD sludge at four different effective normal stresses (500, 1000, 2000, and 3000 psf) using three different deformation rates (0.002, 0.0002 and 0.00002 inches per minute).

The standard rate was 0.0002 inches per minute, referred to as the nominal deformation rate, 'NDR'. The nominal rate of shear deformation (0.0002 inches per minute) was calculated using consolidation data (Gibson and Henkel, 1954) from the final load increment of the consolidation stage of the direct shear test. The rate was increased (NDRI) and decreased (NDRD) by one order of magnitude to examine shearing deformation rate effects on the effective stress (drained) shear strength parameters of the compacted FGD. A failure envelope (c', ϕ') for each deformation rate was obtained using the results from the direct shear testing. The Kaniraj and Gayathri (2004) approach was used to estimate the drained deformation rate. Based on the findings from Kaniraj and Gayathri (2004) it was confirmed that pore pressures were not affecting the shear strength and this lead to further study of aging effects and creep.

1.4 Organization of the Thesis

The thesis is organized into six chapters in which the experimental work, the results and analyses are described in detail. The chapters are organized as follows: The literature review which provides the reader with a background on FGD and shear strength testing is presented in Chapter 2. The information regarding the FGD material and the testing methods used in the laboratory testing program are presented in Chapter 3. Chapter 4 contains the results of the laboratory investigation and Chapter 5 presents discussion of the results. Chapter 6 includes a summary of the findings of this study, conclusions and recommendations for future work.

CHAPTER 2: LITERATURE REVIEW

2.1 Introduction

This chapter contains background information on flue gas desulfurization (FGD) sludge and its applications. Different methods to calculate rate of deformation are presented followed by mineral composition and a brief description of coefficient of consolidation in FGD sludge. When looking at strain rate effects on shear strength of soil, one can consider total stress (undrained) or effective stress (drained) shear strength tests. For undrained tests, effects appear to be significant; therefore, much research has been performed on the shearing rate effects on soils in the undrained condition. However, effects of deformation rates on drained shear strength have not been studied extensively. This study is focused on the shear rate effects on the drained strength (c', ϕ') of compacted FGD.

2.2 FGD sludge background

The U.S. Congress passed strict rules (Clean Air Act, 1970) to place constraints on the emissions from coal burning facilities. In 1977 and 1979, the United States Environmental Protection Agency (US EPA) set up national ambient emission control standards for six criteria pollutants: carbon monoxide (CO), particulate matter (PM), lead (Pb), nitrogen oxide (NOx), ozone (O_3), and sulfur dioxide (SO_2). The Clean Air Act Amendments (CAAA) of 1990 addressed issues like acid rain, ozone depletion and toxic air pollution and mandated reduction of nationwide SO_2 emissions. As a result of the tightened emission controls, SO_2 emissions have declined in the past two decades. This

improvement in air quality occurred simultaneously even though coal consumption by electric utilities was still increasing. In the last few decades, the problem of air pollution has been addressed more seriously throughout the world; hence, environmental regulations have become more and more restrictive towards the emissions of atmospheric pollution produced by combustion systems. Flue-gas desulfurization (FGD) is a set of technologies used to remove sulfur dioxide (SO_2) from exhaust flue gases of fossil-fuel power plants. FGD processes absorb gaseous SO_2 from flue gas to produce solid sulfur compounds, which are collected for safe disposal or beneficial use (Kalyoncu, 2000).

2.2.1 Production of FGD Sludge

The inorganic residues that remain after coal is burned are called Coal Combustion Products (CCPs). CCPs consist (by mass) of roughly 58% fly ash, 24% flue gas desulfurization (FGD) sludge, 16% boiler slag and 3% bottom ash. Generally, heavier and larger particles that fall to the bottom of the boiler are referred to as bottom ash, and the lighter particles that are carried upward through the flue gas are considered fly ash. Boiler slag is molten ash collected at the base of the combustor while FGD sludge is typically the product of an FGD flue gas scrubbing process in which sulfur is removed from the flue gas emission.

The general FGD process is shown in Figure 2.1. Desulfurization of flue gases can be achieved by a variety of methods including: wet scrubbing, dry scrubbing, dry sorbent injection systems, wet sulfuric acid process, and SNOX Flue gas desulfurization.

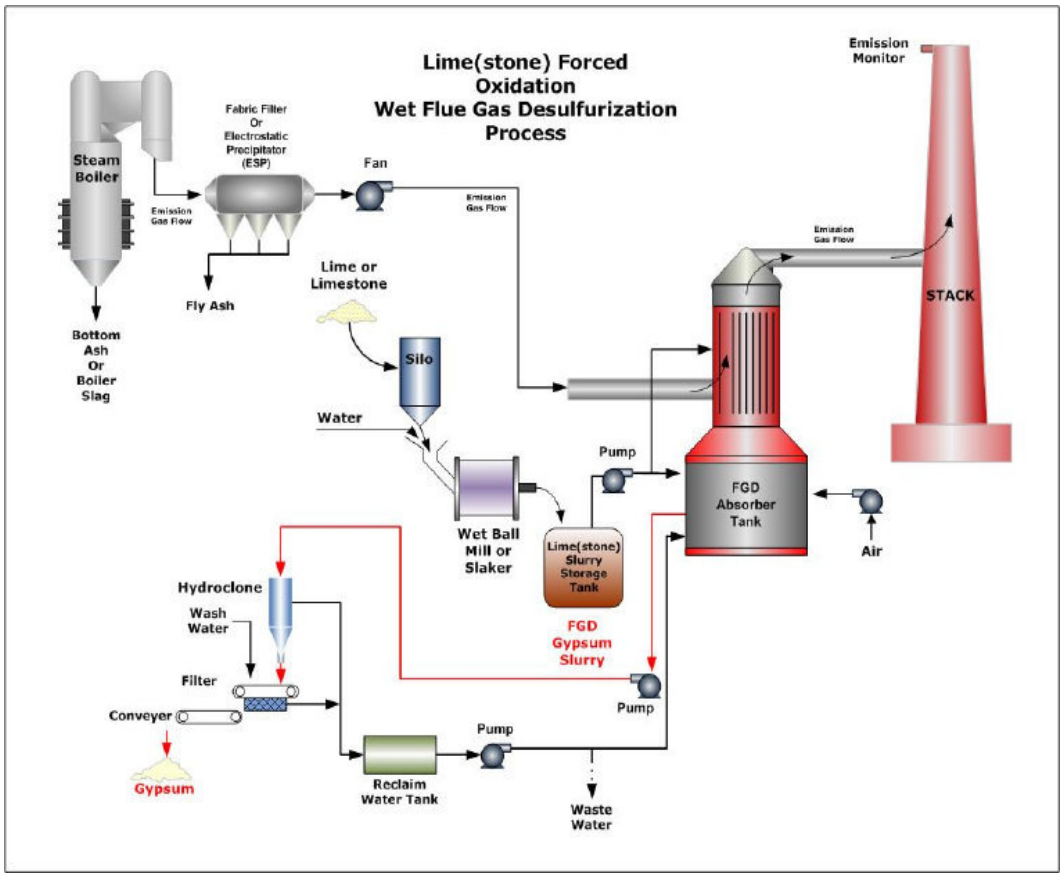

Figure 2.1 Typical diagram of FGD sludge production process using Lime (CaO) or Limestone (CaCO3) (FGDProducts.org, a website sponsored by the American Coal Ash Association Educational Foundation (AAAC 2007).

While the wet and dry processes are the same in their methods, they differ based on the type of sorbents used and the products produced. For a typical coal-fired power station, flue-gas desulfurization (FGD) will remove 90 to 95 percent or more of the SO_2 in the flue gases. Wet scrubbing systems are commercially available in many variations and designs and are the most widely used scrubbing systems employed throughout the world. Depending on the sorbent slurry being introduced, the currently available technologies are classified as: lime/limestone/sludge wet scrubbers, wet lime, fly ash scrubbers, or other wet scrubbers (including seawater, ammonia, caustic soda,

sodium carbonate, potassium and magnesium hydroxide). The preferred sorbent in operating wet scrubbers are limestone followed by lime because of their availability and relatively low cost (Kalyoncu, 2000). Approximately 90 percent of the FGD systems in U.S use limestone/lime as the sorbent (Kalyoncu, 2000).

Sulfur dioxide (SO_2) is an acid gas, and, so, usually the sorbent slurries used to remove the SO_2 from the flue gases are alkaline in nature. The detailed chemistry of absorbing SO_2 from the flue gas using different sorbents is shown below:

a) The reaction taking place in wet scrubbing using a $CaCO_3$ (limestone) slurry produces $CaSO_3$ (calcium sulfite) and can be expressed as:

$$CaCO_3 \text{ (solid)} + SO_2 \text{ (gas)} \rightarrow CaSO_3 \text{ (solid)} + CO_2 \text{ (gas)} \quad (2.1)$$

b) Using a $Ca(OH)_2$ (lime) slurry as a wet scrubbing sorbent, the reaction produces $CaSO_3$ (calcium sulfite) and can be expressed as:

$$Ca(OH)_2 \text{ (solid)} + SO_2 \text{ (gas)} \rightarrow CaSO_3 \text{ (solid)} + H_2O \text{ (liquid)} \quad (2.2)$$

c) The forced oxidation technique is used to reduce the cost of the FGD unit installation in some industries, and it is obtained by using $CaSO_3$ (calcium sulfite) and further oxidizing to produce marketable $CaSO_4 \cdot 2H_2O$ (Gypsum).

$$CaSO_3 \text{ (solid)} + H_2O \text{ (liquid)} + \tfrac{1}{2}O_2 \text{ (gas)} \rightarrow CaSO_4 \text{ (solid)} + H_2O \quad (2.3)$$

d) Seawater is used as a natural alkaline to absorb SO_2.

$$SO_2 \text{ (gas)} + H_2O \text{ (sea water)} + \tfrac{1}{2}O_2 \text{ (added gas)} \rightarrow SO_4^{2-} \text{ (solid)} + 2H^+ \quad (2.4)$$

e) Using a $Mg(OH)_2$ (magnesium hydroxide) slurry as a wet scrubbing sorbent , the reaction produces $MgSO_3$ (magnesium sulfite) and can be expressed as:

$$Mg(OH)_2 \text{ (solid)} + SO_2 \text{ (gas)} \rightarrow MgSO_3 \text{ (solid)} + H_2O \text{ (liquid)} \quad (2.5)$$

Flue gas at the absorber outlet is monitored for SO_2 content, which can be regulated by the quantity of limestone added. The physical nature of FGD sludge varies from a wet, thixotropic sludge to a dry, powdered material, depending on the process.

2.2.2 Applications of FGD sludge

Examples of FGD sludge used for surface reclamation of coal refuse piles (gob piles) are presented in Figures 2.2, 2.3 and 2.4 (Wolfe W., Butalia T., Daniels J. and Baker R. (2010)). The alkaline nature of the FGD helps to ameliorate the acidic nature of seepage through the coal refuse. The lower hydraulic conductivity of the FGD layer also restricts the amount of precipitation that infiltrates into the coal refuse and thus reduces the volume of acidic drainage that may develop.

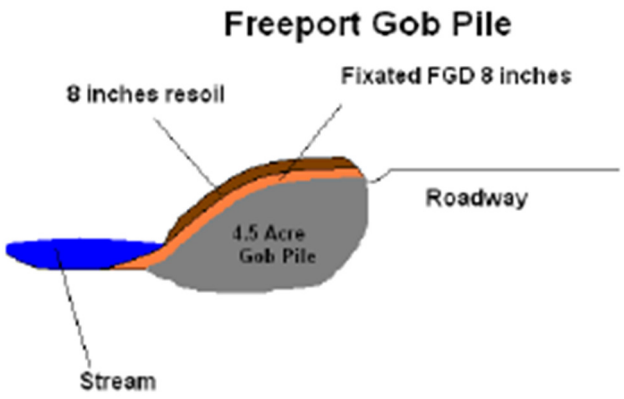

Figure 2.2 Cross-section of Freeport coal refuse (gob) surface reclamation plan (located in Lafayette Township, Coshocton County, Ohio).

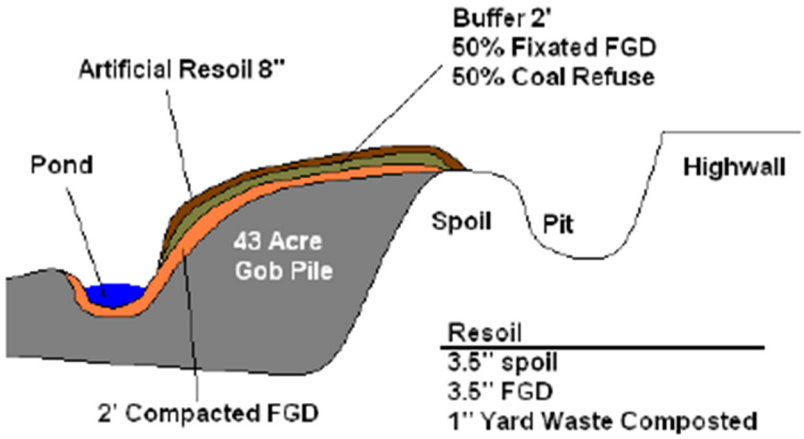

Figure 2.3 Rehoboth FGD application for surface reclamation of coal refuse (gob) (Clayton Township, Perry County, Ohio).

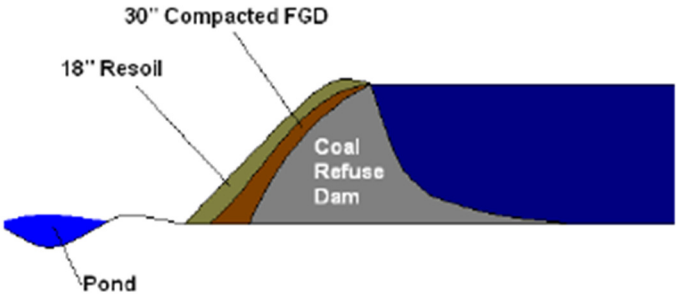

Figure 2.4 Central Ohio Coal Company cross section of surface reclamation of coal refuse embankment by application of layer of FGD (Meigsville Township, Morgan County, Ohio).

2.3 Gibson and Henkel (1954), Rate of deformation

Shear strength of soil is defined as the magnitude of the shear stress (measure of soil's resistance) that a soil can sustain against failure and sliding along any plane (deformation) inside the soil mass. It is important to study the nature of shearing resistance in order to analyze soil stability problems such as bearing capacity, slope stability and lateral pressures on earth retaining structures. When considering the shear

strength of soil, two main types of tests are used to determine deformation and strength characteristics of saturated soils: fully drained and undrained shear strength tests. While no volume change occurs in an undrained test, drained shear strength of soil is the strength obtained from the test in which pore water pressures, generated during the course of shearing the soil, are allowed to dissipate during shearing, i.e., excess pore water pressures remain nearly zero and result in considerable amount of volume change.

The shear strength of a soils, in terms of effective stress is given by the equation

$$S = c' + \sigma' \tan \phi' \tag{2.6}$$

where:

σ’ = Effective normal stress on plane of shearing = σ – u

σ = Total stress

u = Pore water pressure

c’ = Effective cohesion

ϕ’ = Effective internal angle of friction

Effective stress governs soil behavior. It is important to understand the two terms, static pore water pressure and excess pore water pressure, which combine to produce the change in the effective stress within the soil. Hydrostatic pore water pressure (u) also called neutral stress (as it does not produce any compression of the soil nor increase the shear strength of soil) is the pressure that exists in the water present in the pores of the soil. It is measured by inserting a tube or a stand pipe at a particular point where pore

pressure must be determined and by recording the increase in water level as it rises in the stand pipe (piezometer) (Equation 2.7).

$$u_0 = \gamma_w x\, h \tag{2.7}$$

where h = height of water rise in piezometer above the point

Excess pore pressure (Δu) is pore water pressure generated by shearing soil. Considering the loading of a sponge soaked with water. As the sponge is loaded, water drains out; a similar process happens when saturated soil is loaded. Clay is not very permeable and does not release water quickly, so the pore water pressure initially increases, but then gradually decreases as water drains from the soil pores. Sands and gravels are more permeable; hence, they rarely generate significant excess pore pressures during shear. The excess pore water pressure generated by loading highly permeable soils dissipates almost immediately. Thus, pore water pressure at any point is given by Equation 2.8:

$$u = u_0 + \Delta u \tag{2.8}$$

In drained tests on sand, free drainage of water is allowed out of, or into, the specimen because no excess pore pressure is desired anywhere in the specimen. The excess pore water pressure is a result of loose sands compressing during shearing, whereupon the pore water is squeezed out of sand. However, dense sands dilate (expand) as they are sheared creating a negative pressure in the pore water which results in water flowing into the sand. Significant volume change (expansion) can occur in the sand. For fully drained conditions the soil either compresses or dilates (expands) during shear and the

excess pore water pressure remains zero, Δu = 0. Thus, the pore water pressure in the sand remains constant at the neutral stress value, $u = u_0$.

The conditions of a fully drained test are satisfied only if the rate of loading is slow enough to allow any excess pore water pressures to fully dissipate during the shearing stage; otherwise, an excess pore water pressure (Δu) remains undissipated as illustrated in Figures 2.5(a) and (b). Therefore, finding an appropriate deformation rate for shear testing of a specific type of soil, which will yield the effective stress (fully drained) behavior of that particular soil, is always a challenge for engineers. Gibson and Henkel (1954) assumed that for a drained test, any increment of deformation produces the same increase in pore water pressure as does the same increment in an undrained test, but that the pore water pressures now dissipate in accordance with Terzaghi's theory of one-dimensional consolidation as shown in Figure 2.5(b) (Teraghi, 1942).

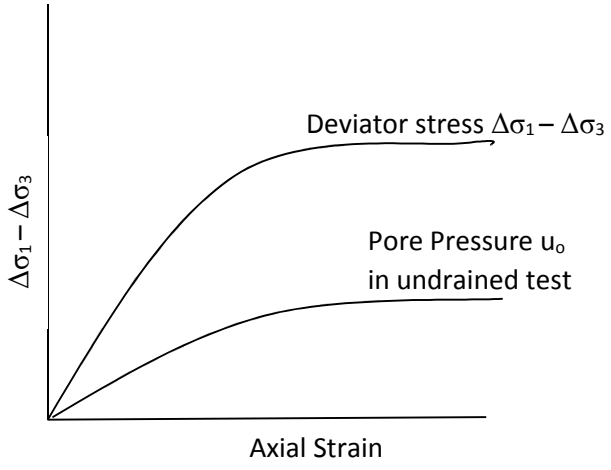

Figure 2.5(a) Idealized excess pore water pressure and stress difference versus axial strain during shear in undrained triaxial tests (after Gibson and Henkel, 1954).

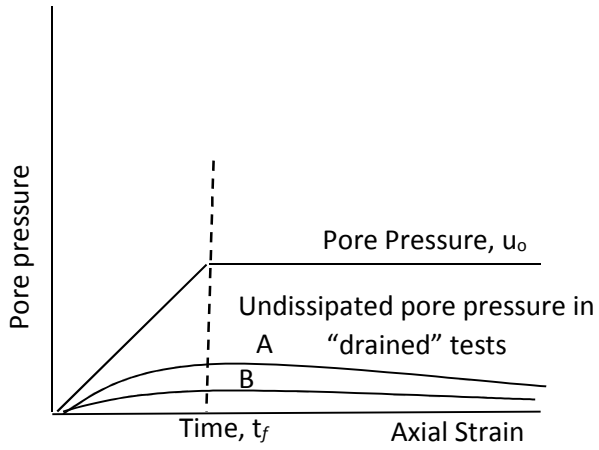

Figure 2.5(b) Idealized excess pore water pressure in soil specimens (A and B) at two successively slower axial strain (deformation) rates in "drained" triaxial tests (after Gibson and Henkel, 1954).

Stresses applied to the soil specimen are prevented from becoming fully effective by an amount dependent upon the magnitude of the undissipated pore-water pressure at the time of failure. Thus, the measured strength differs from the fully drained strength. The dissipation of the pore water pressure in a drained test depends on the hydraulic conductivity and compressibility of the soil as well as the location of the drainage surfaces around the specimen, and the rate of loading. Because of this dependent set of pore water pressure processes, Gibson and Henkel (1954) recommended that before carrying out drained tests on a particular soil, a suitable rate of shearing (testing) must be estimated to ensure that the effect of any undissipated porewater pressure on the strength is negligible. To estimate a satisfactory strain rate for shearing a soil specimen, a series of trials are necessary to measure the strength of specimens which are free to drain in the same way but are tested at different strain rates (Gibson and Henkel, 1954). This allows a theoretical estimate of the shear rate required to achieve full dissipation of

excess pore water pressures. Gibson and Henkel (1954) developed a theory to estimate duration of the test needed to ensure a shearing rate close to fully drained conditions.

Gibson and Henkel (1954) performed a series of drained triaxial and direct shear tests with different rates of strain. They used three clays: 1) silty Weald clay with a liquid limit (LL) of 43 and a plastic limit (PL) of 18, and 2) remolded London clay with an LL of 72 to 74 and a PL of 25 to 28 3) Kaolinite with LL 64 and PL 42 to determine a suitable rate of loading for drained tests. Along with these tests, triaxial tests with different rates of loading on kaolinite (LL = 64; PL = 42) were also performed. The test results are shown in Figures 2.6 to 2.9 as curves of percentage of the fully drained strength mobilized in a particular test against the time to reach failure (peak shear resistance). The purpose of their study was to develop a theory and to derive expressions connecting time of shearing or loading with degree of dissipation of excess pore water pressure at failure for typical laboratory shear tests. This would result in some degree of reliability regarding the comparisons made between results of drained tests and the predictions of the theory.

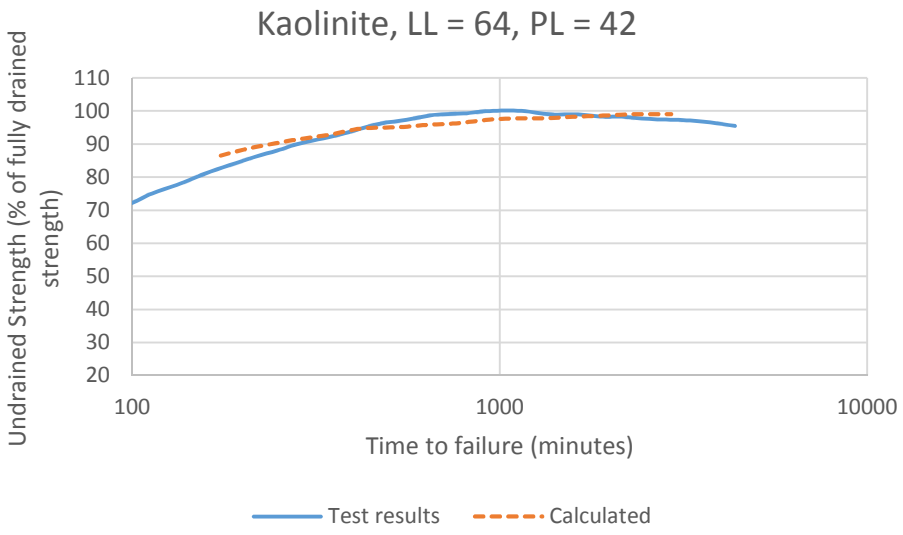

Figure 2.6 Percentage of the fully drained strength versus duration of deformation for direct shear tests on Kaolinite clay (after Gibson and Henkel, 1954).

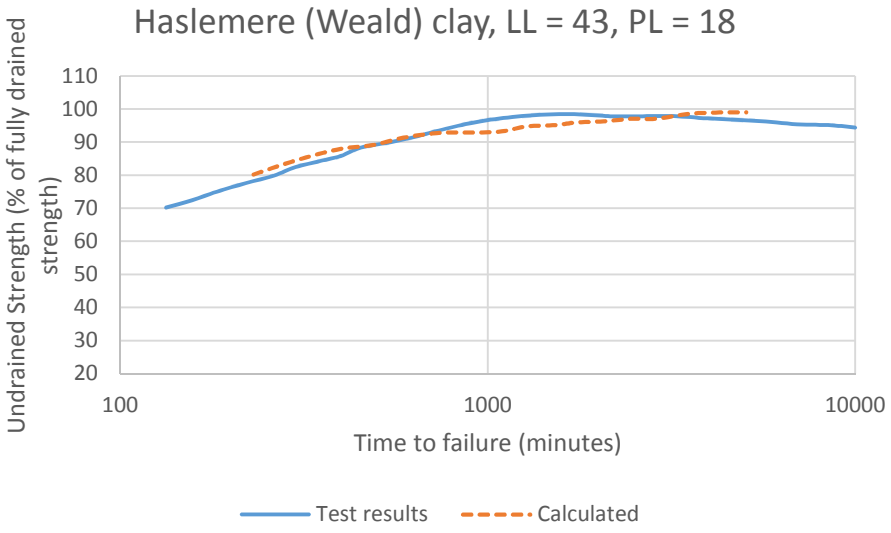

Figure 2.7 Percentage of the fully drained strength versus duration of deformation for direct shear tests on Haslemere clay (after Gibson and Henkel, 1954).

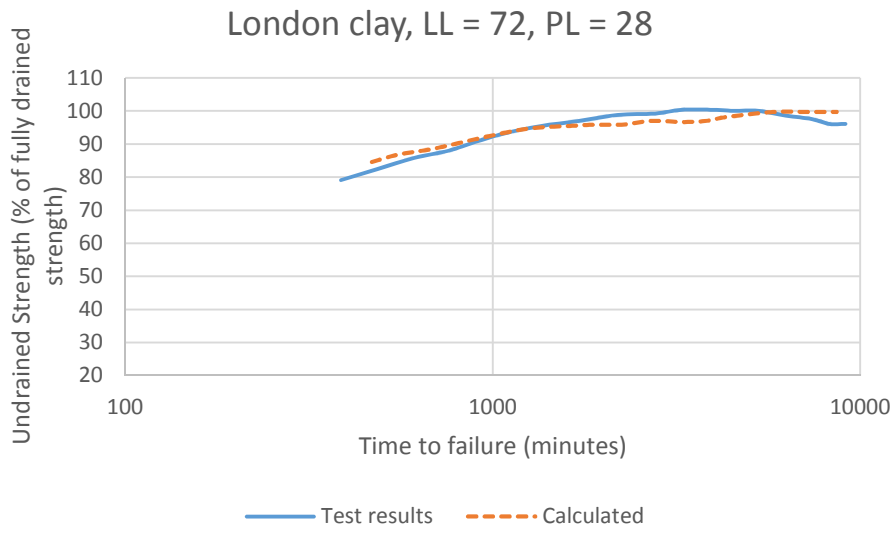

Figure 2.8 Percentage of the fully drained strength versus duration of deformation for direct shear tests on London clay after (Gibson and Henkel, 1954).

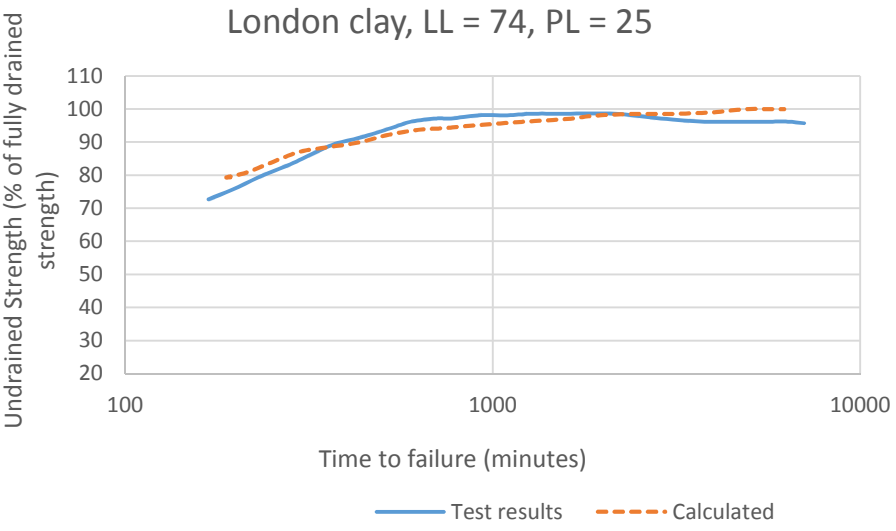

Figure 2.9 Percentage of the fully drained strength versus duration of deformation for direct shear tests on London clay (after Gibson and Henkel, 1954).

Based on their results (Figs 2.6 to 2.9), the measured strength increased with increasing duration of shearing up to a peak strength, but for still slower rates of shear the strength again decreased. An average degree of consolidation at failure was about 95 percent (nearly completion of primary consolidation) at peak drained strength.

For a "drained" test, (Gibson and Henkel, 1954) assumed that the excess pore water pressures dissipated in accordance with Terzaghi's theory (1942) of one-dimensional consolidation. Figure 2.5(a) shows curves to represent the excess pore water pressure and related deviator stress with axial strain as obtained from a consolidated, undrained triaxial test carried out at a constant rate of axial strain. The excess pore water pressure curve has been idealized in Figure 2.5(b) to consist of two straight lines representing the drained triaxial test. From the start of the test up to the time of failure, t_f, the rate of increase of pore pressure is linear; thereafter, the pore water pressure remains constant. With the assumptions mentioned previously, it was found that in a drained test the undissipated excess pore water pressure can be given by Equation 2.9:

$$c_v * \Delta v^2 * \mathrm{u} = \frac{\partial u}{\partial t} - \frac{\partial u_0}{\partial t} \qquad \text{For } 0 \le t \le t_f$$

$$c_v * \Delta v^2 * \mathrm{u} = \frac{\partial u}{\partial t} \qquad \text{For } t \ge t_f \quad (2.9)$$

where:

u is the excess pore water pressure, t is time, c_v is the coefficient of consolidation, and Δv is volume change per unit volume. The solution of Equation 2.9 is an infinite Fourier series. The degree of consolidation at failure, U_f, in terms of test failure time is given by Equation 2.10.

$$\mathrm{U_f} = 1 - \frac{u_f}{u_0} \qquad (2.10)$$

where:

u_f is the excess pore water pressure at failure and u_0 is the excess pore water pressure that would have existed in the absence of any drainage. In a fully drained test, excess pore water pressure, u_f, would be zero and the average degree of consolidation, U_f, would then be 1.0. The infinite series solution for U_f can be truncated after the first term for large values of U_f (say over 0.8) to yield a simple solution:

$$\mathrm{U_f} = 1 - \frac{H_s^2}{2c_v t_f} \tag{2.11}$$

where:

H_S is the average drainage distance during shear; subscript "s" denotes the shearing stage, and for the case of top and bottom drainage, H_S is half of the thickness of the specimen; c_v is the coefficient of consolidation, and t_f is the time to failure. Equation 2.11 can be rearranged to yield:

$$\mathrm{t_f} = \frac{H_s^2}{2c_v(1-U_f)} \tag{2.12}$$

The time to failure is infinite if U_f is set equal to one. In principle, the coefficient of consolidation, c_v, can be evaluated for the last consolidation loading increment following the methods based on Terzaghi's theory. If the curve fitting is performed at 50 percent average degree of consolidation the the calculated coefficient of consolidation, c_v, becomes:

$$\mathrm{c_v} = \frac{0.197 \times H_c^2}{t_{50}} \tag{2.13}$$

where:

H_C is the average drainage distance (half the thickness of the soil specimen in the direct shear test) during the consolidation stage, and t_{50} is the time to achieve 50 percent average degree of consolidation. Substitution of Equation 2.13 into Equation 2.12 leads to:

$$t_f = \frac{H_S^2 \times t_{50}}{2 \times 0.197 \times H_C^2 (1 - U_f)} \quad (2.14)$$

In order to estimate a reasonable value of average degree of consolidation, U_f, Gibson and Henkel (1954) performed a number of direct shear tests using various strain rates. They used three different types of soft remolded clays. As the shearing time increased the strength also increased until it reached a peak strength after which any further increase in the time of failure caused a gradual reduction in strength (Figures 2.6 to 2.9). The peak strength corresponded to a calculated average degree of consolidation at failure of about 0.95. So, U_f has been assigned a value of 0.95 in most of the examples discussed in this thesis.

Equation 2.14 can be simplified by assuming that the drainage distances during consolidation and shear are essentially identical, and that satisfactory results can be achieved using U_f = 0.95. Thus, with time of failure given as Equation 2.15, the rate of deformation can be then calculated by Equation 2.16:

$$t_f = 50 \times t_{50} \quad (2.15)$$

The above formula makes estimating the rate of deformation possible with the following equation:

$$\dot{\delta} = \frac{\delta_h peak}{t_f} \quad (2.16)$$

where:

$\delta_h$peak = Horizontal deformation at peak shear resistance,

t_f = time to reach peak shear resistance (time of failure) = 50 x t_{50} (Equation 2.15)

2.4 Head (1981), Rate of deformation

Head (1981) suggests using a version of the square root of time method (Taylor 1948) to plot the vertical deformations during the final consolidation loading prior to beginning the shearing stage in order to calculate the time to failure and subsequently the appropriate deformation rate to yield effective stress (drained) shear strength parameters in the direct shear test.

In this version of Taylor's method, a plot of settlement (in mm) versus square root time (minutes) (Figure 2.10) is obtained from the last consolidation loading on the specimen (the effective stress under which the specimen will be sheared). A tangent is drawn in the early straight line portion of the consolidation curve. This line is extended to intersect the horizontal line representing 100 percent consolidation. The point of intersection gives the value of $\sqrt{t_{100}}$, which when multiplied by itself gives the time intercept as t_{100} (min).

The time required to reach peak shear resistance (failure), t_f, in a shear test is given by the empirical Equation 2.17:

$$t_f = 12.7\ x\ t_{100(minutes)} \quad (2.17)$$

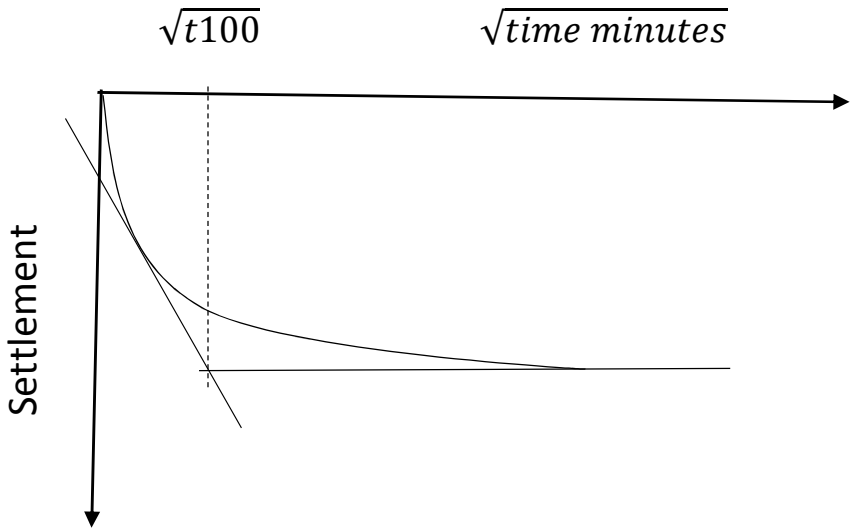

Figure 2.10 Derivation of time to failure from consolidation curve using square root time plotting method.

The coefficient of consolidation, c_v, can be calculated using Equation 2.18 (Gibson and Henkel, 1954).

$$c_v = \frac{0.103 \times H^2}{t_{100}} \tag{2.18}$$

where:

H is the specimen height (mm) and t_{100} is in minutes.

The estimation of rate of deformation is then found by using Equation 2.16 as was used for Gibson and Henkel's work.

Regardless of the method of calculating time to reach peak shear resistance (t_f) (peak shear strength) for fully drained conditions, one needs to first estimate the displacement at which the peak strength is likely to be mobilized. This is usually based on experience, although general guidance for horizontal deformation at peak strength is given in Table 2.1 (Head 1981).

Table 2.1 Typical displacements to reach peak shear strength in 60 mm shear box (after Head, 1981)

Type of soil	Shear box displacement for peak strength	
	(mm)	(inches)
Loose sand	5 to 8	0.2 to 0.3
Dense sand	2 to 5	0.08 to 0.2
Plastic clay	8 (typical limit of travel)	0.3
Stiff clay	2 to 5	0.08 to 0.2
Hard clay	1 to 2	0.04 to 0.08

2.5 Mineral composition of FGD sludge

In order to understand the behavior of FGD sludge, it is important to know the mineral composition. Bigham et al. in 2005 collected 59 coal combustion products from six coal fired plants throughout United States, all of which used different types of flue gas scrubbing technologies to remove SO_2. The FGD scrubbing technologies included duct injection, lime injection multistage burner (LIMB), fluidized bed combustion and spray dryer. Detailed descriptions of these technologies are in Kost et al. (2005).

Bigham et al. (2005) conducted X-ray diffraction tests, swelling tests, long term equilibrium studies and equilibrium geochemical modeling. X-ray diffraction revealed that the primary contents of FGD sludge were $Ca(OH)_2$ (Portlandite), $CaSO_3 \bullet 0.5H_2O$ (Hannebachite), CaO (Lime), $CaSO_4$ (Anhydrite), $CaCO_3$ (Calcite) and MgO (Periclase). Two distinct swelling episodes were observed. One episode occurred immediately after water was applied due to a hydration reaction, especially the conversion of CaO to $Ca(OH)_2$ and $CaSO_4$ to $CaSO_4 \bullet 2H_2O$ (Gypsum). The second began between 10 and 50 days later and involved formation of the mineral Ettringite ($Ca_6(Al(OH)_6)(SO_4)_3 \bullet 26H_2O$).

Bigham et al. (2005) found that if FGD byproducts were under 'closed' and alkaline weathering conditions such as found in road embankments or mine reclamation, Gypsum and Portlandite are initially formed followed by the conversion of the Gypsum to Ettringite (highly swelling in nature). In the present study the specimen was confined for testing for as long as 7 to 8 days wherein formations of some of the above mentioned compounds were possible.

2.6 Coefficient of consolidation

There are several methods to determine c_v from the settlement-time data which are obtained during the consolidation phase of the direct shear test. In this thesis, the log-time method (Casagrande and Fadum, 1940) and square-root-time method (Taylor, 1948) were both used. However these methods were originally developed for plastic clays where it potentially takes a long time to complete primary consolidation under a given loading. For non-plastic fines such as fly ashes, FGD sludge and non-cohesive soils, settlement (and full dissipation of excess porewater pressures) occurs very quickly and often within 30 minutes upon application of load (Moghal and Sivapullaiah, 2011). Krizek et al. (1987) reported the time to reach end of primary consolidation, t_{100}, as less than one minute for FGD sludge. The c_v values for the compacted FGD sludge calculated by Casgrande and Taylor's methods in the present study were reconsidered. Pandian and Balasubramonian (1999) determined the value of c_v's for two Indian fly ashes using the Casagrande method, Taylor's method, and the rectangular hyperbola method. They observed that there was a significant variation in the c_v determined by the three methods, and Taylor's method gave a value 21 times higher than the rectangular

method. Taylor's method gave a faster rate of consolidation than the other methods. Porbaha et al. (2000) back-calculated the hydraulic conductivity, k, using Equation 2.19 and found that there were large variations between the measured and back-calculated values of k:

$$k = c_v * m_v * \gamma_w \quad (2.19)$$

where:

m_v = coefficient of volume compressibility, and

γ_w= unit weight of water

The discrepancies among c_v's by the conventional methods (Casagarnde and Fadam, 1940 and Taylor, 1948), can be evaluated by direct measurement of hydraulic conductivity (k) and the coefficient of volume compressibility (m_v). Kaniraj and Gayathri (2004) recommended using the theory of Gibson and Henkel (1954). The first step is to measure the hydraulic conductivity, k and the coefficient of volume compressibility m_v for the final consolidation load increment before shearing and use them to calculate c_v using Equation 2.19. Kaniraj and Gayathri (2004) studied the compressibility parameters coefficient of compressibility (a_v) and m_v in a Casagrande-type consolidometer. The values of c_v were calculated by substituting the measured value of m_v and the measured value of k into Equation 2.19.

2.7 Summary

Clean coal technology requires cleanup of flue gases for removal of sulfur compounds. Calcium carbonate ($CaCO_3$, limestone) injected into the flue gases absorbs the sulfur and results in a byproduct of calcium sulfite ($CaSO_4$) which is known as FGD

sludge. The FGD sludge is underutilized and most often disposed in embankment landfills. Analysis of the stability of the embankments and other beneficial reuses of the FGD sludge requires knowledge of the shear strength parameters (c' and Φ').

Gibson and Henkel have shown that to obtain effective stress strength parameters (drained strength), shearing rates must be slow enough to allow time for dissipation of any excess pore water pressures generated due to shearing. They provided a procedure to calculate the time necessary to reach peak drained shear strength based on knowledge of the consolidation properties of a soil. Head (1981) suggested using Taylor's square root of time method for calculating time to reach peak drained shear strength. He also provided typical deformations to reach peak strength for several general soil types.

In the present thesis, the methods of Gibson and Henkel (1954) is used to determine appropriate deformation rates for specimens of compacted FGD to ensure that effective stress strength parameters are measured; i.e., ensure the specimens are sheared under fully drained conditions. Mineral composition of the FGD sludge is also presented in this chapter. The coefficient of consolidation in FGD sludge is also discussed in the chapter.

CHAPTER 3: MATERIALS AND METHODS

3.1 Introduction

The materials and methods used in the testing program to gain a better understanding of the deformation rate effects on the drained shear strength of compacted FGD sludge are described in this chapter. The laboratory methods used for measuring the shear strength, coefficient of consolidation, hydraulic conductivity and particle size distribution are described.

3. 2 Material

Flue gas desulfurization (FGD) sludge was the primary material used in the research presented herein. The FGD sludge was received in air-tight buckets in two different batches on 09 April 2013 and 19 July 2013. The as-received moisture content of FGD sludge for both batches is given in Appendix Table A.1. The samples were always completely air-tight sealed to reduce the potential for change in as-received moisture.

3.3 Direct shear test

Direct shear testing is used to evaluate the drained shear strength of soils. For both loading stages (consolidation and shearing), complete drainage is allowed and leads to fully drained conditions where excess pore water pressure is negligible when sheared slow enough relative to the hydraulic conductivity of the material being sheared. Normal stress and shear stress on a horizontal plane are calculated where vertical displacement and relative horizontal displacement are between two halves of the specimen. It should be noted that the complete state of stresses and strains are

non-uniform and cannot be known throughout the specimen except on the horizontal plane of failure. Also, the plane of failure is forced to be horizontal, which may or may not be the weakest plane in the specimen. Though there are some disadvantages with this test, it is still useful because it is relatively quick, inexpensive, and conceptually simple, requires a small specimen and can shear to large displacements.

The direct shear test actually consists of two different ways of loading the specimen: stress controlled or strain controlled. In the present research, the direct shear test is used where the deformation rate is controlled in order to study the effects of deformation rate on the drained shearing strength of compacted FGD sludge. In a strain-controlled test a constant rate of deformation is applied and forces/stresses are measured. Figure 3.1 shows a schematic of the direct shear test device. Figures 3.2(a) and (b) show a photograph of the experimental setup used for the testing reported herein.

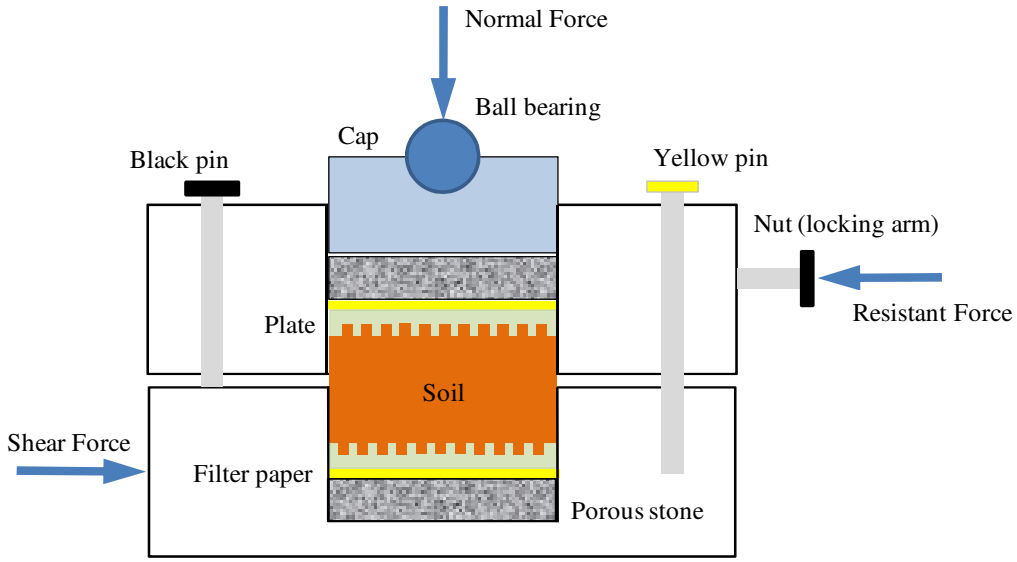

Figure 3.1 Elevation view of direct shear device with test components and forces (Direct shear manual, Geotechnical Engineering Program, University of Missouri, Columbia, 2012).

As seen in Figure 3.1, the test was arranged by first placing the following components: a saturated porous stone in the direct shear mold overlain with a filter paper to ensure freely draining surfaces, followed by a gripper plate. The 2.5-inch diameter compacted FGD sludge specimen is placed on top of the filter paper, and then the above mentioned components are placed in reverse order on the specimen to fill the mold. As shown in Figure 3.1 yellow pins hold the two halves of the shear box together, while black pins are used to create a shearing gap that minimizes friction between the two halves of the shear box. The mold is then placed in a holding box, and a load distribution cap and ball bearing are placed over the top porous stone.

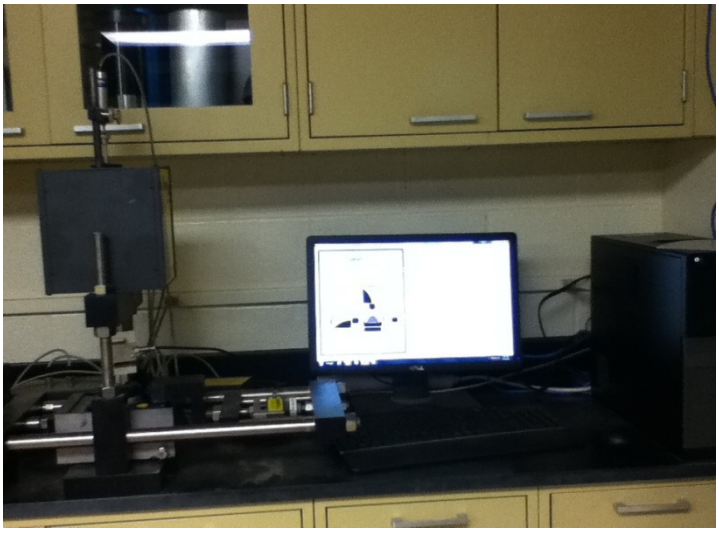

Figure 3.2 (a) Direct shear test setup in the Geotechnical laboratory of the University of Missouri.

As seen in Figure 3.2 (b) from the lab setup, a yoke connects to the top half of the shear box through the external bolt to lock it in position, while the bottom half is free to slide when a shear force is applied to the shear box.

A S2220 DigiShear™ automated Direct Shear System was used for shear tests on the compacted FGD. The system uses a computer software program to drive the test, display results during the test and simultaneously record the data in an electronic file to see the current position of loading at any time during the test. Also, the three different sensors, namely, the vertical load cell, horizontal load cell, and the lateral displacement gauge, can each be viewed on the Digishear software interface to monitor current loadings on the specimen and allow the operator to see the results as the deformation is in process.

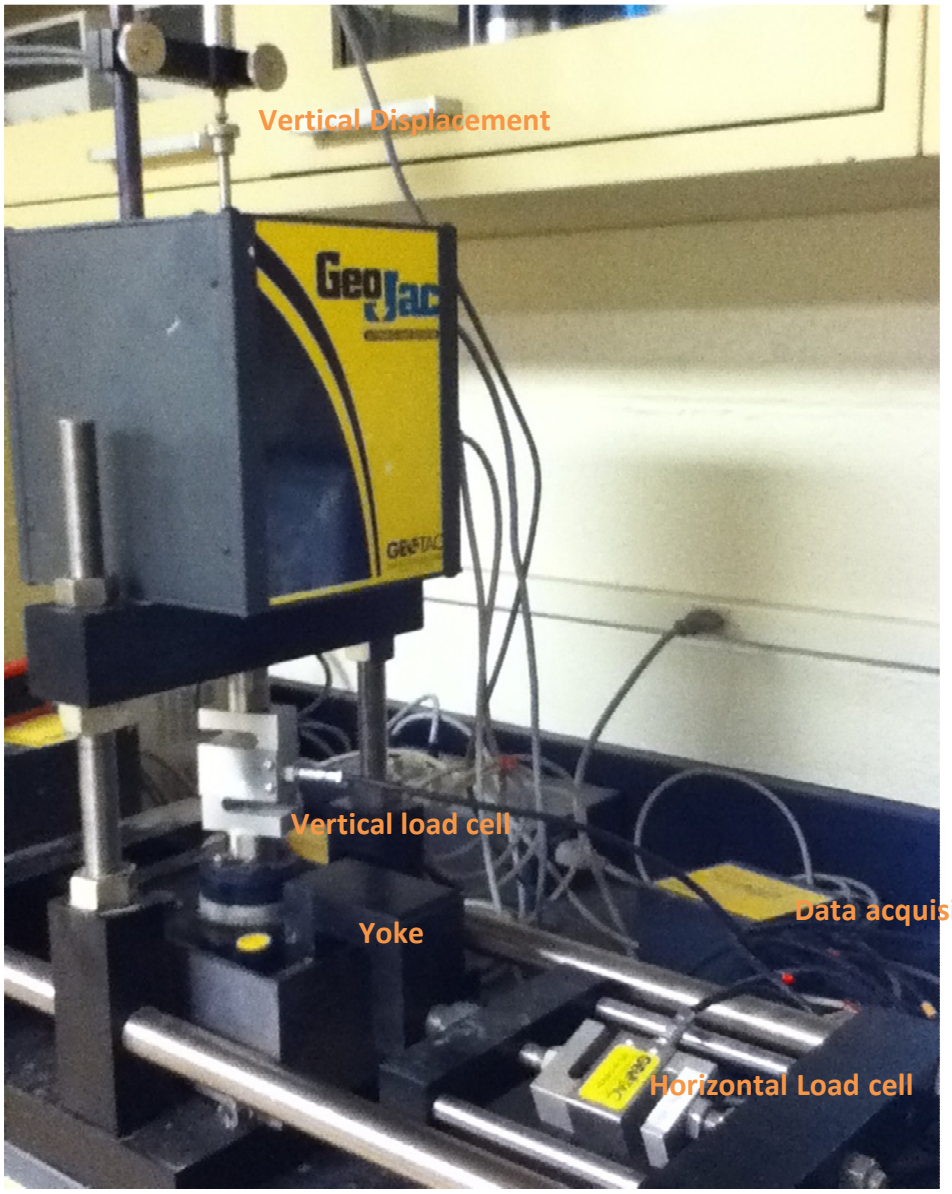

Figure 3.2 (b) Direct shear test setup in the Geotechnical laboratory of the University of Missouri.

The first phase of the direct shear test is the consolidation stage. The consolidation loading schedule can be entered into the computer program before the start of the test, and then, the constant rate of displacement (shearing speed range of 0.000002 to 0.2 inches per minute) is entered for the second stage of the direct shear

test, which is the shearing stage. The computer program automatically consolidates the soil specimen as per the loading schedule entered. The load applied to the specimen was measured using a GEOTAC load cell with a maximum capacity of 500 lbs. (vertical and horizontal cell). The vertical deformation during the consolidation stage as well as shear stage was measured using a DCDT (an electronic displacement measuring device). The maximum horizontal travel of the machine is +/- 0.5 inches. The machine deflections during the consolidation stage were not taken into consideration.

3.3.1 Test procedure for direct shear test

The shear tests were performed in accordance with the American Society for Testing and Materials (2011), ASTM standard D-3080, "Standard Method for Direct Shear Test on Soils under Consolidated Drained Conditions". A detailed procedure of the test is also included in the UMC CEE Geotechnical Engineering Program (2012) device manual, “Automated Direct Shear System.” The testing program is summarized as follows.

The FGD material was first compacted using standard Proctor energy at the as-received moisture content (38 to 48 percent, dry mass basis). After compaction, 2.5-inch diameter direct shear specimens were trimmed from the center of the 4-inch diameter Proctor specimens for placement in the direct shear device. All the specimens were free to drain in a similar way. The specimens were consolidated under vertical load increments shown in Table 3.1.

Table 3.1 Effective normal stresses and constant rate of deformations employed in the research presented herein.

Consolidation (effective normal stress) Pressure at the start of the Shearing Stage	Consolidation Load Steps			t_{50}	$\dot{\delta}$ Constant Rate of Deformation (NDR)	
	Load Step 1 Final Pressure	Load Step 2 Final Pressure	Load Step 3 Final Pressure			
(psf)	(psf)	(psf)	(psf)	(min)	(in/min)	(mm/min)
500	125	250	500	9	0.000240	0.006
1000	250	500	1000	12	0.000190	0.005
2000	500	1000	2000	11	0.000208	0.005
3000	500	1500	3000	12	0.000190	0.005

After the consolidation stage was completed, the shear stage was started. The constant rate of deformation was calculated using the following formula.

$$\dot{\delta} = \frac{\delta_h peak\ average}{t_f} \tag{3.1}$$

where:

δ_h = horizontal deformation at peak shear was assumed to be 0.11 inch which was the average deformation at peak shear stress from previous drained shear tests on compacted FGD sludge Table 3.2 (Bowders and Day, 2013).

t_f = time of to failure = 50 x t_{50} in minutes (Gibson and Henkel, 1954)

Table 3.2 - Results of previous drained direct shear tests on compacted Flue Gas Desulfurization (FGD) Sludge. Specimens 1 through 7 were tested in 2007/2008. Specimens 8 through 11 were tested in 2013 on FGD (Bowders and Day 2013).

Speci-men No.	Molding water content (%)	Dry Unit Weight (pcf)	Water Content at start of DS (%)	$\dot{\delta}$ Horizontal Deformation Rate (in/min)	Peak Shear Stress (psf)	Effective Normal Stress at peak shear stress (psf)	δpeak Horizontal Deformation at Peak Shear (inch)
1	41.7	69.4	25.2	0.000018	4584	4762	0.17
2	41.0	68.5	25.2	0.000018	1362	1562	0.09
3	32.3	65.1	25.4	0.004370	3882	5224	0.27
4	30.0	66.9	25.3	0.000531	1264	1515	0.07
5	41.0	68.6	25.3	na	na	na	na
6	32.3	66.2	25.3	0.004370	914	9410	0.11
7	30.0	60.9	25.3	0.004370	786	4156	0.23
8	41.0	69.0	41.0	0.0000472	1654	1971	0.12
9	46.0	70.0	46.0	0.0000472	2068	1953	0.10
10	40.0	73.0	40.0	0.0000472	1407	981	0.09
11	47.0	70.0	47.0	0.0000472	854	498	0.07

The shaded area in Table 3.2 includes direct shear tests on compacted FGD sludge in which deformation rates were considered to be high and possibly resulting in undrained conditions during shearing. Only the non-shaded results shown in Table 3.2 were used to calculate an average horizontal deformation at peak shear resistance (δpeak). The average peak horizontal deformation was calculated to be 0.11 inch and was used to calculate the drained shearing deformation rate for the direct shear tests in the research reported herein.

The deformation rate obtained from Equation 3.1 is referred as the *nominal* deformation rate (NDR). The deformation rate was calculated such that complete

drainage of any excess pore water pressure generated by shearing should be dissipated. The deformation rates during shear are given in Table 3.1 for each effective normal stress and are about 0.0002 inches per minute (0.005 mm per minute). Drained direct shear tests were conducted on compacted FGD sludge specimens at four different effective normal stresses (500, 1000, 2000, and 3000 psf) using three different deformation rates: 0.002 inches per minute (NDRI), 0.0002 inches per minute (NDR) and 0.00002 inches per minute (NDRD). Where NDRI is the nominal deformation rate increased by one order of magnitude, NDR is the nominal deformation rate and NDRD is the nominal deformation rate decreased by one order of magnitude.

The reproducibility of direct shear tests was evaluated by performing six (6) tests at the effective normal stress of 2000 psf using the deformation rate of 0.0002 inches per minute (NDR). A total of 16 direct shear tests were performed on specimens of compacted FGD sludge.

3.3.2 Data Interpretation

During the consolidation phase of the direct shear tests, time rate of settlement curves were produced for each load step using the square root of time plotting method (Taylor, 1948). The vertical deformation versus square root of time procedure for determining deflections at 90 percent and 50 percent consolidation and time to 50 percent average degree of consolidation, t_{50} (Taylor, 1948) were used for determining the rate of deformation for the shearing phase of the direct shear test for each effective normal stress. The data collected using the computer software program for a S2220 DigiShear™ Automated Direct Shear System was transferred to an Excel® spreadsheet

for further reduction. The raw data from the Digishear machine were in volts. The detailed equations for calculating the engineering parameters including: shear stress, normal stress, deformation rate, horizontal and vertical stress, and normalized displacement, are included in the Appendix. The calculated parameters were then used to determine the shear strength parameters for the compacted FGD; i.e., effective friction angle, Φ' and effective cohesion, c'.

3.4 Consolidation tests

Two additional consolidation tests were conducted on compacted FGD specimens, one in the incremental load test (ILT) (ASTM D2435/D2435M, 2011) apparatus (Figure A.36) and the other in the Direct Shear System at an effective normal stress of 3000 psf. The load was applied in three steps: $\Delta\sigma$ = 500 psf, $\Delta\sigma$ = 1000 psf and $\Delta\sigma$ = 1500 psf to reach a final effective normal stress of 3000 psf in both tests. These consolidation tests were conducted to observe the consolidation curves to further evaluate the creep behavior of the compacted FGD sludge under constant load. The consolidation curves for these tests are in the Appendix (Figure A.10 to A.15)

3.5 Permeability tests

To study the influence of confining stress and time on hydraulic conductivity, flexible wall permeability tests were conducted in accordance with ASTM-D5084 (2010) on compacted FGD specimens. Two different permeability tests were performed on the compacted FGD specimens of the same size as used in the direct shear tests (2.5-inch diameter and 1-inch height). Permeability test specimens A and B were trimmed from the same compacted FGD specimen to ensure both were at same dry density. During

the permeability test, specimen A was maintained at a constant effective confining stress of 500 psf (3.5 psi) and the hydraulic conductivity was measured at 0, 7, 14 and 28 days after compaction to determine if there were any aging effects on hydraulic conductivity. During the test, an average pore pressure of 2 psi was applied on the specimen with three psi headwater pressure and one psi tail water pressure in both specimens A and B, while maintaining the desired cell pressure. During the waiting period (7 days between k measurements for specimen A), the effective stress at the center of the sample was maintained at 3.5 psi by keeping the headwater and tail water at 2 psi pressures while still maintaining the cell pressure as 5.5 psi. Additional details of the permeability test are given in Tables A.7 and A.8. The hydraulic conductivity of specimen B was measured at six different effective confining stresses. All six measurements were performed on the same day. The test was conducted by changing the cell pressure after each permeability measurement was completed and hydraulic conductivity was determined.

The falling-head, rising-tail equation was used for determining the hydraulic conductivity:

$$k = \frac{a_{in} * a_{out} * L}{(a_{in} + a_{out}) * A * \Delta t} ln(\frac{\Delta h_1}{\Delta h_2}) \quad (3.2)$$

where:

k = hydraulic conductivity, cm/s,

a_{in} = cross sectional area of the reservoir containing the influent/inflow liquid, cm^2,

a_{out} = cross sectional area of the reservoir containing the effluent/outflow liquid, cm^2,

L = length of specimen, cm,

A = cross sectional area of specimen, cm^2,

Δt = interval of time (seconds) over which the flow ΔQ occurs ($t_2 - t_1$),

t_1 = time at the start of permeation trial, date: hr:min:sec,

t_2 = time at the end of permeation trial, date: hr:min:sec,

Δh_1 = head loss across the specimen at t_1, cm of water

Δh_2 = head loss across the specimen at t_2, cm of water

The permeability test was conducted with inflow and outflow reservoirs of equal area, $a_{in} = a_{out}$ and thus Equation 3.2 reduces to

$$k = \frac{a*L}{2*A*\Delta t} ln(\frac{\Delta h_1}{\Delta h_2}) \quad (3.3)$$

where:

a = cross sectional area of the reservoirs containing either influent/inflow or effluent/outflow liquid, cm^2

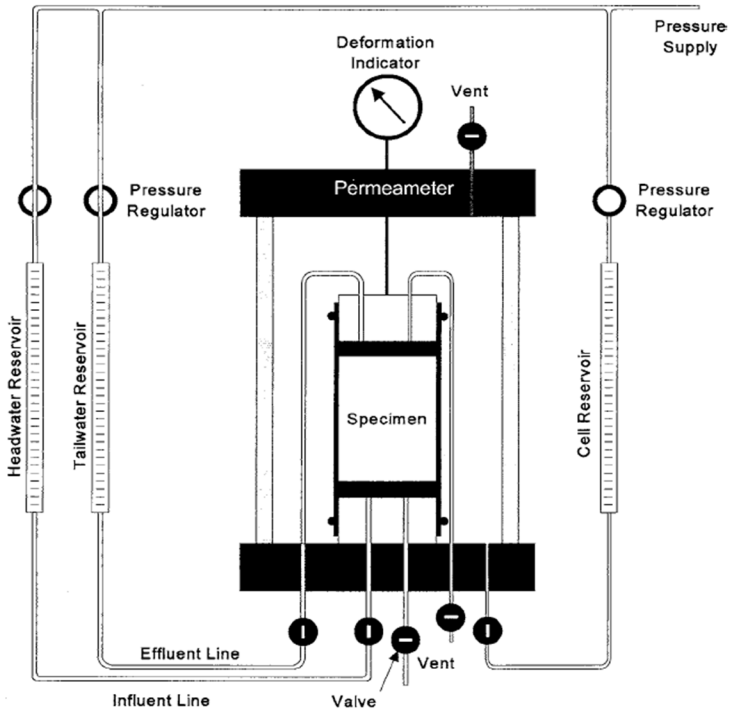

Figure 3.3 Falling head-Rising tail system Method C (ASTM-D5084-10).

Figure 3.4 Permeability apparatus in MU geotechnical engineering laboratory.

3.6 Particle size distribution of the FGD sludge

The particle size distribution (D 422-63, 2007) of soil fraction passing a 75-micron sieve was determined by sedimentation analysis. The pipette method was used in this research, which consists of drawing off samples of soil suspension (10 ml in volume) by means of a pipette from a specified depth (10 cm) at known time intervals after the commencement of sedimentation. Each sample was dried to get the weight of solids per ml (W_d).

The percent finer N can be found using Equation 3.4:

$$\mathrm{N} = \frac{\mathrm{Wd} - w/\mathrm{V}}{\mathrm{Wd/V}} x\ 100 \qquad (3.4)$$

where:

w is the weight of dispersing agent present in total suspension of volume V.

3.7 Summary

A description of the flue gas desulfurization material, testing equipment and procedures used to analyze the FGD sludge were presented in this chapter. Data interpretation used for direct shear testing was also discussed here. Permeability tests, additional consolidation tests and particle size distribution measurement procedures were described in detail in this chapter.

CHAPTER 4: RESULTS

4.1 Introduction

Flue gas desulfurization sludge is a byproduct resulting from clean coal energy technology in which flue gasses are cleaned by removing sulfur and nitrogen compounds. The primary objective of the research presented herein is to quantify the strength behavior of compacted FGD sludge when sheared at different deformation rates in 'drained' direct shear tests. More specifically, determine if a deformation rate of 0.0002 inches per minute results in fully drained behavior of the compacted FGD sludge. Secondly, if necessary estimate a deformation rate that will yield fully drained shear strength parameters. The results of the laboratory testing are presented in this chapter.

4.2 Index properties and dry densities

The FGD sludge used in this research was received in two different batches; both batches were tested individually for their properties and compared with each other for their behavior. Both batches had similar Atterberg limits and as-received moisture contents (first batch LL = 57, w % = 43 and second batch LL = 57, w % = 40). The specific gravity was measured and found to be 2.31.

The dry unit weight of compacted FGD sludge specimens in the present study ranged 69 pcf to 70 pcf(Table 4.1, Column 10) and as-received moisture contents ranged from 38 to 48 percent (Table 4.1, Column 6).

Table 4.1 Shear data for compacted FGD sludge specimens tested in this study.

Specimen No.	Batch No.	Test ENS (psf)	Deformation rate	Deformation rate(in/min)	Water content from trimming (%)	Water content pre-test (%)	Water content post-test (%)	Dry density from ring (pcf)	Dry Density compaction mold (pcf)	δh @peak shear stress (inches)	Peak shear stress (psf)	Peak ENS (psf)
(1)	(2)	(3)	(4)	(5)	(6)	(7)	(8)	(9)	(10)	(11)	(12)	(13)
1	1	3000	NDR	0.000190	41.1	41.0	60.0	na	69.8	0.091	3495	3016
2	2	2000	NDR	0.000208	41.0	Na	52.6	na	72.5	0.082	2512	2024
3	1	1000	NDR	0.000190	48.4	48.6	52.6	75.1	na	0.064	1313	1010
4	1	500	NDR	0.000244	48.0	42.0	53.5	74.4	na	0.063	841	504
5	1	3000	NDRD	0.000019	39.1	39.1	51.9	na	70.7	0.140	4384	3028
6	1	1000	NDRD	0.000019	45.8	38.7	59.7	74.5	na	0.155	2125	1012
7	1	500	NDRD	0.000024	43.7	45.9	60.0	74.3	na	0.110	1070	513
8	1	3000	NDRI	0.001903	41.1	43.8	56.6	na	70.7	0.099	1912	3021
9	1	2000	NDRI	0.002148	42.1	43.3	57.4	75.9	na	0.067	1841	2012
10	1	1000	NDRI	0.001903	42.1	43.8	51.4	75.3	na	0.089	1193	1005
11	1	500	NDRI	0.002444	47.6	45.3	54.6	73.6	na	0.054	575	517
12	1	2000	NDR	0.000208	41.0	42.4	52.9	76.7	na	0.070	1238	2024
13	2	2000	NDR	0.000208	38.3	41.7	47.7	77.8	73.7	0.097	2581	2041
14	2	2000	NDR	0.000208	na	na	na	na	na	0.070	2977	2146
15	2	2000	NDR	0.000208	na	40.9	na	na	na	0.067	1416	2028
16	2	2000	NDR	0.000208	na	46.9	na	na	na	0.064	2124	2005

ENS-Effective normal stress, NDRI-Nominal deformation rate increase 0.002 in/min, NDR-Nominal deformation rate 0.0002 in/min and NDRD-Nominal deformation rate decrease 0.00002 in/min.

4.3 Classification of FGD sludge

4.3.1 Unified Soil Classification system (USCS)

Both batches of FGD sludge had a LL = 57 but were non-plastic (PL = 0) and classified as low-plasticity inorganic silt (ML) in the standard practice for classification of soils for engineering purposes, Unified Soil Classification System (ASTM D2487, 2011). In the plasticity chart, the "A-Line" separates silts from clays. Soils identified as "non-plastic" (NP) are classified as ML. It should be noted here that although the point representing the FGD sludge plots as if an inorganic clay of high plasticity, because the plastic limit is zero, the FGD is identified as ML. The key to distinguishing silts (and FGD sludge) from clays is its response to changes in water content. Clays are relatively strong when dry and can absorb a significant amount of water and remain in a moldable, plastic state. Silts have a lower dry strength than clays and absorb less water. If one attempts to break a dried clump of the soil about the size of a small marble with fingers, clays will be difficult to break, whereas silts will break or crumble easily (Coduto, 2010). Compacted FGD sludge responds similar to silts when dried then compressed, it crumbles like silt.

4.3.2 USDA soil classification system (USDA)

The grain size distribution of the FGD sludge is given in Table 4.2. FGD is classified as Silt Loam (Figure 4.1) in the textural classification chart adapted from the US Department of Agriculture (USDA).

Table 4.2 Grain size distribution of FGD sludge

% Total			% of Silt size particles		% of Sand size particles				
<0.002 mm	0.002-0.05 mm	0.05-2.00 mm	0.002-0.02 mm	0.02-0.05 mm	0.05-0.10 mm	0.10-0.25 mm	0.25-0.50 mm	0.50-1.00 mm	1.00-2.00 mm
Clay size	Silt size	Sand size	Fine	Coarse	V fine	Fine	Medium	Coarse	V Coarse
4.7	59.4	35.9	10.3	49.1	24.3	10.7	0.8	0.1	0.0

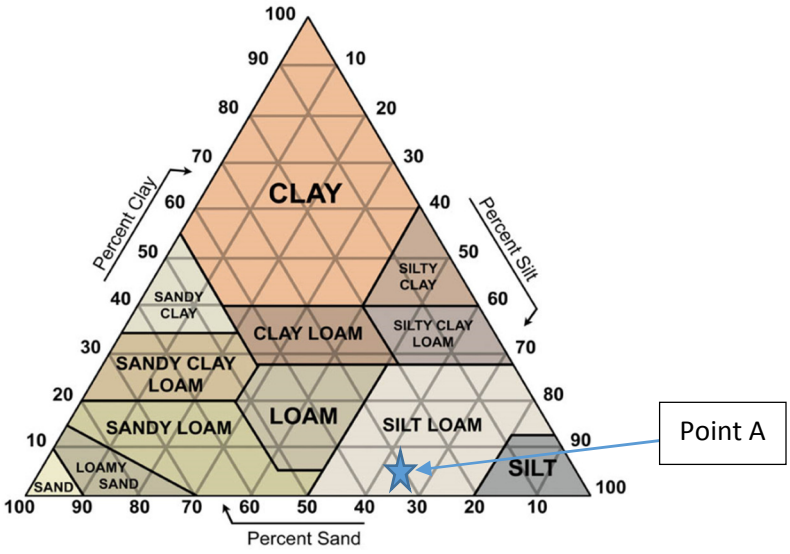

Figure 4.1 USDA soil classification triangle. Point A in the chart represents the data in Table 4.1 for FGD sludge (www.soilsensor.com).

4.4 Consolidation and Shear behavior of FGD sludge

The results of the drained direct shear tests on compacted FGD sludge are presented in this section. The consolidation curves (Figure 4.2(a)-(c)) for each specimen are shown first followed by the shear stress versus horizontal displacement plots (Figures 4.3(a) - 4.5(a)). Vertical deformation (from vertical actuator) during the shearing stage of direct shear test at different effective normal stresses (psf) and horizontal displacement for three deformation rates are shown in Figures 4.3 (b) – 4.5(b). The moisture contents of the specimen pre-and post-test (Table 4.1, Column 6 and 8 respectively), deformation rates (Table 4.1, Column 5) along with dry densities (Table 4.1, Column 9 and 10), peak horizontal deformation (Table 4.1, Column 11) and peak shear stresses (Table 4.1, Column 12) are listed in Table 4.1. It should be noted here that the DCDT vertical displacement gauge was not always trustworthy, so the vertical displacement of the actuator is used to plot Figures 4.3 (b) – 4.5(b).

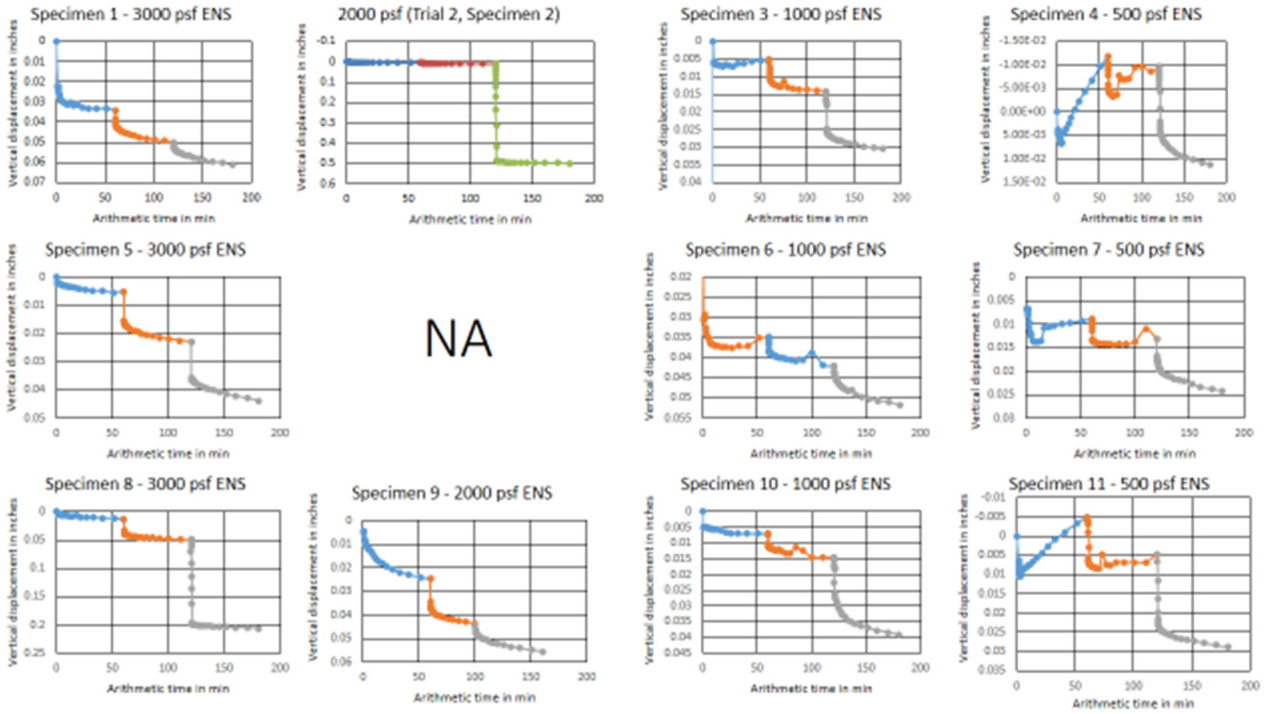

Figure 4.2 (a) Consolidation curves (arithmetic time) for compacted FGD sludge. The first row consist of specimens sheared at NDR, the second row consist of specimens sheared at NDRD and the third row consist of specimens sheared at NDRI.

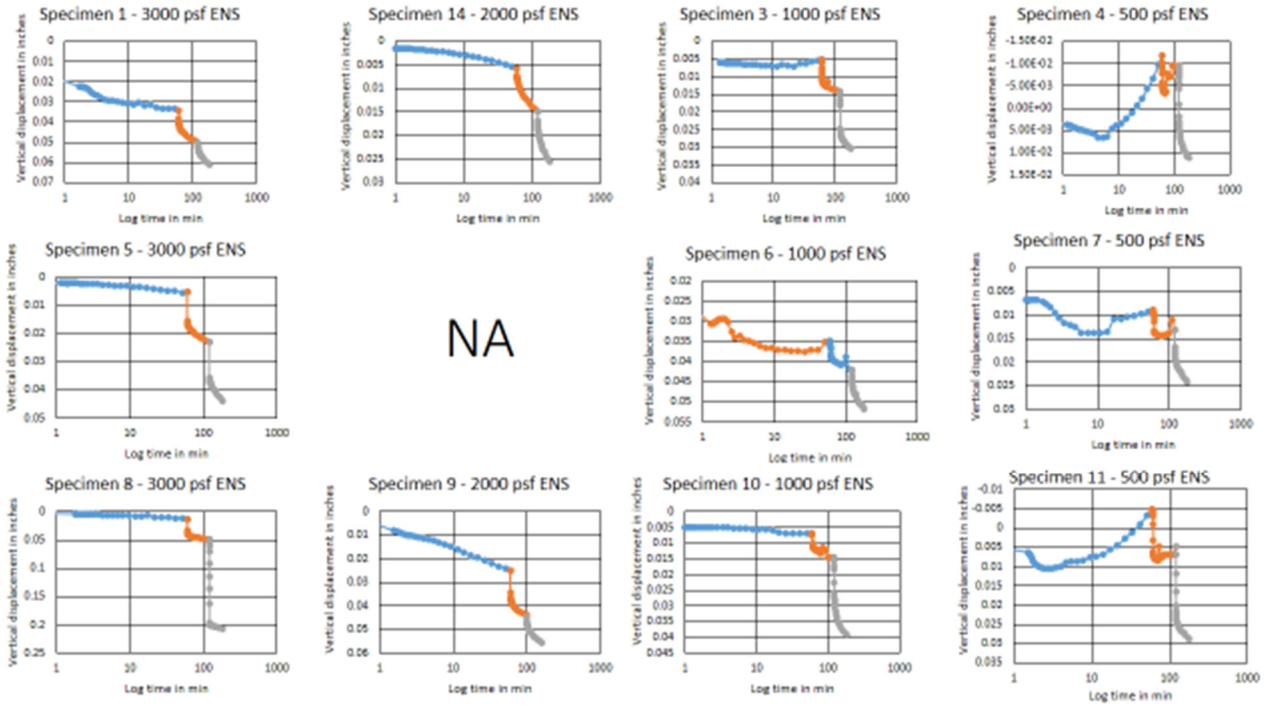

Figure 4.2 (b) Consolidation curves (Log time) for compacted FGD sludge. The first row consist of specimens sheared at NDR, the second row consist of specimens sheared at NDRD and the third row consist of specimens sheared at NDRI.

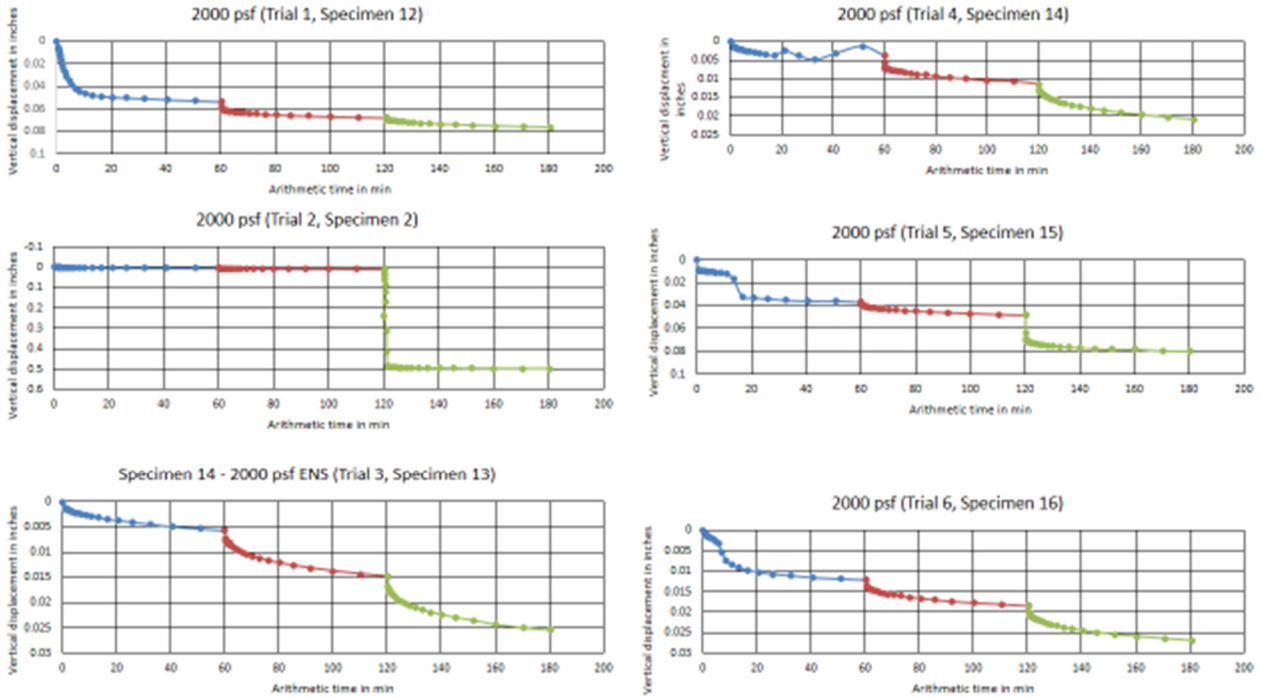

Figure 4.2 (c) Consolidation curves (arithmetic time) for compacted FGD sludge. All the specimens sheared at NDR.

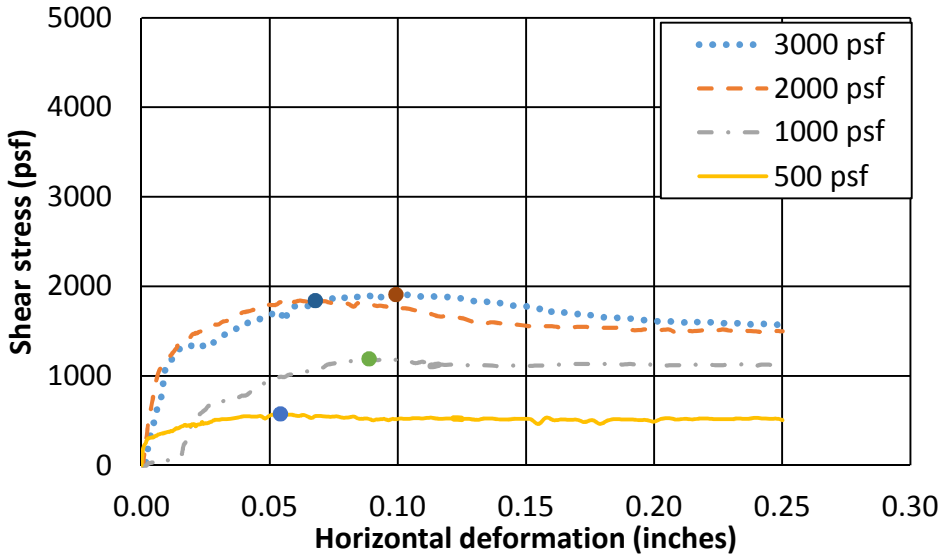

Figure 4.3 (a) Stress versus horizontal displacement for compacted FGD sludge and peak points for different effective normal stresses (psf) at a horizontal displacement rate of 0.002 inches per minute (0.05 mm/min) (NDRI).

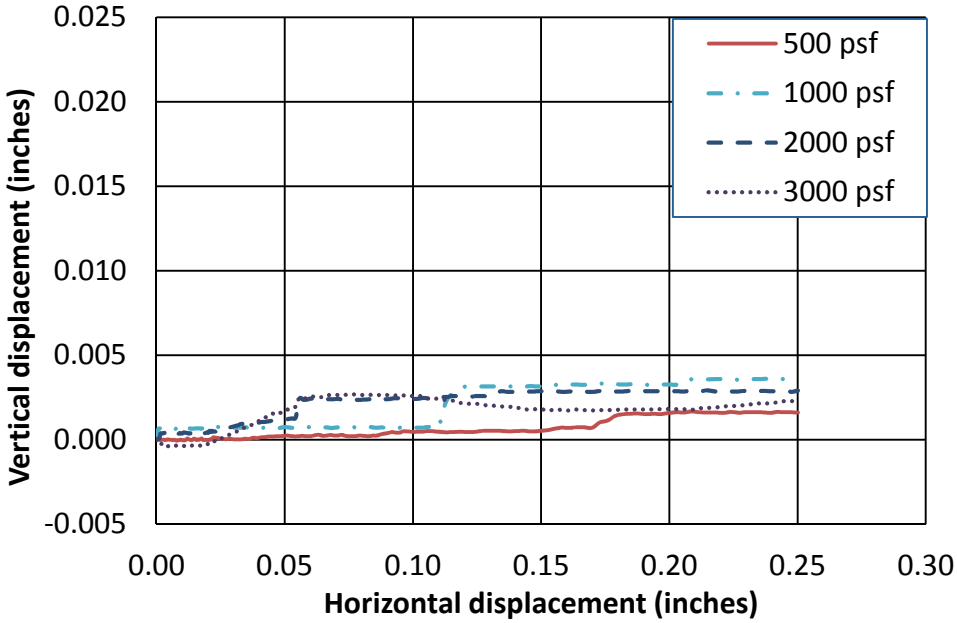

Figure 4.3 (b) Vertical deformation (from vertical actuator) during the shearing stage of direct shear test for different effective normal stresses (psf) at a horizontal displacement rate of 0.002 inches per minute (0.05 mm/min) (NDRI).

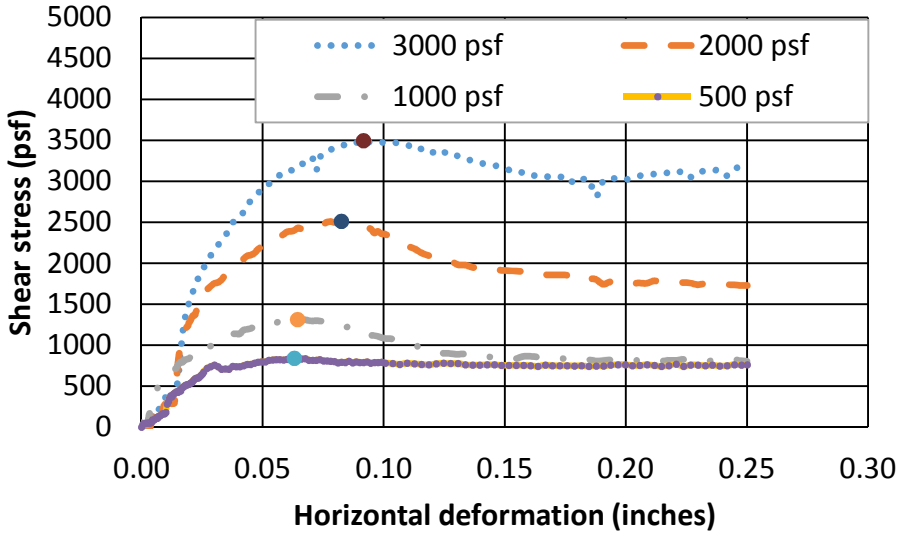

Figure 4.4 (a) Stress versus horizontal displacement for compacted FGD sludge and peak points for different effective normal stresses (psf) at a horizontal displacement rate of 0.0002 inches per minute (0.005 mm/min) (NDR).

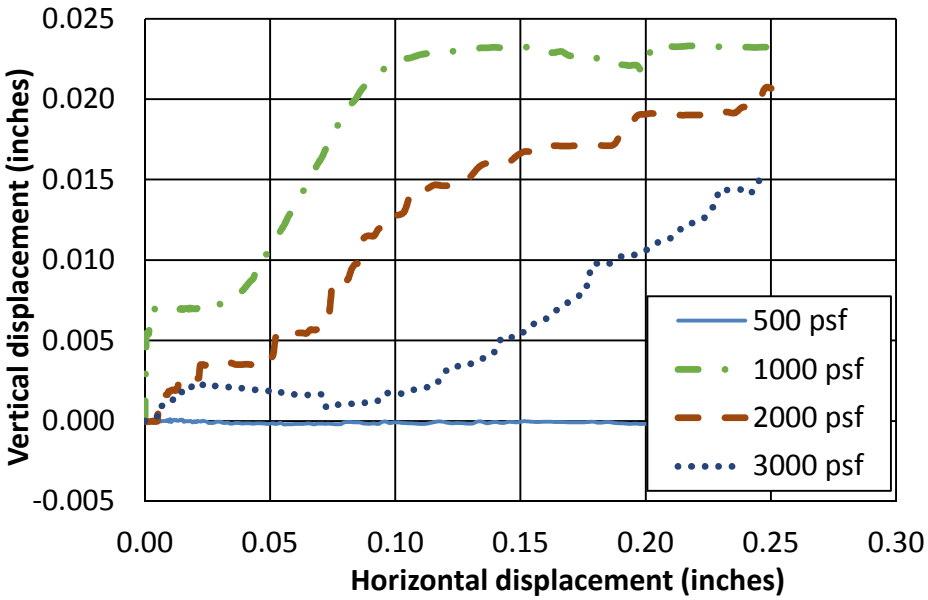

Figure 4.4 (b) Vertical deformation (from vertical actuator) during the shearing stage of direct shear test for different effective normal stresses (psf) at a horizontal displacement rate of 0.0002 inches per minute (0.005 mm/min) (NDR).

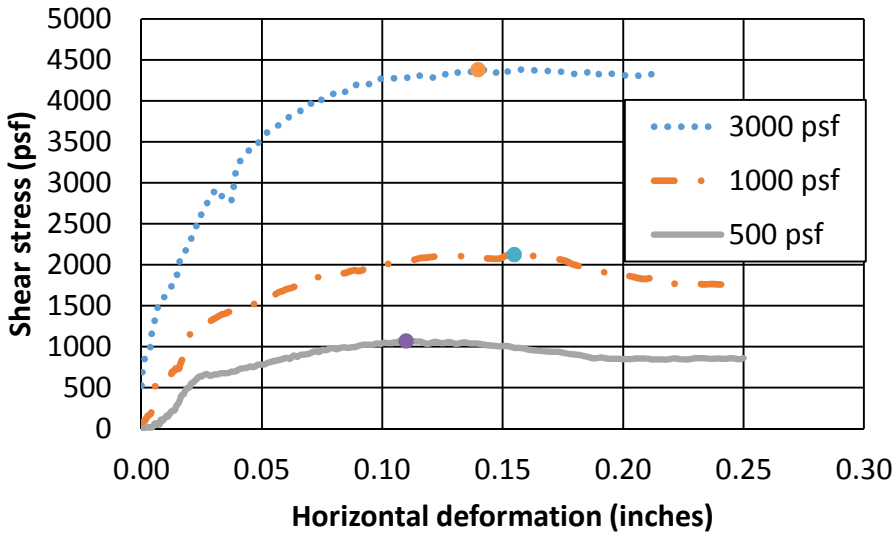

Figure 4.5 (a) Stress versus horizontal displacement for compacted FGD sludge and peak points for different effective normal stresses (psf) at a horizontal displacement rate of 0.00002 inches per minute (0.0005 mm/min) (NDRD).

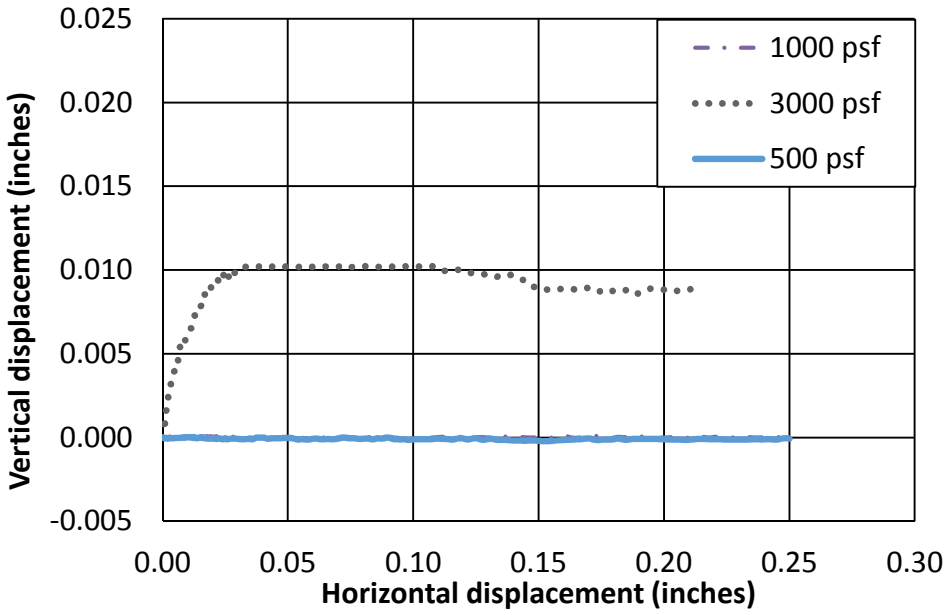

Figure 4.5 (b) Vertical deformation (from vertical actuator) during the shearing stage of direct shear test for different effective normal stresses (psf) at a horizontal displacement rate of 0.00002 inches per minute (0.0005 mm/min) (NDRD).

4.5 Permeability

The permeability test on specimen A was done to study aging effects on hydraulic conductivity of compacted FGD sludge and specimen B was to investigate impact of different effective normal stresses on hydraulic conductivity of compacted FGD sludge. The hydraulic conductivity, of specimen B varied from 2.01E-05 to 8.51E-06 cm/s (Figure 4.6), as the effective confining stress was increased from 500 psf to 6000 psf. Detailed results of the permeability test on specimen A and B are provided in Table A.7 and A.8 (Appendix).

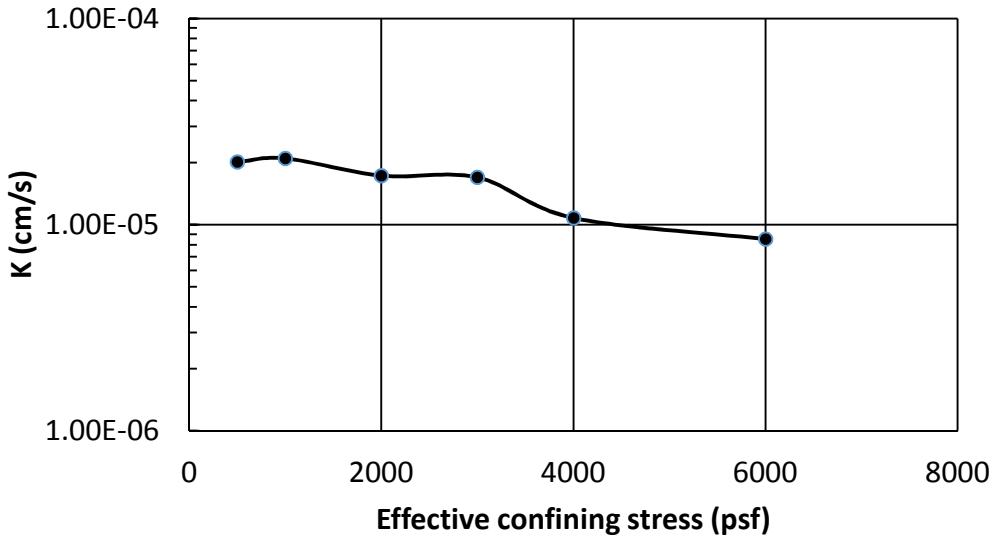

Figure 4.6 Hydraulic conductivity (k) versus confining effective stress for compacted FGD specimen, B.

4.6 Summary

Results of index properties, dry densities and particle size analysis of compacted FGD sludge were presented in this chapter followed by consolidation and shear behavior. There was a gain in strength with decreasing deformation rates.

CHAPTER 5: DISCUSSION

5.1 Introduction

The results presented in Chapter 4 are discussed in this chapter. Analyses of the data were performed using two different approaches for calculating the time to failure of the shearing specimen. The first approach consisted of Gibson and Henkel (1954). The second approach consisted of measuring hydraulic conductivity in the flexible wall permeability test, taking the coefficient of volume compressibility from last load increment of consolidation and then calculating a new coefficient of consolidation of compacted FGD sludge (Kaniraj and Gayathri,2004). The coefficient of consolidation is used to estimate the time to failure during shear for a compacted FGD specimen. Several possible factors resulting in strength increase with decreasing deformation rates are also discussed.

5.2 Index properties and dry densities

Krizek et al. (1987) Atterberg limit tests indicated a liquid limit ranging from 44 percent to 65 percent along with a plasticity index as low as 8 to 17. In the FGD tested for the presented thesis LL = 57 and PL = 0. The results are in agreement with the findings of Krizek et al (1987). Bowders and Day (2013) reported dry unit weights from 66 pcf to 71 pcf and as-received moisture contents from 41 to 57 percent.

Figure 5.1 presents comparison of dry unit weight versus molding moisture content for compacted FGD sludge from the present investigation to various investigators working on FGD (Freeman 2013). The dry unit weights and as-received moisture contents of compacted FGD sludge in the present study (Table 4.1 Column 10 and 6 respectively, Figure 5.1, Khan 2013) are comparable to those by past investigators.

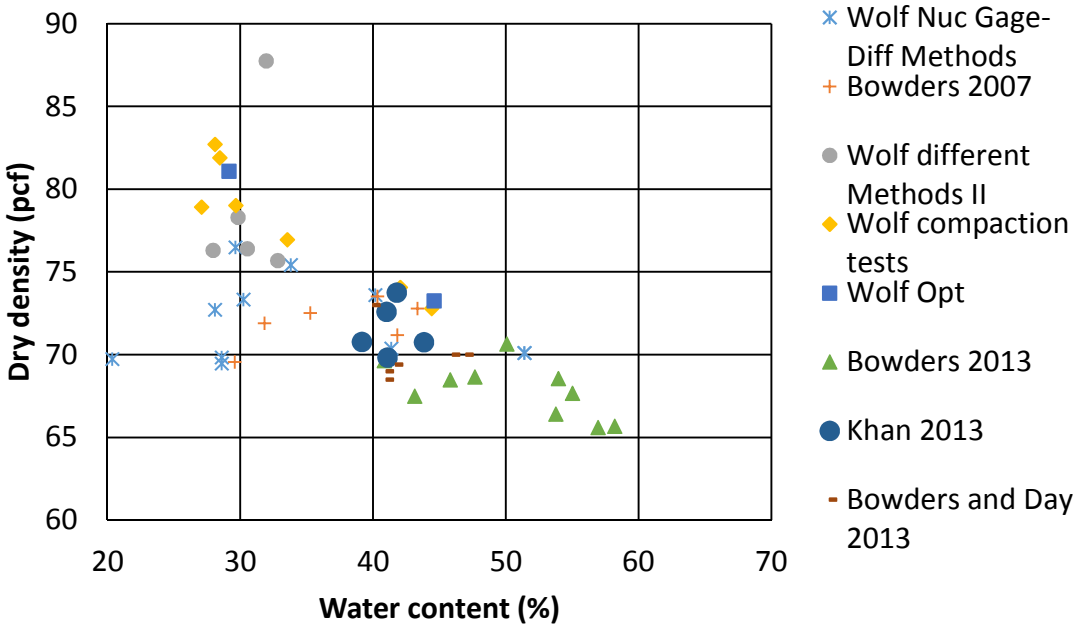

Figure 5.1 Comparison of dry unit weight versus molding moisture content for compacted FGD sludge from this investigation and by various investigators (Freeman 2013).

5.3 Classification of FGD sludge

Krizek et al. 1987 observed that the particle sizes of FGD sludge are rather uniform and lie primarily in the range of silt and fine sand. The FGD sludge used for the present research did not include fly ash or other coal combustion products and the particle sizes are in the range of (0.002 mm to 2 mm) silt and fine sand (Table 4.2). Therefore it can be expected that the FGD sludge specimen behaves like a silt or sand when considering the permeability.

5.4 Shear behavior of FGD sludge

The FGD sludge is classified as low plasticity inorganic silt (ML) in the Unified Soil Classification System thus shear strength is expected to be a result of inter-particle friction rather than from cohesion. The peak shear stress (Figures 4.3(a) - 4.5(a)) occurs at about 0.1 inches of horizontal displacement regardless of the displacement rate. It is also evident that as the displacement rate decreases, the peak shear strength increases (Figure 5.2).

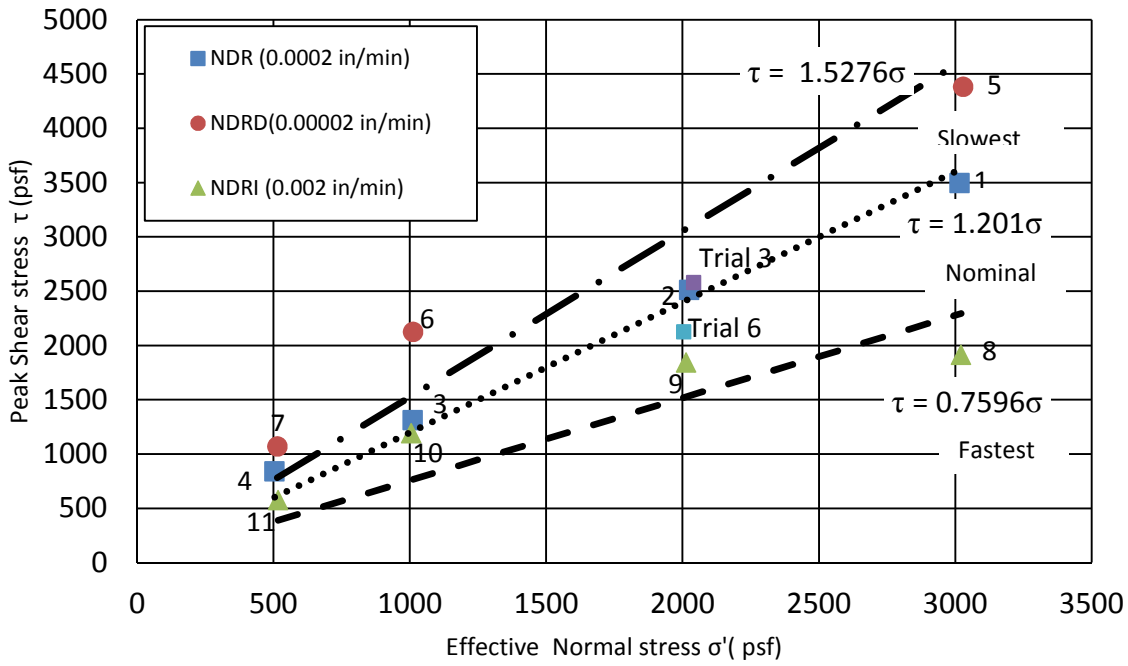

Figure 5.2 Failure envelopes for direct shear results using three different deformation rates: NDRI = 0.002 in/min (Specimens 8 to 11), NDR = 0.0002 in/min (Specimens 1 to 4) and NDRD = 0.00002 in/min (Specimens 5 to 7) and forcing envelope through the origin, i.e. zero cohesion intercept. Specimen numbers are from Table 4.1 for shear data.

The resulting internal friction angles of the compacted FGD (assuming no cohesion, c' = 0) are as follows: NDRI (ϕ' = 37°), NDR (ϕ' = 46°) and NDRD (ϕ' = 57°) (Figure 5.2). It was expected that the deformation shear rate calculated from the consolidation data would be slow enough for excess pore pressures to remain zero during shear. If such is the case, then the peak shear stresses for specimens at a given effective normal stress should yield the same magnitude of peak shear stress regardless of the rate of deformation; however, this behavior is not seen here (Figure 5.2). Rather, at each effective normal stress, the peak shear stress was greatest for the slowest rate of deformation, and smallest for the fastest rate. Such behavior can indicate that deformation rates may not have been slow enough to allow complete drainage of excess pore pressures resulting in shear parameters that are not fully drained.

The peak shear strength and percentage changes in peak shear stress for each effective normal stress at different deformation rates is calculated with respect to peak shear stress measured for a deformation rate of 0.002 in/min (NDRI) (Table 5.1). Observing failure envelopes in Figure 5.2 and values shown in Table 5.1, it can be seen that decreasing the deformation rate by an order of magnitude (0.002 to 0.0002 in/min) resulted in an increase in peak shear stress by 10 to 80 percent. A further order of magnitude decrease in the deformation rate to 0.00002 in/min resulted in an 80 to 130 percent increase in the peak shear stress, relative to the fastest deformation rate (0.002 in/min). The differences in the peak stresses were less at smaller effective normal stresses of 500 and 1000 psf; however, the difference became greater at higher effective normal stresses 2000 and 3000 psf.

Table 5.1 Peak shear strength and percentage increase in peak shear strength with respect to shear strength at 0.002 in/min deformation rate (NDRI).

ENS (psf)	3000	2000	1000	500
NDRI (0.002 in/min)	1912 psf (0 %)	1841 psf (0 %)	1193 psf (0 %)	575 psf (0 %)
NDR (0.0002 in/min)	3495 psf (+83 %)	2512 psf (+31 %)	1313 psf (+10 %)	841 psf (+46 %)
NDRD (0.00002 in/min)	4384 psf (+129%)	NA	2125 psf (+78 %)	1070 psf (+86 %)

ENS-Effective normal stress, NDR-Nominal deformation rate, NDRI-Nominal deformation rate increase, and NDRD-Nominal deformation rate decrease.

The question now arises as to whether the deformation rates were slow enough to allow complete dissipation of all excess pore water pressure generated during shear, or, are there other mechanisms resulting in higher strength (in these drained shear tests) as deformation rate is decreased.

Other possible mechanisms could be aging effects, creep or structural water in FGD sludge. The possible factors contributing to increase of strength in compacted FGD sludge with decreasing deformation rate are discussed in the following section.

5.5 Factors contributing to gain of strength in FGD sludge with slow deformation rate

5.5.1 Pore Pressures

The first item to note is that all of the specimens in the direct shear tests dilated (expanded vertically) during shearing (Figure 4.3 (b), 4.4 (b) and 4.5(b)). The specimens were submerged in a water bath and open to drainage at the top and bottom of the shear box during shearing. If the specimens are fully drained (porewater pressures generated due to shearing dissipate as soon as they are generated and do not build up), then there should be no excess porewater pressures in the specimen. If the specimen is undrained, or partially drained, then in the case of dilation one would expect the excess porewater pressures to be less or even negative, thus resulting in a higher strength with increasing shear rate. The opposite behavior was seen in the data in Figure 5.2. The faster the shear rate the lower the strength - a case for positive pore water pressures, which are not likely given the specimens dilated.

The FGD sludge is a non-plastic silt with a hydraulic conductivity of 1.5 x 10^{-4} to 2.5 x 10^{-4} cm/s (Bowders and Coffman, 2007), whereas the hydraulic conductivity of soft clay is 10^{-6} to 10^{-8} cm/s. Thus, the compacted FGD sludge specimens would be expected to drain faster than soft clays such as those shown by Gibson and Henkel (1954) Figures 2.6 to 2.9.

The shearing time to reach failure, t_f, in the present study was based on the coefficient of consolidation, c_v, which was calculated from the last loading increment during the consolidation stage of direct shear test using the $50*t_{50}$ approach of Gibson and Henkel (1954). For faster draining (higher hydraulic conductivity) soils, time to failure, t_f was expected to be less than that for soils with lower hydraulic conductivities. Using the same value of average degree for consolidation, U_f from Gibson and Henkel's (1954) theory to calculate times to failure for the FGD sludge should have assured that the FGD material reached complete drainage (U_f > 95 %, no excess porewater pressures) at the time of failure (peak shear stress). However, even though Gibson and Henkel's (1954) procedure for calculating t_f was used there was still an apparent deformation rate effect on the strength of the compacted FGD sludge indicating either the specimens were not draining or other mechanisms are at play.

Another procedure to check on the time to failure (t_f) for fully drained conditions was suggested by Kaniraj and Gayathri (2004). The procedure consists of measuring the hydraulic conductivity, k, and the coefficient of volume compressibility, m_v for the final consolidation load increment before shearing and using them to calculate c_v (Equation 2.19).

$$k = c_v * m_v * \gamma_w \tag{2.19}$$

where:

k = hydraulic conductivity

m_v = slope of Є vs σ' curve till the end of primary consolidation = coefficient of volume compressibility = $a_v/(1+e_i)$

e_i = initial void ratio over the effective stress change $d\sigma'$

$a_v = de/d\sigma'$

de = change in void ratio over change in effective stress $d\sigma'$

γ_w= unit weight of water

c_v = coefficient of consolidation

In the present study, consolidation tests for load increments of 250, 500, 1000, and 2000 psf were performed to obtain m_v. The resulting m_v's are given in Table 5.2. Hydraulic conductivity was measured at different effective normal stresses (Figure 4.6, specimen B) and are used in the calculation of c_v.

Table 5.2 Calculated coefficient of consolidation, c_v, using measured hydraulic conductivity, k, and measured coefficient of volume compressibility, m_v.

Final Consol Stress σ' (psf)	Load increment Δσ' (psf)	Initial void ratio e_0	Void ratio at end of primary consolidation e_f	Change in void ratio Δe	Coeff of vol. Compress m_v = Δe/ Δσ' (psf^{-1})	Hydraulic conductivity (specimen B) k (cm/s)	Coeff of consol, c_v (cm^2/s)
500	250	1.000	0.964	0.036	7.309E-05	2.01E-05	0.13
1000	500	0.897	0.869	0.027	2.936E-05	2.10E-05	0.35
2000	1000	0.829	0.815	0.014	7.677E-06	1.73E-05	1.10
3000	1500	0.831	0.819	0.011	4.355E-06	1.70E-05	1.90

The calculated coefficients of consolidation c_v varied from 0.13 to 1.9 cm^2/s. The results shown in Table 5.2 indicate that both the hydraulic conductivity and coefficient of consolidation of the compacted FGD sludge are comparable to those of non-plastic silts (Kaniraj and Gayathri, 2004).

The calculated c_v's were then used in Equation 2.12 (Gibson and Henkel, 1954) to calculate time to reach peak shear.

$$t_f = \frac{H_S^2}{2c_v(1-U_f)} \quad (2.12)$$

where:

H_S = the average drainage distance during shear; sub-s denotes the shearing stage, and for the case of top and bottom drainage, H_S is half of the thickness of the specimen

c_v = the coefficient of consolidation

t_f = the time to reach peak shear

U_f = average degree of consolidation

The t_f was calculated for an average degree of consolidation (U) of 99 percent.

From Equation 2.12, time to U_f = 99 % is about t_f = 43 seconds ≈ 1 minute to reach peak drained strength. Given that the horizontal deformation at peak shear stress is taken to be 0.1 inch, the resulting deformation rate, $\dot{\delta}$, is 0.11 in/min (Equation 3.1) for an effective normal stress of 3000 psf. The variation in hydraulic conductivity, with variation in effective normal stress will result in different c_v's and times to failure t_f; however, the times to failure remain small (Table 5.3). Any rate slower than 0.11 in/min for 3000 psf effective normal stress should yield drained shear strength parameters for the compacted FGD sludge. Table 5.3 shows the times to failure and resulting deformation rates for all direct shear tests used in the present study. The measured hydraulic conductivity used to calculate c_v, was at 99 percent average degree of consolidation for that particular effective stress. Calculated deformation rates are based on measured hydraulic conductivity, k (specimen B), coefficient of volume

compressibility, m_v, used in Equation 2.12 to get time to shear failure, t_f and for an assumed δ_h peak = 0.11 inch.

The nominal deformation rate NDR was calculated using the t_f from Gibson and Henkel (1954) ($50*t_{50}$) and the assumed δ_h peak = 0.11 inch. The t_{50} was calculated from the final loading in the consolidation stage for each specimen in the direct shear test.

Table 5.3 Comparison of the shear rate used in the present study with the shear rate from measured k (Specimen B) and m_v (Table 5.2).

Specimen no.(Table 4.2)	Effective normal stress (psf)	Time to reach failure (sec ≈ min)	Calculated Drained deformation rate (in/min)(Kaniraj and Gayathri, 2004)	Deformation rates actually used in the present study (Gibson and Henkel method, 1954)		
				NDRI (in/min) fastest	NDR (in/min) nominal	NDRD (in/min) slowest
1	3000	43 ≈ 1	0.1100	0.0019	0.00019	0.000019
13	2000	293 ≈ 5	0.0220	0.0021	0.00020	na
3	1000	923 ≈ 16	0.0068	0.0019	0.00019	0.000019
4	500	1216 ≈ 21	0.0052	0.0024	0.00024	0.000024

The peak deformation of compacted FGD sludge (0.11 inches) is in the range of that for dense sands (Table 2.1). It is observed from Table 5.3 that the slowest required deformation rate 0.00523 in/min to measure drained shear behavior is three times faster than the fastest deformation rate 0.0019 in/min used in the present research. It is concluded that all the deformation rates used in the present research should result in fully drained behavior. The increase in strength (friction angle, Figure 5.2) with decrease in deformation rate is not due to drainage of excess porewater pressure.

5.5.2 Creep behavior of FGD sludge

Since excess pore pressure dissipation was not the reason for the gain in strength as shear rate decreased in the drained direct shear tests then there must be some other reasons for the observed behavior. It is possible that the increase in strength with

decreasing deformation rate is due to mechanisms which result in strength gain with time (aging) (Mitchell, 1986). One possible mechanism is strain hardening, or densification, due to vertical compression (creep) densification under constant vertical stress. Creep is defined here as deformation after the end of primary consolidation (t_{eop}) under a constant load. Although the consolidation curves from the incremental load test (ILT) (Appendix, Figures A.10 to A.12) were not used for calculations (there was extrusion of the specimen from the consolidation ring), the time-settlement curves (Figures A.10 to A.12) were similar, with respect to creep behavior, to the curves obtained during the consolidation stage of the direct shear tests (Appendix, Figures A.13 to A..15). The time-settlement curve in Figure 5.3 (Appendix, Figure A.1 to A.17) shows the typical shape of the curves. Secondary consolidation behavior as typically seen for clays (slope of time-settlement curve dramatically decreases after the end of primary consolidation) is not seen in the compacted FGD sludge. In fact, the primary consolidation occurred in less than 20 minutes and in many specimens in less than one or two minutes in the present study. Moghal and Sivapullaiah (2011) noted that the primary consolidation of the compacted FGD occurs within 30 minutes. Krizek et al. (1987) observed the completion of primary consolidation for FGD sludge usually occurred within the first minute after application of a load increment (Table 5.3). Most of the vertical deformation observed during the consolidation tests performed in the present study may be attributed to creep or plastic deformations of the skeleton rather than primary consolidation as a result of dissipation of excess pore water pressure.

There is a volume decrease in inundated FGD specimens under a constant stress with time. This behavior is quantified in Table 5.4.

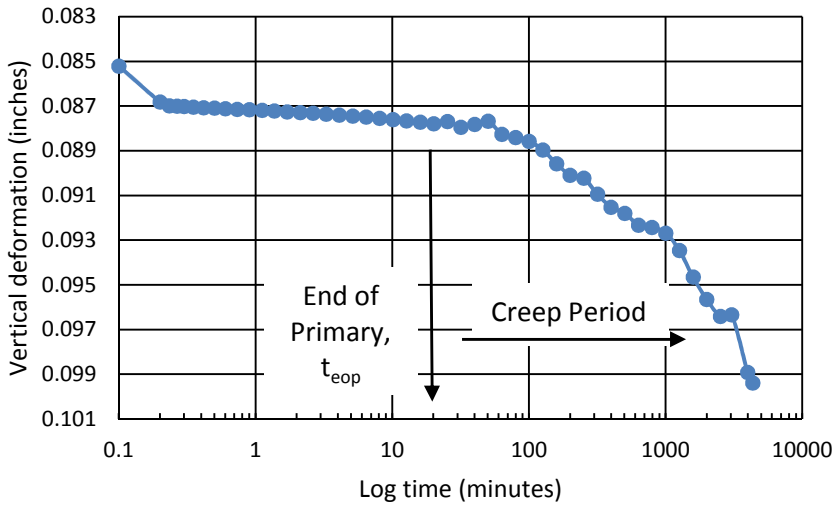

Figure 5.3 Typical FGD sludge consolidation curve for a compacted specimen under load increment from 1500 psf to 3000 psf (End of primary consolidation, t_{eop} = 20 min, after this time, specimen is considered to be undergoing creep).

Creep refers to vertical deformation under a constant stress. The creep rate is a function of the magnitude of stress. As shown in Table 5.4, at higher stresses, the creep deformation rate is slightly greater compared to that at lower stresses. Specimens on which the constant stress was held for less than about 100 minutes showed a constant creep rate (Appendix, Figures A.1 through A.17). While specimens on which the constant stress was held for more than about 1600 minutes exhibited a decreased creep rate with time (Appendix Figures A.10, A.13 and A.14). One would expect the creep rate to decrease over time, so it is possible that the specimens exhibiting constant creep rates were simply not monitored for a sufficient length of time.

Observing the failure envelopes in Figure 5.2, it can be seen that the difference in the peak stresses is less at smaller effective normal stresses (500 psf and 1000 psf) compared to the higher effective normal stresses (2000 psf and 3000 psf). A possible reason for this behavior may be that at higher normal stresses, creep deformation is making the specimen more dense resulting in higher strength (strain hardening). Slower shear rates lead to longer duration of testing and thus a greater amount of creep, which could lead to more strain-hardening for the direct shear tests performed at slower shearing rates. However, all the specimens exhibited either dilation or no vertical displacement during shear, thus the creep (strain hardening) factor is not likely to be a cause of increase in strength with decreasing shear rate.

Table 5.4 Creep rates based on compressibility data for compacted FGD sludge

Shear Data				Consolidation Data						
Specimen no.	Nominal Vertical Effective Stress (psf)	Deformation Rate Type	Deform. Rate (in/min)	Load Increment Δσ (psf)	Vertical Reading at End of Primary Consolidation, t_{eop} (inches)	Vertical Reading at End of Creep Period (inches)	Vertical Creep Deformation for Final Load Increment Δσ (inches) (7)-(6)	Time to Reach End of Primary Consol, t_{eop} (min)	Time from t_{eop} Consol to tcreep (min)	Vertical Creep Deformation Rate (in/min) (8)/(10)
(1)	(2)	(3)	(4)	(5)	(6)	(7)	(8)	(9)	(10)	(11)
1	3000	NDR	0.000190	1500	0.0577	0.0613	$3.6x10^{-3}$	21	40	$9.0x10^{-5}$
2	2000	NDR	0.000208	1000	0.4961	0.4986	$2.5x10^{-3}$	21	40	$6.2x10^{-5}$
3	1000	NDR	0.000190	500	0.0285	0.0305	$2.0x10^{-3}$	21	40	$5.0x10^{-5}$
4	500	NDR	0.000244	250	0.0087	0.0111	$2.4x10^{-3}$	18	42	$5.7x10^{-5}$
5	3000	NDRD	0.000019	1500	0.0402	0.0437	$3.5x10^{-3}$	21	40	$8.7x10^{-5}$
6	1000	NDRD	0.000019	500	0.0491	0.0518	$2.7x10^{-3}$	21	40	$6.7x10^{-5}$
7	500	NDRD	0.000024	250	0.0219	0.0242	$2.3x10^{-3}$	21	40	$5.7x10^{-5}$
8	3000	NDRI	0.001903	1500	0.2029	0.2061	$3.2x10^{-3}$	21	40	$8.0x10^{-5}$
9	2000	NDRI	0.002148	1000	0.0523	0.0555	$3.2x10^{-3}$	21	40	$8.0x10^{-5}$
10	1000	NDRI	0.001903	500	0.0356	0.0390	$3.4x10^{-3}$	21	40	$8.5x10^{-5}$
11	500	NDRI	0.002444	250	0.0266	0.0288	$2.2x10^{-3}$	21	40	$5.5x10^{-5}$
12	2000	NDR	0.000208	1000	0.0224	0.0254	$3.0x10^{-3}$	21	40	$7.5x10^{-5}$
13	2000	NDR	0.000208	1000	0.0180	0.0208	$2.8x10^{-3}$	21	40	$7.0x10^{-5}$
14	2000	NDR	0.000208	1000	0.0770	0.0797	$2.7x10^{-3}$	21	40	$6.7x10^{-5}$
15	2000	NDR	0.000208	1000	0.0245	0.0269	$2.4x10^{-3}$	21	40	$6.0x10^{-5}$
-	4000	na	na	2000	0.0060	0.0136	$7.6 x10^{-3}$	20	341	$2.2x10^{-5}$
-	6000	na	na	3000	0.0025	0.0225	$2.0 x10^{-2}$	20	3116	$6.4x10^{-6}$
-	6000	na	na	3000	0.0020	0.0160	$1.4 x10^{-2}$	20	1205	$1.1x10^{-5}$
-	6000	na	na	3000	0.0010	0.0090	$8.0 x10^{-3}$	20	1580	$5.1x10^{-6}$

The 4000 and 6000 psf ENS data are from Zhang (2013)

5.5.3 Effect of pozzolanic reactions on consolidation and shear strength characteristics of FGD sludge.

The term pozzolan refers to a siliceous or siliceous and aluminous material which, in itself, possesses little or no cementitious value but which will, in finely divided form and in the presence of water, react chemically with calcium hydroxide at ordinary temperature to form compounds possessing cementitious properties (ASTM C125). Pozzolan basically refers to a material's capability of reacting with calcium hydroxide and water. The rate of the pozzolanic reaction is dependent on the intrinsic characteristics of the pozzolan such as the specific surface area, the chemical composition and the active phase content.

It is possible that the FGD in the present study FGD may be pozzolanic thus resulting in an increase in strength with time as the pozzolans react. Slower shearing rates would allow longer times for a pozzolanic reaction to occur and could result in higher shear strengths. FGD sludge develops strength (Moghal and Sivapullaiah, 2011) due to pozzolanic behavior when mixed with siliceous/aluminous material; e.g., fly ash. Although primary consolidation is completed very quickly, maybe even within a minute (Krizek et al. 1987, Pandian and Balasubramonian, 1999) to 20 minutes (Kaniraj and Gayathri, 2004) with pozzolanic behavior, the duration of the load increment may not reflect the true nature of consolidation behavior when tested with the conventional approach of 24-hour load in the consolidation test as the pozzolan develops sufficient strength even during this period (Moghal and Sivapullaiah, 2011). In the present work, for most of the direct shear specimens, the final consolidation stage lasted for 60 minutes to ensure reaching the end of primary consolidation. According to Moghal and

Sivapullaiah (2011) one hour can be assumed to be insufficient for development of strength due to pozzolanic reactions. However, shear durations ranged from a day to several days during which pozzolanic reactions could possibly contribute to strength increase.

It should be noted from Figures 4.3 (a), 4.4 (a) and 4.5 (a) that the stress versus horizontal deformation curves for NDRI (fast shear rate), NDR (moderate shear rate) and NDRD (slow shear rate) are different in shape as the duration of the test increases. The initial slopes of the stress versus horizontal displacement curves becomes steeper and horizontal deformation at peak shear stress increases as the rate of deformation decreases and the length of the test increases. This may indicate that the pozzolanic reactions are occurring at different rates at various times during the test. The duration and dates of all the direct shear tests are given in Table 5.5.

A change in hydraulic conductivity with time might indicate a pozzolanic reaction occurring in the compacted FGD. A permeability test was performed on a compacted specimen of FGD sludge to obtain hydraulic conductivity (k) versus time behavior. The hydraulic conductivities varied from 2.3E-05 to 9.4E-06 cm/s over 28 days under an effective confining stress of 500 psf (Figure 5.4). The range of measured hydraulic conductivities is in the typical range of the hydraulic conductivity of non-plastic silts (Kaniraj and Gayathri, 2004). The general trend is a reduction in hydraulic conductivity over time with a maximum reduction of about 50 percent (factor of two) (Figure 5.5). Based on the single permeability test (specimen A), there was no appreciable change in

hydraulic conductivity over time and thus no evidence of a pozzolanic or other time-rate (aging) reaction in the compacted FGD sludge.

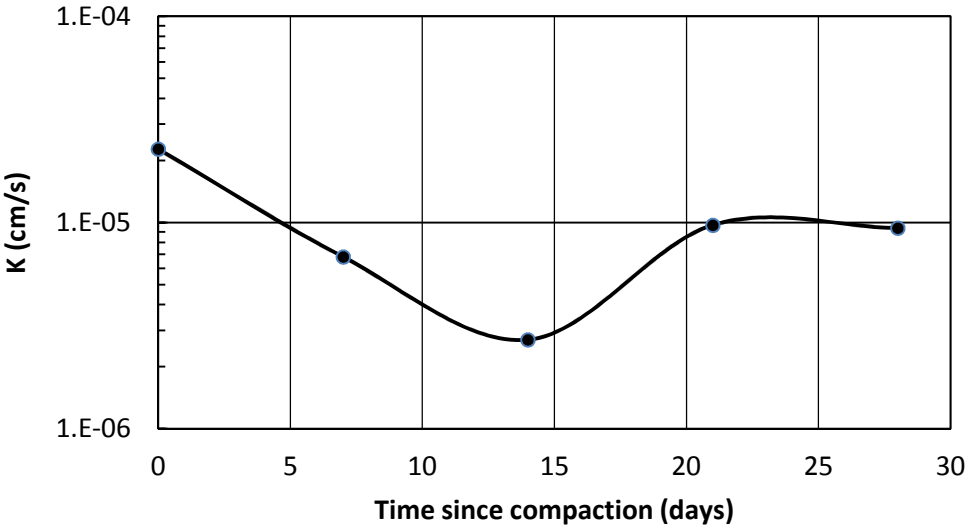

Figure 5.4 Variation of hydraulic conductivity (k) with time since compaction for FGD specimen A to look for changes as possible evidence of pozzolanic reactions occurring in the specimen.

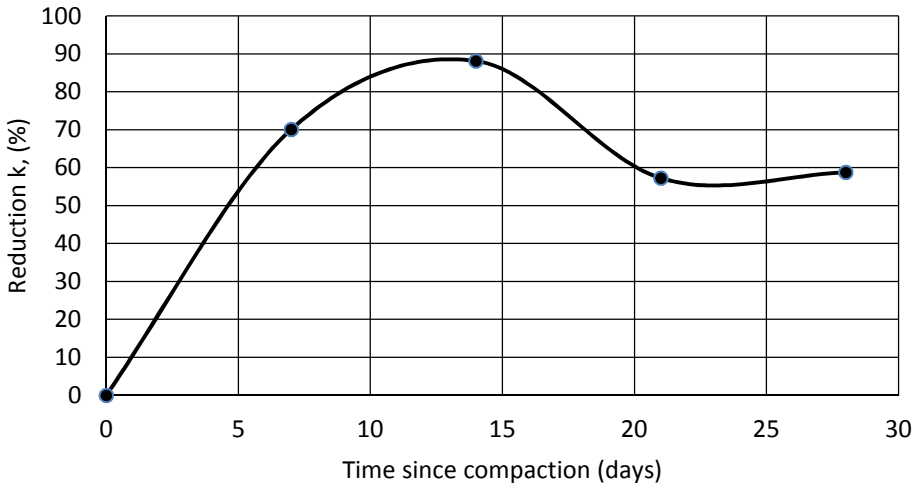

Figure 5.5 Reduction in hydraulic conductivity (k) of compacted FGD sludge with time since compaction, specimen A.

Table 5.5 Consolidation and shear data for compacted FGD sludge

Batch /Specimen No.	Test ENS (psf)	Deform-ation rate (in/min)	Pre-test water (%)	Dry mass, $M_{d,}$ ring (g)	Vol. of solid V_S	Height of solid H_s	e_o	S_r	e_{f1}	Post shear water content (%)/S_{rf}	e_{f2}	Duration of Consolidation			Duration of Shear		Shear time (days)
												Step 1	Step 2	Step 3	Start	End	
(1)	(2)	(3)	(4)	(5)	(6)	(7)	(8)	(9)	(10)	(11)	(12)	(13)			(14)		(15)
1/1	3000	NDR 0.000190	41.1	96.6	2.54	0.52	0.93	1.02	0.81	60.0/1.59	0.87	5/23/13 11:58	5/23/13 12:58	5/23/13 13:58	5/24/13 10:43	5/25/13 8:38	1
2/3	1000	NDR 0.000208	48.4	96.8	2.55	0.52	0.92	1.21	0.87	52.6/1.37	0.89	6/7/13 10:33	6/7/13 11:33	6/7/13 12:33	6/7/13 17:52	6/8/13 15:47	1
1/4	500	NDR 0.000190	48.0	93.9	2.47	0.50	0.98	1.13	0.51	53.5/2.28	0.54	6/11/13 10:25	6/11/13 11:25	6/11/13 12:25	6/11/13 14:17	6/12/13 7:19	1
1/5	3000	NDRD 0.000019	39.1	96.7	2.54	0.52	0.92	0.98	0.84	51.9/1.58	0.76	5/25/13 14:09	5/25/13 15:09	5/25/13 16:09	5/26/13 13:25	6/3/13 9:33	7
1/6	1000	NDRD 0.000019	45.8	91.3	2.40	0.50	0.99	1.07	0.89	59.8/1.39	0.99	6/24/13 15:15	6/24/13 16:15	6/24/13 17:16	6/25/13 9:36	7/4/13 12:12	8
2/7	500	NDRD 0.000024	43.7	96.5	2.54	0.52	0.93	1.09	0.88	60.0/1.5	0.93	6/16/13 13:47	6/16/13 14:48	6/16/13 15:48	6/17/13 9:12	6/24/13 11:14	8
1/8	3000	NDRI 0.0019	41.1	97.1	2.56	0.52	0.92	1.04	0.52	56.6/1.64	0.80	6/4/13 12:40	6/4/13 13:40	6/4/13 14:40	6/4/13 18:16	6/4/13 20:27	2 hr
1/9	2000	NDRI 0.0021	42.0	97.9	2.57	0.52	0.90	1.08	0.80	57.4/1.61	0.83	6/6/13 14:02	6/6/13 15:02	6/6/13 16:02	6/6/13 18:36	6/6/13 20:32	2 hr < 1 day
1/10	1000	NDRI 0.0019	42.1	98.1	2.58	0.52	0.90	1.09	0.82	51.4/1.42	0.84	6/10/13 10:24	6/10/13 11:24	6/10/13 12:24	6/10/13 13:34	6/10/13 15:46	2 hr < 1 day
1/11	500	NDRI 0.0024	47.6	93.6	2.46	0.50	0.99	1.11	0.93	54.7/2.26	0.56	6/14/13 14:51	6/14/13 15:51	6/14/13 16:51	6/14/13 23:04	6/15/13 0:47	< 1day
1/13	2000	NDR 0.000208	38.3	100.3	2.64	0.53	0.86	1.04	0.81	47.7/1.47	0.75	7/26/13 14:35	7/26/13 15:35	7/26/13 16:35	7/27/13 9:55	7/28/13 5:55	1 day
1/16	2000	NDR 0.000208	39.0	102.9	2.71	0.55	0.81	1.14	0.76	54.0/1.8	0.69	8/1/13 10:07	8/1/13 11:08	8/1/13 12:08	8/1/13 18:18	8/2/13 13:52	1 day

ENS is effective normal stress, H initial = 1 inch, e_o = initial void ratio in the ring, e_{f1} = end of consolidation stage (60 minutes), e_{f2} = at peak shear stress, Sr = Degree of saturation more than 100 % in case of both the pre and posttest sample.

5.5.4 Structural water in FGD sludge

FGD sludge is calcium sulfite ($CaSO_3$). Over time, the $CaSO_3$ will oxidize in the presence of water (H_2O) to form gypsum ($CaSO_4 \cdot 2H_2O$). The "$2H_2O$" is now structural water; however, the structural water can be removed by over drying at temperatures of around 110° C. Three 100 grams specimens of moist FGD sludge were dried using three different procedure. The first sample was placed in a desiccator, the second in the open air, and the third in a forced-air oven at 110° C to observe the moisture loss (Figure 5.6).

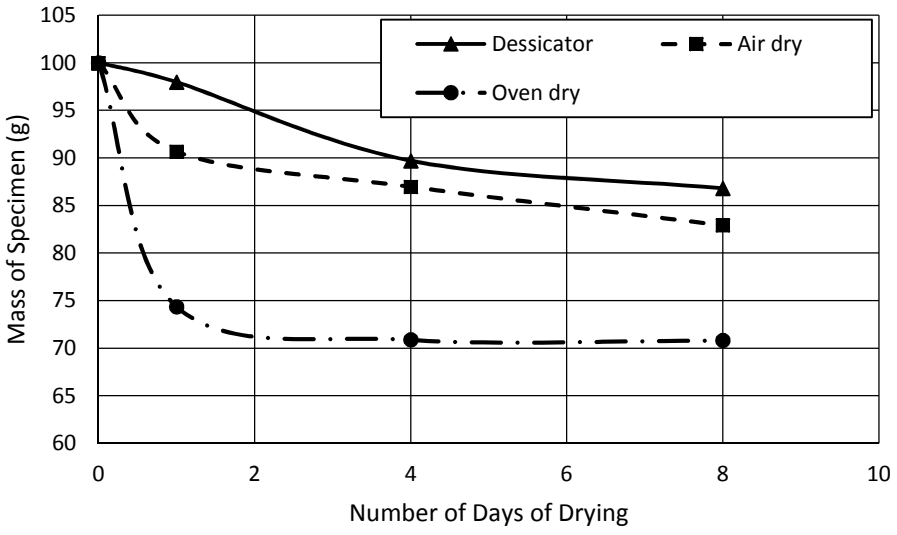

Figure 5.6 Mass of initial 100-gm specimens of FGD versus time for different methods of drying.

The amount of moisture lost at equilibrium was 15 percent for the desiccator sample, 20 percent for the air dry sample, and 41 percent in the case of the oven dry sample possibly indicating that the Gypsum ($CaSO_4 \cdot 2H_2O$) sludge loses some structural water at high drying temperatures (110° C). The water in the structure of the FGD sludge

is capable of being released at high temperature (Kirzek et al., 1987). In the present study, all moisture content determinations shown in Table 5.5 were by the oven-drying method (@ 110◦ C). Thus, the moisture content calculations may include some structural water which is likely reflected by the degree of saturation being calculated to be more than 100 percent. Since all of the specimens were oven dried it is assumed that about the same relative amount of structural water was lost from each specimen.

It was also observed that the FGD sludge's as-received moisture content decreased with time even though the FGD was stored in a closed, airtight plastic drum. This might indicate that the as-received water content present in the FGD sample has started being absorbed in the structure of FGD sludge. The FGD sludge keeps on absorbing the water in its structure at room temperature and the $CaSO_3$ (calcium sulfite) is further oxidized to produce $CaSO_4 \cdot 2H_2O$ (gypsum) (Freeman, 2013). This phenomenon is known as oxidation:

$$CaSO_3 \text{ (solid)} + 2H_2O \text{ (liquid)} + \tfrac{1}{2}O_2 \text{ (gas)} \rightarrow (CaSO_4 \cdot 2H_2O) \qquad (5.1)$$

Absorption of water in the FGD sludge can result in free calcium being converted to calcium hydroxide (CaOH) which, in the presence of siliceous and aluminous material, accelerates pozzolanic reactions and results in a gain in strength with time. There is no evidence of pozzolanic material in the FGD used in this thesis as demonstrated by the absence of change in hydraulic conductivity during the long-term test on Specimen A.

5.6 Reproducibility of the direct shear test

Philipp (1991) stated that the shear strength parameters include uncertainties due to specimen preparation even when performed by the same laboratory and the

same person). Lumb (1974) noted that scatter in direct shear test results may be due to the apparatus used, heterogeneity of the soil material tested and specimen preparation. In the present work, a study was performed to qualify the reproducibility of the direct shear tests on the compacted FGD.

Six compacted FGD specimens were compacted and sheared using a deformation rate of 0.00019 in/min (NDR) at 2000 psf effective normal stress. All tests were conducted by the same person using the same procedure and apparatus for specimen preparation as well as testing. Specimen preparation included: FGD sludge homogenization, Proctor compaction, cutting cylindrical direct shear specimens from the Proctor specimens, installation in the direct shear apparatus and consolidating the specimens prior to initiating shear.

Peak shear stress versus effective normal stress for all six specimens are shown in Figure 5.7. Specimens 12 and 15 show a peak shear stress, τ_p lower than the effective normal stress, σ'. Such behavior was attributed to fine cracks (not visible from the outside of the specimen) in the compacted specimens generated as the specimens were trimmed or during the placement in the direct shear box. Therefore, the results from specimens 12 and 15 are not considered further in the discussion. Specimen 14 was a good test; however, at peak shear stress, the normal effective stress was 2,150 psf or about 8 percent greater than the other specimens. One would expect the strength to be higher for specimen 14 simply because of the increased effective normal stress. Thus, specimen 14 should not be used in the analysis of reproducibility.

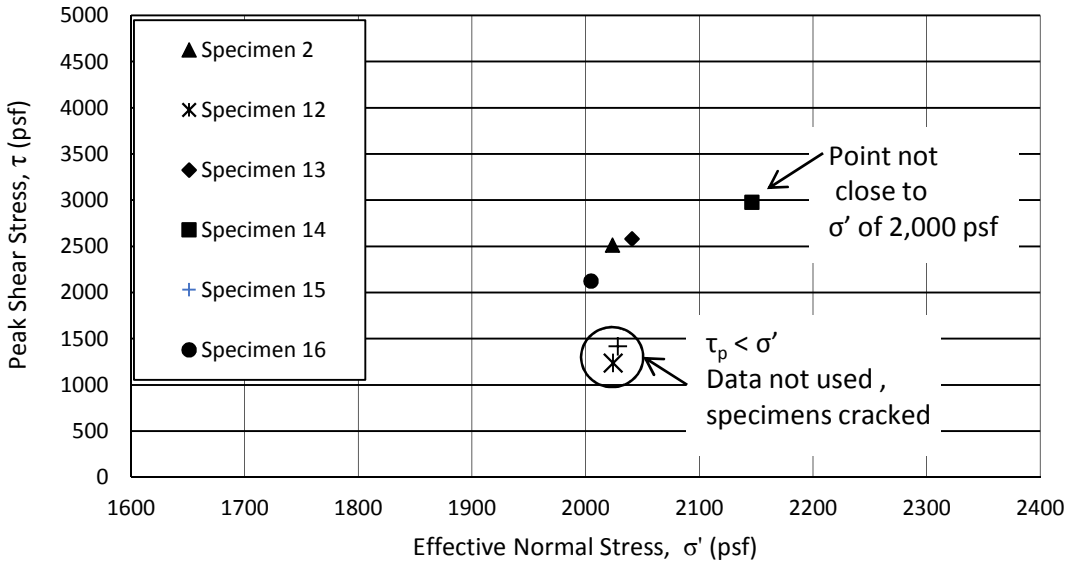

Figure 5.7 Peak shear stress at 2000 psf effective normal stress for six different specimens.

Considering specimens 2, 13 and 16, the average value of peak shear stress was 2406 psf. Specimen 2 (peak shear stress = 2512 psf) was used to define the failure envelope for the nominal deformation rate (0.0002 in/min). The shear stress versus horizontal displacement behavior for specimens 2, 13, 14 and 16 are similar as shown in Figure 5.8. The standard deviation from the peak shear stress for specimens 2, 13 and 16 was 246 psf and the cov was 0.102 (10 %). The friction angles for each test (assuming a cohesion intercept of zero) are shown in Table 5.6. The mean friction angle was 48°. The standard deviation of tan(ϕ) is 0.072 and the cov is seven percent. Lumb (1974) noted that the coefficient of variation (cov) of tan(ϕ) for a cohesive soil is six percent in direct shear tests which is surprisingly close to the findings of the present study. The results of the direct shear tests are considered to be reproducible with a high degree of precision (cov ≤ 10%).

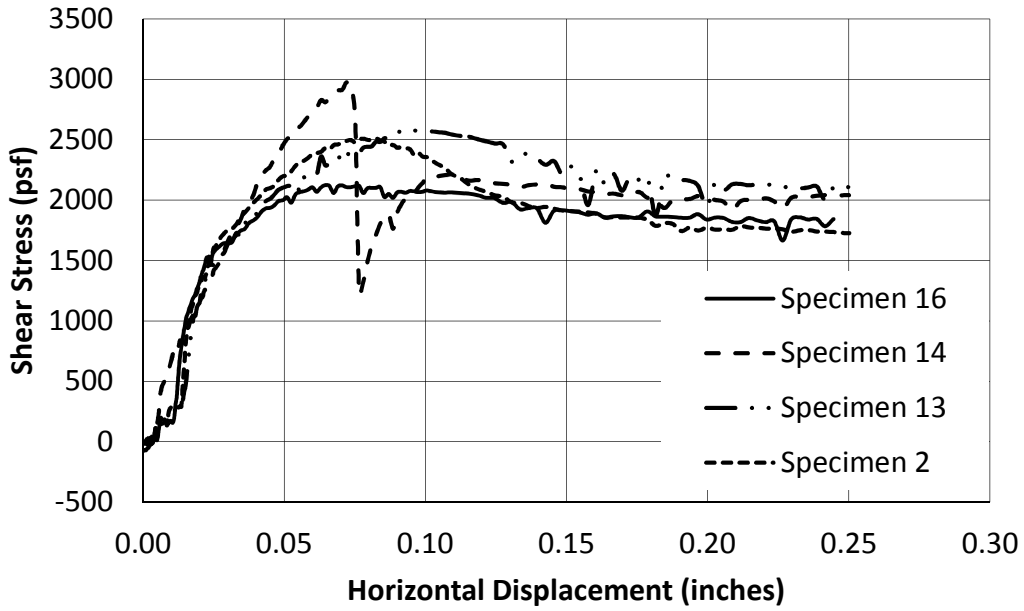

Figure 5.8 Shear stress path at 2000 psf effective normal stress for six different specimens.

Table 5.6 Friction angle of compacted FGD sludge with the different specimens at deformation rate 0.0002 in/min (NDR).

Specimen No.	Friction Angle (°)	Tan(φ)
2	46	1.035
13	50	1.191
16	49	1.150
Mean	48.3	1.1
Stdev	2.08	0.08
cov	0.043	0.072

5.7 Interpreting direct shear test results

It was decided to interpret shear test results, assuming the compacted FGD was cohesionless (c=0), so that the shear strength is purely friction based. This prcedure yielded the failure envelopes shown in Figure 5.2 and friction angles given in Table 5.7. However, it is also possible to interpret the data as cohesion and friction based (c and ϕ) resulting in the failure envelopes shown in Figure 5.9 and given in Table 5.7. Both

methods yield the same shear strength (τ) at same effective normal stress (σ')(Equation 5.2).

$$\tau = c' + \sigma' \tan(\phi') \quad (5.2)$$

where:

τ = shear strength

c'= effective cohesion

σ'= effective normal stress

ϕ' = effective friction angle

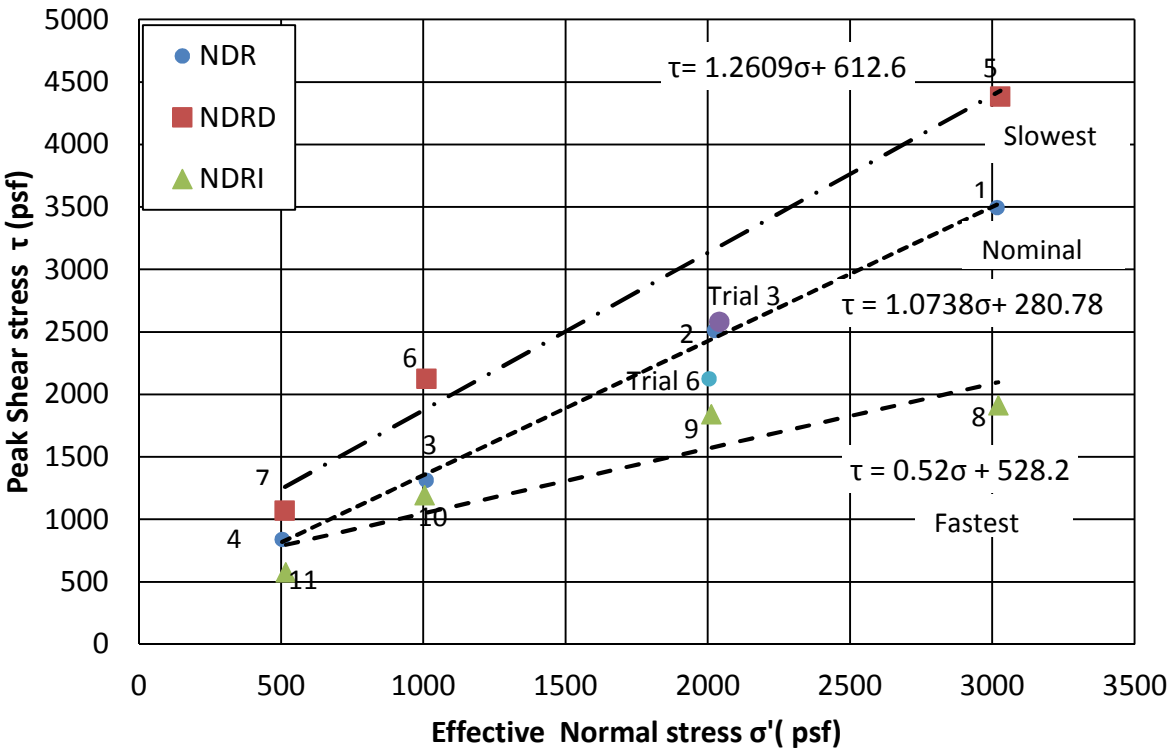

Figure 5.9 Failure envelopes from the direct shear test with cohesion (failure envelope not forced through origin) (NDR-Nominal deformation rate (specimens 1 to 4), NDRI-Nominal deformation rate increase (specimens 8 to 11) and NDRD- Nominal deformation rate decrease (specimens 5 to 7) All Specimen numbers are from Table 4.1 for shear data).

Table 5.7 Shear strength parameters for compacted FGD sludge.

Deformation Rate	Cohesion Considered (Figure 5.9)		Cohesion Ignored, c' = 0, (Figure 5.2)
(inches/minute)	Effective friction Angle (ϕ°)	Effective Cohesion, c' (psf)	Effective friction Angle (ϕ°)
NDRI 0.002	27	528	37
NDR 0.0002	47	280	46
NDRD 0.00002	52	613	57

5.8 Summary

Peak shear strength increased as the deformation rate during shear was decreased for a series of drained direct shear tests on compacted flue gas desulfurization (FGD) sludge. Shearing rates were calculated for each test such that fully drained behavior; i.e., no excess pore water pressures, should have resulted during shearing of the specimens (Table 8, column 2). The initial assumption was that excess (positive) pore water pressures were being generated during shear resulting in the strength dependence on shear rate. Results of independent tests (consolidation and hydraulic conductivity, Table 5.8, column 5) on the compacted FGD were used to re-calculate shearing rates to yield drained behavior. The independently calculated rates further confirmed that the shearing rates used should have produced fully drained behavior (Table 5.8, column 3). The specimen volume change during shearing was examined and found to show a slight dilation to no volume change during shearing (Table 8, column 1) further supporting the theme that no excess pore water pressures (positive or negative) were being generated during shear.

Several other mechanisms that could possibly lead to strength changes with time (time being the time during shearing of the compacted FGD specimen) were

hypothesized including: creep or specimen compaction under a constant normal stress, mineralogical reaction (calcium sulfite changing to gypsum) and a pozzolanic reaction. The consolidation portion of the direct shear tests, supported the possibility of vertical creep under constant load (specimen densification) (Table 5.8, column 6). However, volume change (specimen height) during the shearing phase of the tests did not support the creep hypothesis (Table 5.8, column 1). Both, reaction of calcium sulfite to gypsum and pozzolanic reactions will make the FGD stronger. Both processes require time (a day to a few weeks) to yield an appreciable change in shear strength of the FGD. Neither consolidation tests (Table 5.8, column 6) nor a long-term hydraulic conductivity tests (Table 5.8, column 4) supported the hypotheses of strength gain under these two mechanisms.

Re-examination of the time-settlement curves for each consolidation load on the direct shear specimens (Appendix Figures A.1 through A.17) indicate that the times to reach end of primary consolidation may be much longer than calculated in this thesis. Four specimens (Figures A.10, A.11, A.13 and A.14) show a substantial flattening of the time-settlement curve after more than 900 to 2500 minutes under a given consolidation stress. Based Figures A.10, A.11, A.13 and A.14, time to failure for fully drained behavior could be 25,000 to 65,000 minutes resulting in deformation rates of 4E-5 to 2E-6 inches/minute, which further suggests that only the slowest deformation rates used in this thesis (0.00002 inches/minute) should yield fully drained behavior of the compacted FGD sludge.

Table 5.8 Possible mechanisms leading to different shear strengths measured at different shearing deformation rates, methods used to evaluate the mechanisms and .

Mechanism	Method used to evaluate possible mechanism affecting shear strength of compacted FGD sludge					
	(1)	(2)	(3)	(4)	(5)	(6)
	Volume change during shear of the specimen (Vol increased or no change during shearing)	Fully drained Deform. Rate Gibson and Henkel (1954)	Fully drained Deform. Rate Kaniraj and Gayathri (2004)	Long term k test $k \approx 10^{-5}$ cm/s (No change with time)	k @ different effective normal stress (ENS) $K \approx 10^{-5}$ cm/s (No change with increase in ENS)	Consol tests (Vertical deformation gradually increases under constant load)
Positive pore water pressure (strength decrease)	Not supported	Not supported $\dot{\delta}_{\text{actual}} < \dot{\delta}_{\text{fully drained}}$ therefore should not be any excess pore water pressures		Not supported no change in k with time specimen free to drain No pore pressure	Not supported no change in k with increase in effective stress specimen free to drain No pore pressure	NA
Negative pore water pressure (strength increase)	Supported by dilation in some specimens					NA
Creep (specimen compresses/ densifies) (strength increase)	Not supported dilation or no vol change during shear	NA	NA	Not supported no change in k with time	NA	Supported (Steady volume decrease under constant load)
Reaction (Oxidation) to Gypsum (strength increase)	NA	NA	NA	Not supported no change in k with time	NA	Not supported (expect defm to stop if gypsum forming)
Aging-Pozzolanic (strength increase)	NA	NA	NA	Not supported no change in k with time	NA	Not supported (expect defm to stop if possolan rxn)

CHAPTER 6: CONCLUSIONS AND RECOMMENDATIONS

6.1 Summary

Flue gas desulfurization (FGD) sludge is produced during the clean-up of the gas stream from the combustion of coal. The FGD is calcium oxide, injected into the hot off gases to remove sulfur (SO_x) compounds. The resulting FGD is primarily calcium sulfite $CaSO_3$ and gypsum $CaSO_4 \cdot 2H_2O$. Although FGD has several beneficial reuses (agricultural lime, gypsum wallboard), most is disposed of in embankment landfills. To expand the potential reuses and to ensure stability and safety of the disposal embankments, shear strength parameters of the compacted FGD are required. The main objectives of this research were to: (1) quantify the shear strength behavior of compacted FGD when sheared at different deformation rates in 'drained' direct shear tests. More specifically, determine if a deformation rate of 0.0002 inches per minute results in fully drained behavior of the compacted FGD and (2), if necessary estimate a deformation rate that will yield fully drained shear strength parameters.

The FGD used in this study classified as low plasticity silt (ML) with a plastic limit of zero. Specimens were compacted using standard Proctor energy and drained direct shear tests were performed at three different deformation rates. The nominal deformation rate was calculated from the consolidation data (NDR = 0.0002 inches per minute). A deformation rate one order of magnitude slower (NDRD = 0.00002 inches per minute) and another rate one order of magnitude faster (NDRI = 0.002 inches per minute) were also used. Plots of shear stress versus horizontal deformation were

prepared for analysis. One-dimensional consolidation tests were performed to determine the coefficient of volumetric compressibility (m_v) and flexible-wall permeability tests were performed to measure hydraulic conductivity (k) as a function of time and as a function of effective stress.

6.2 Conclusions

There was a noticeable change in shear strength for specimens sheared at the same effective normal stress but at different deformations rates. Lower shear strengths were recorded for faster deformation rates. Assuming zero cohesion and calculating the slope of the best linear-fit failure envelopes yielded internal frictions angles of 57°, 46°, and 37° for deformation rates of 0.00002, 0.0002 and 0.002 inches per minute, respectively. The decrease in shear strength (friction angle) with increasing deformation rate seemed to indicate that excess pore water pressures generated during shear may not be dissipating thereby leading to a decrease in the shear strength. However, the compacted FGD specimens tended dilate slightly (volume expansion) or have no volume change during shear which leads to reduced or even negative pore water pressures which should result in an apparent increase in the drained shear strength. (Reduced or negative pore water pressures lead to increased effective stress and therewith increased shear strength.)

An independent check on the shearing rate; i.e., time to reach peak shear resistance, was performed by measuring the hydraulic conductivity, k, of the compacted FGD and the coefficient of volume compressibility, m_v, and using them to calculate a coefficient of consolidation, c_v. The coefficient of consolidation was then used to

calculate a deformation rate that yielded peak shear strength for the compacted FGD with a 99 percent average degree of consolidation, meaning 99 percent of any excess pore water pressures generated due to shear should be dissipated by the time the specimens reach peak shear strength. The slowest deformation rate required for "fully drained" shear behavior was calculated to be 0.0052 inches per minute which is more than two times faster than the fastest deformation rate used in the present study (0.002 inches per minute). Thus, it was concluded that excess pore water pressures were not generated by the deformation rates used in the present study. Other mechanisms for the shear strength dependence on deformation rate were considered including strain-hardening by creep, mineralogical change of the FGD sludge from calcium sulfite ($CaSO_3$) to gypsum ($CaSO_4 \cdot 2H_2O$) and pozzolanic reactions.

Initial analysis of the consolidation curves for the compacted FGD indicated that the excess pore water pressure dissipated within minutes after loading (very rapid) but vertical deformation under the constant load (creep) continued for hours to days. Such creep (in this case compression) behavior can lead to strain-hardening of the material being sheared such that as the horizontal shearing deformation rate is slowed, the specimen remains under a constant vertical stress and creep continues, even during shear, resulting in a stiffer specimen which is more resistant to shear.

Mineral change from calcium sulfite to gypsum and pozzolanic reaction in the compacted FGD would also tend to lead to greater resistance to shear. It was hypothesized that these changes, if occurring, would lead to decreasing hydraulic conductivity during long term hydraulic conductivity tests. The maximum shearing

duration was eight days. The mechanisms were evaluated by measuring the hydraulic conductivity of a compacted FGD specimen over a period of 30 days. There was a slight change (less than a factor of two) in the hydraulic conductivity over the measurement period. The small change is indicative of no major mineral alteration or pozzolanic reactions in the FGD over that period of time and thus one would not expect these mechanisms to be impacting the shear strength measured over a period of one to eight days.

Re-examination of the time-settlement curves for each consolidation load on the direct shear specimens indicate that the times to reach end of primary consolidation may be much longer than originally assumed. Four specimens of the 17 show a substantial flattening of the time-settlement curve after more than 900 to 2500 minutes under a given consolidation stress. However, these four test results yield deformation rates of 4E-5 to 2E-6 inches/minute for fully drained behavior, which further suggests that only the slowest deformation rate (2E-5 inches/minute) used in this thesis should yield fully drained behavior of the compacted FGD sludge. For now, it is recommended that designers use the lowest shear strength parameters (obtained from the direct shear tests with the highest deformation rates), for design of FGD disposal embankments; i.e., internal friction angle of 37 degrees with zero cohesion.

6.3 Recommendations

Several recommendations are presented to gain a better understanding of the time/shear rate dependence of shear strength for compacted FGD.

1. Perform a strength versus aging-time study. Compact a series of cylindrical FGD specimens at the same molding water content and dry density. Store the specimens in a sealed chamber with a high relative humidity at room temperature (20°C). Select two specimens periodically (0, 7, 14, 28, 56 days) and measure their compressive strength (UU test). Analyze the strength versus time. An increase in strength with time would indicate some aging phenomenon such as a pozzolanic reaction or mineralogical change from calcium sulfite to gypsum. Repeat the experiment but, keep the specimens at 4°C. Low temperatures slow the rate of mineralogical and pozzolanic reactions.

2. Perform an investigation of the excess pore water pressure dissipation with time. Compact an FGD sludge specimen. Use a one-dimensional consolidometer with a pore water pressure measurement system in the base of the consolidometer. Trim the specimen into the consolidometer. Perform an incremental load test on the FGD specimens and measure the excess pore water pressure versus time for each incremental load. Analyze the time required for the excess pore water pressure to dissipate under each loading. Back-calculate coefficients of consolidation for each load increment and use them to calculate time to failure t_f, (Equation 2.12) and analyze the t_f with regard to times to failure for fully drained shear tests presented in this thesis.

3. Perform parallel shear strength studies on compacted FGD using drained triaxial tests (CD), undrained triaxial tests with porewater pressure measurements ($\overline{CU}$) and direct simple shear tests using the constant volume procedure (DSS-CV). Compare

the shear strength deformation behaviors, the pore water pressures during shear, the shear strength, and the effective shear strength parameters c' and ϕ'.

4. Investigate the mineralogy, composition, and skeletal structure of the compacted FGD as a function of time at the microscopic scale. Special emphasis should be placed on determining the rate at which calcium sulfite converts to gypsum.

5. Investigators of any future study of FGD sludge must be very cognizant of the time duration during sampling, transport, storage, and in all aspects of testing since it is likely that the FGD undergoes some type of 'aging' effects that appear to have bearing on the index and strength properties of compacted FGD sludge.

6. It is recommended that air drying or a desiccator should be used when determining the moisture content of the FGD sludge in order to eliminate the issue of removing structural water during oven drying,

REFERENCES

AAACA Educational Foundation (2007). "Diagram of a Typical FGD Gypsum Production Process," http://www.fgdproducts.org/FGDGypsumIntro.htm, (8/8, 2013).7

ASTM (2007). "Standard Test Method for Particle-Size Analysis of Soils", Annual Book of ASTM Standards, D 422-63, 04.08, ASTM, West Conshohocken, PA.

ASTM (2010). "Standard Test Methods for Measurement of Hydraulic Conductivity of Saturated Porous Materials Using a Flexible Wall Permeameter", Annual Book of ASTM Standards, Designation D 5084, ASTM, West Conshohocken, PA.

ASTM (2011). "Classification of Soils for Engineering Purposes", Annual Book of ASTM Standards, D 2487-11, 04.08, ASTM, West Conshohocken, PA.

ASTM (2011). "Standard Test Method for Direct Shear Test of Soils under Consolidated Drained Conditions", Annual Book of ASTM Standards, Designation D 3080, Vol. 4.09, ASTM, West Conshohocken, PA.

ASTM (2011). "Standard Test Methods for One-Dimensional Consolidation Properties of Soils Using Incremental Loading", Annual Book of ASTM Standards, ASTM D2435/D2435M, 04.08, ASTM, West Conshohocken, PA.

ASTM (2012). "Standard Terminology Relating to Concrete and Concrete Aggregates", Annual Book of ASTM Standards, Designation C125-13a,Vol. 4.02, ASTM, West Conshohocken, PA.

Bigham, J. M., Kost, D. A., Stehouwer, R. C., Beeghly, J. H., Fowler, R., Traina, S. J., & Dick, W. A. (2005). "Mineralogical and engineering characteristics of dry flue gas desulfurization products", *Fuel*, 84(14):1839-1848.

Bowders, J. J., and Day, T. J. (2013). "Report No.: 2013-FGD-DS Flue Gas Desulfurization (FGD) sample (Weststar 'gypsum') laboratory results direct shear testing." For *Weststar Energy & Burns and Macdonnell Engineering, Inc,* 9400 Ward Parkway, Kansas city, Missouri, 64114, Institute of Interdisciplinary Geotechnics, Department of Civil and Environmental Engineering, The University of Missouri-Columbia (UMC), Missouri.

Casagrande, A. and Fadum, R. E. (1940). Notes *on Soil Testing for Engineering Purposes.* Harvard Soil Mechanics Series: Harvard University, Graduate School of Engineering, Cambridge, MA, p.74.

Coduto, D.P., Yeung, M.R., and Kitch, W.A. (2010). "*Geotechnical Engineering: Principles and Practices"*, 2ed, Printice-Hall, New York, pp. 164-186.

Coffman, R. A., and Bowders, J. J. (2007). "Report no.: 2007-FGD-a, Flue gas desulfurization (FGD) sample laboratory results addendum." For Weststar Energy & Burns and McDonnell Engineering, Inc. , 9400 Ward Parkway, Kansas City, Missouri 64114, Institute for Interdisciplinary Geotechnics, University of Missouri-Columbia.

Freeman, E (2013). "Dry unit weight versus molding moisture content for FGD," Environmental Engineering Department, Burns & McDonnell, Kansas City, Missouri (April 2013).

Gibson, R. E., and Henkel, D. J. (1954). "Influence of duration of tests at constant rate of strain on measured drained strength," *Geotechnique*, 4(1):6-15.

Head, K. H., and Epps, R. (1981). "Manual *of soil laboratory testing", Volume 2, Permeability, shear strength and compressibility tests*, Pentech Press, London, UK, 489pp.

Kalyoncu, R. S., and Olson, D. W. (2000). "Coal combustion products" <http://pubs.usgs.gov/fs/fs076-01/fs076-01.html>. (4/29, 2014).

Kaniraj, S. R., & Gayathri, V. (2004). "Permeability and consolidation characteristics of compacted fly ash", Journal *of Energy Engineering*, *130*(1):18-43.

Kost, D. A., Bigham, J. M., Stehouwer, R. C., Beeghly, J. H., Fowler, R., Traina, S. J., & Dick, W. A. (2005). "Chemical and physical properties of dry flue gas desulfurization products", *Journal of Environmental Quality*, *34*(2):676-686.

Krizek, R. J., Chu, S. C., and Atmatzidis, D. K. (1987). Geotechnical Properties and Landfill Disposal of FGD Sludge, *Proceedings* of the ASCE Specialty Conference on Geotechnical Practice for Waste Disposal, Ann Arbor, Michigan, pp. 625-639.

Lumb, P. (1974). "Application of Statistics in Soil Mechanics", In: LEE, I.K. S*oil Mechanics – New Horizons*, Newnes-Butterworths, London, 44-111.

Mitchell, J. K. (1986). "*Practical problems from surprising soil behavior"*. Journal of Geotechnical Engineering, 112(3), 259-289.

Moghal, A. A. B., & Sivapullaiah, P. V. (2011). "Effect of pozzolanic reactivity on compressibility characteristics of stabilised low lime fly ashes", *Geotechnical and Geological Engineering*, *29*(5):665-673.

Pandian, N. S., & Balasubramonian, S. (1999). "Permeability and consolidation behavior of fly ashes", *Journal of Testing and Evaluation*, 27(5):337-342.

Phillip, H. (1991). "About the test accuracy of soil parameters determined in the laboratory", *Geotechnik*, 14(4):184-189 (in German).

Porbaha, A., Pradhan, T. B. S., & Yamane, N. (2000). “Time effect on shear strength and permeability of fly ash”, *Journal of Energy Engineering*, *126*(1):15-31.

Taylor, D. W. (1948). “*Fundamentals of Soil Mechanics*”, Chapman and Hall, London, John Wiley and sons, New York, pp. 239-241.

Terzaghi, K. (1942). “*Theoretical Soil Mechanics*”, Chapman and Hall, London, John Wiley and sons, New York, pp.7-10.

UMC Geotech (2012). “*Automated Direct Shear System*”, Department of Civil And Environmental Engineering, Geotechnical Engineering Program, Unpublished internal report, University of Missouri-Columbia, pp. 1-7.

United States Environmental Protection Agency USEPA (2013). "Overview - the clean air act amendments of 1990." <http://epa.gov/oar/caa/caaa_overview.html>. (4/29, 2014).

Wolfe W., Butalia T., Daniels J. and Baker R. (2010). “Final Report for Project CDO/D-07-06”, The Ohio State University. <http://ccpohio.eng.ohio-state.edu/sites/ccp.web.engadmin.ohio-state.edu/files/uploads/cdo-d-07-6_final_report.pdf>. (4/29, 2014).

Zhang G (2013). “Shear Strength of Flue Gas Desulfurization By-Product”, *MS Thesis*, Department of Civil and Environmental Engineering, University of Missouri, Columbia, 62pp.

APPENDIX

A. AS RECEIVED MOISTURE CONTENT IN PERCENT OF THE SAMPLES

Table A.1 As-received moisture content in percent of the samples in the buckets

	Bucket 1	Bucket 2	Bucket 3	Bucket 4
Top	36.40	43.88	34.84	40.53
Middle	38.56	43.12	34.40	39.90
Bottom	37.08	43.97	35.68	39.55

Buckets 1 and 2 are from batch 1 and buckets 3 and 4 are from batch 2. Bucket 3 was not used as it had low moisture content compared to that of the other buckets. Batch 1 was received on 9 April 2013 and batch 2 on 19 July 2013.

B. DIRECT SHEAR TEST CALCULATIONS AND PERMEABILITY TEST

1. DETERMINATION OF THE SHEAR DEFORMATION RATE FROM CONSOLIDATION DATA

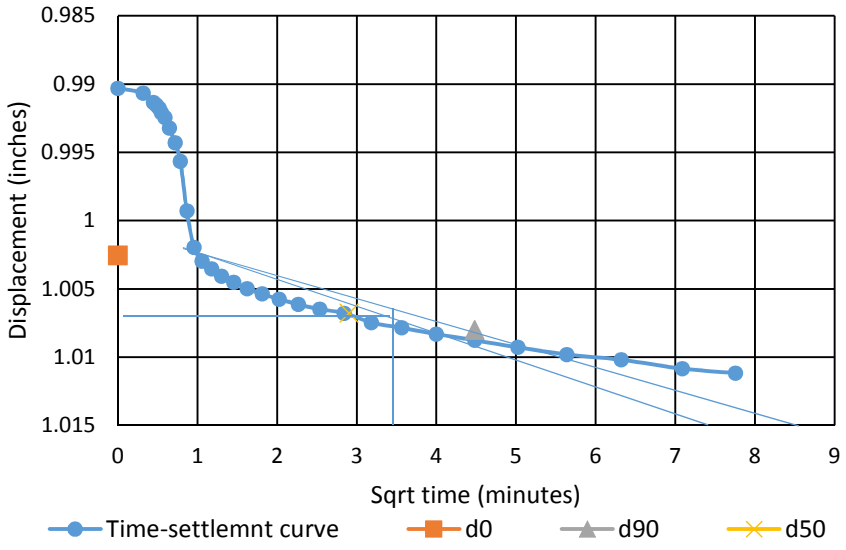

Figure A.1 Consolidation curve for 500 psf ENS on square root time scale (deformation rate NDR, specimen 4, Table 4.1) at last load increment from 250 to 500 psf.

Table A.2 Calculation of deformation rate for 500 psf effective normal stress.

x intercept * 1.15	= 6.9*1.15 = 8	Vertical actuator (inches)
	d90	1.0080
	d0	1.0025
	d0-d90	0.0054
d50	5/9 * (d0-d90)	0.0030
	d0+d50	1.0067
t50 (mins)	= 2.9*2.9 = 9	
50*t50	450	
Shear rate (in/min) NDR	0.000244	
NDRD	0.0000244	
NDRI	0.002444	

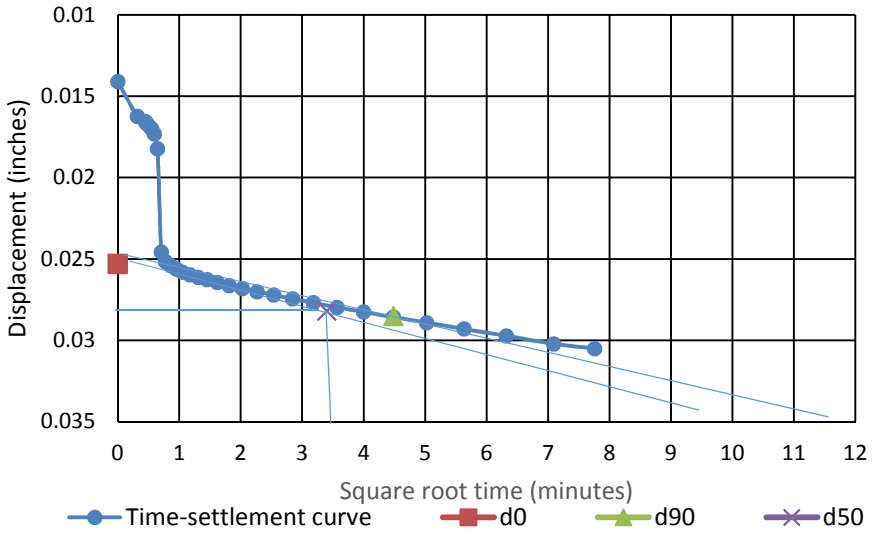

Figure A.2 Consolidation curve for 1000 psf ENS on square root time scale (deformation rate NDR, specimen 3, Table 4.1) at last load increment from 500 to 1000 psf.

Table A.3 Calculation of deformation rate for 1000 psf ENS

x intercept * 1.15	= 9.2*1.15 = 10.58	Vertical actuator (inches)
	d90	0.0285
	d0	0.0253
	d0-d90	0.0050
d50	5/9 * (d0-d90)	0.0028
	d0+d50	0.0282
t50 (mins)	= 3.4*3.4 = 11.56	
50*t50	578	
Shear rate (in/min) NDR	0.00019	
NDRD	0.000019	
NDRI	0.0019	

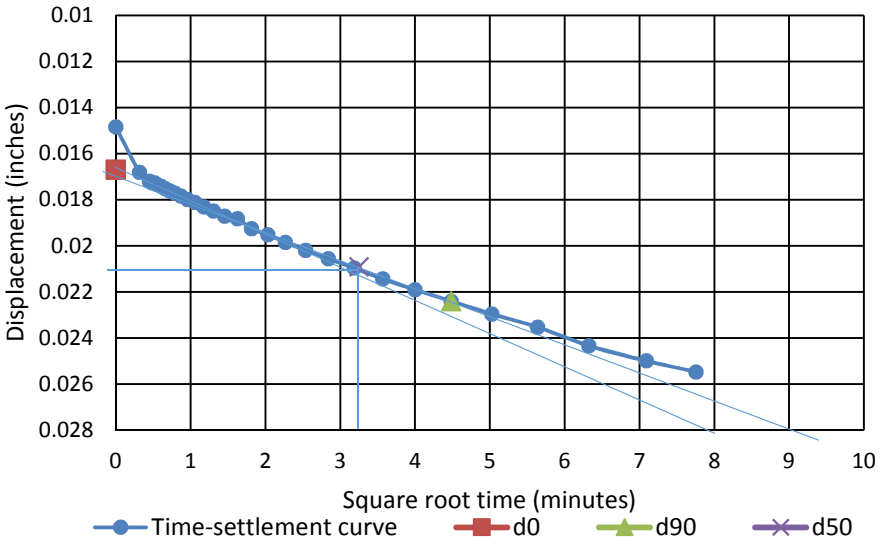

Figure A.3 Consolidation curve for 2000 psf ENS on square root time scale (deformation rate NDR, specimen 14, Table 4.1) at last load increment from 1000 to 2000 psf.

Table A.4 Calculation of deformation rate for 2000 psf ENS

x intercept * 1.15	= 8.4*1.15=9.66	Vertical actuator (inches)
	d90	0.0224
	d0	0.0167
	d0-d90	0.0076
d50	5/9 * (d0-d90)	0.0042
	d0+d50	0.0209
t50 (mins)	= 3.25*3.25= 10.56	
50*t50	528.12	
Shear rate(in/min)NDR	0.000208	
NDRD	0.0000208	
NDRI	0.00208	

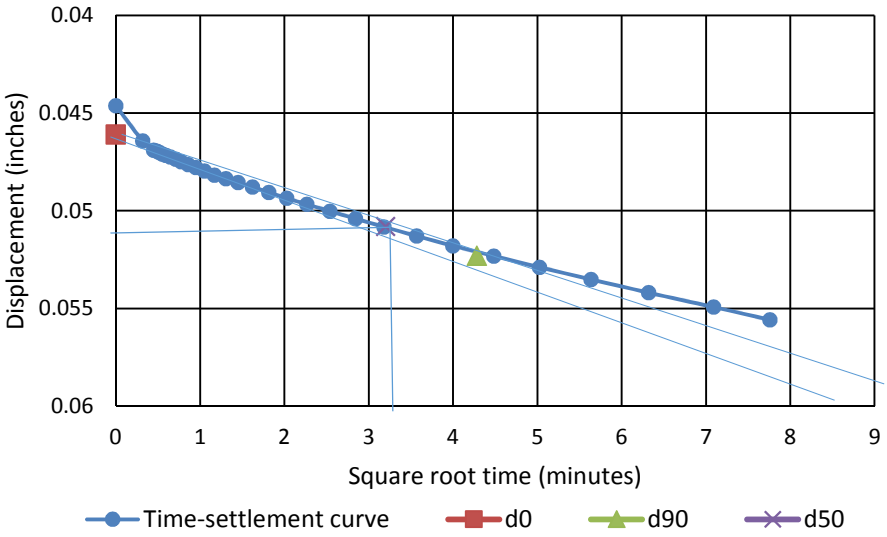

Figure A.4 Consolidation curve for 2000 psf ENS on square root time scale (deformation rate NDRI, specimen 9, Table 4.1) at last load increment from 1000 to 2000 psf.

Table A.5 Calculation of deformation rate for 2000 psf ENS

x intercept * 1.15	= 8.5*1.15=9.7	Vertical actuator (inches)
	d90	0.0523
	d0	0.0461
	d0-d90	0.0083
d50	5/9 * (d0-d90)	0.0046
	d0+d50	0.0508
t50 (mins)	= 3.2*3.2= 10.24	
50*t50	512	
Shear rate (in/min) NDR	0.0002148	
NDRD	0.00002148	
NDRI	0.002148	

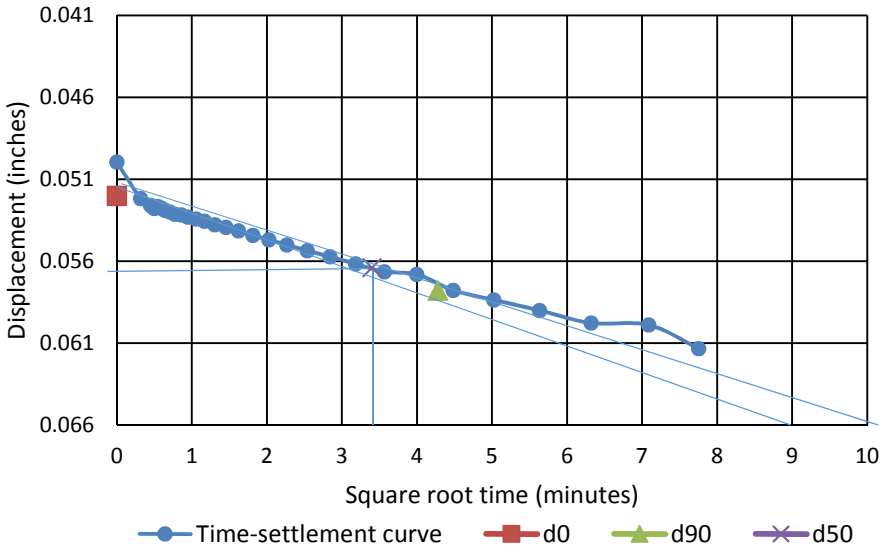

Figure A.5 Consolidation curve for 3000 psf ENS on square root time scale (deformation rate NDR, specimen 1, Table 4.1) at last load increment from 1500 to 3000 psf.

Table A.6 Calculation of deformation rate for 3000 psf ENS

x intercept * 1.15	= 8.8*1.15 = 10.12	Vertical actuator (inches)
	d90	0.0578
	d0	0.05203
	d0-d90	0.00786
d50	5/9 * (d0-d90)	0.00437
	d0+d50	0.0564
t50 (mins)	= 3.4*3.4 = 11.56	
50*t50	578	
Shear rate(in/min)NDR	0.00019	
NDRD	0.000019	
NDRI	0.0019	

2. CONSOLIDATION CURVES AT DIFFERENT EFFECTIVE NORMAL STRESS, ENS.

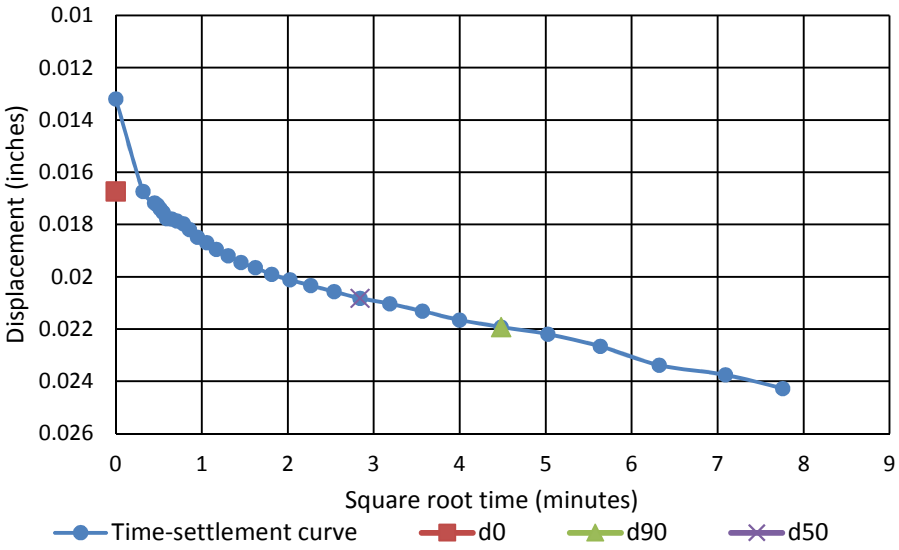

Figure A.6 Consolidation curve for 500 psf ENS on square root time scale (deformation rate NDRD, specimen 7, Table 4.1) at last load increment from 250 to 500 psf.

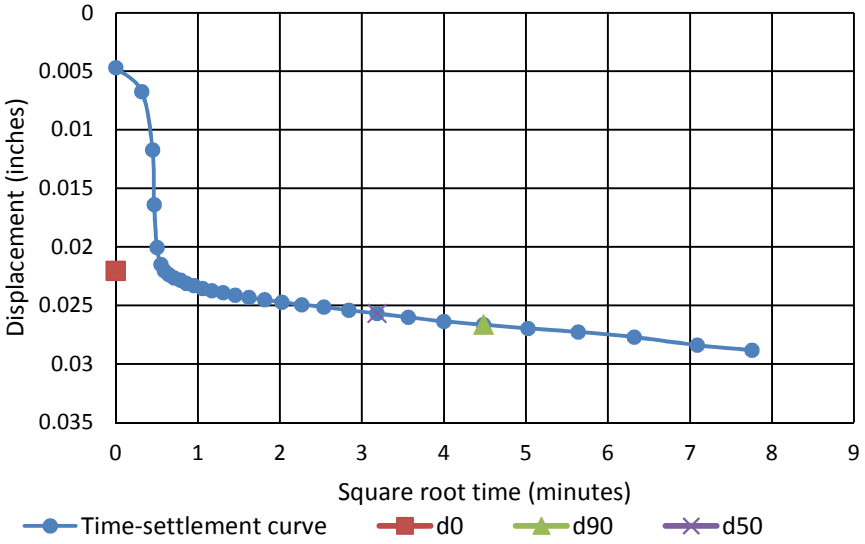

Figure A.7 Consolidation curve for 500 psf ENS on square root time scale (deformation rate NDRI, specimen 11, Table 4.1) at last load increment from 250 to 500 psf.

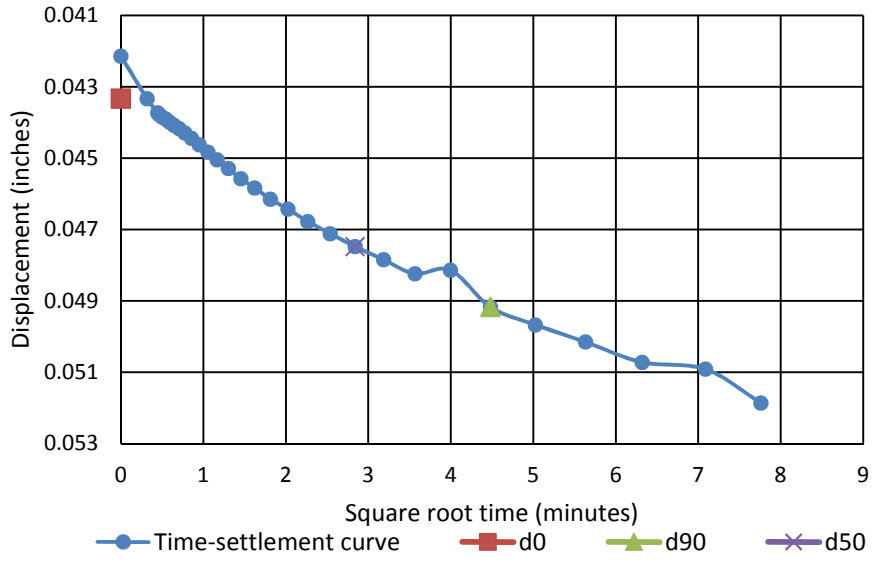

Figure A.8 Consolidation curve for 1000 psf ENS on square root time scale (deformation rate NDRD, specimen 6, Table 4.1) at last load increment from 500 to 1000 psf.

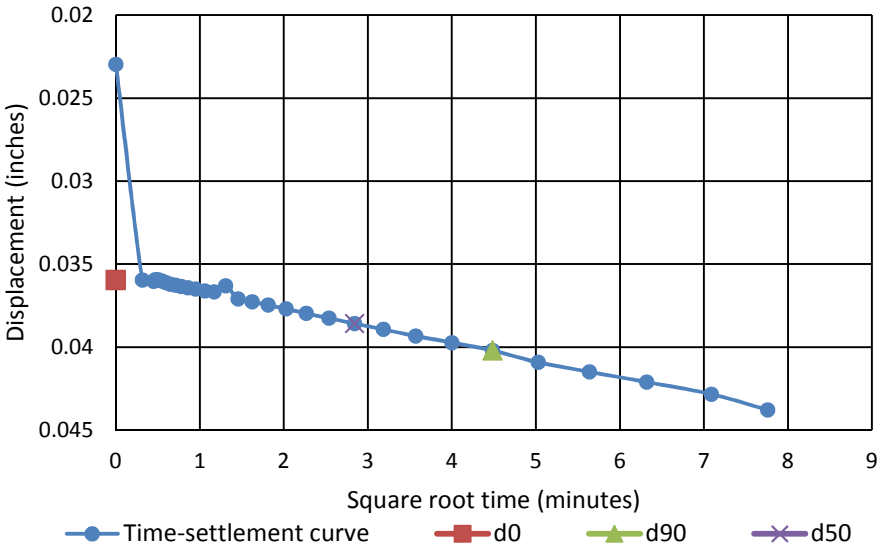

Figure A.9 Consolidation curve for 3000 psf ENS on square root time scale (deformation rate NDRD, specimen 5, Table 4.1) at last load increment from 1500 to 3000 psf.

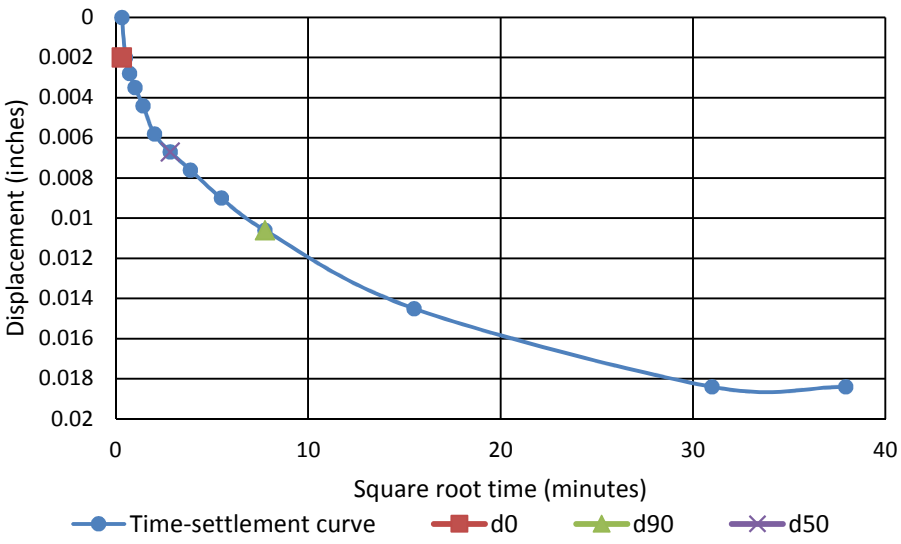

Figure A.10 Consolidation curve (ILT) for 3000 psf ENS on square root time scale at first load increment from 0 to 500 psf.

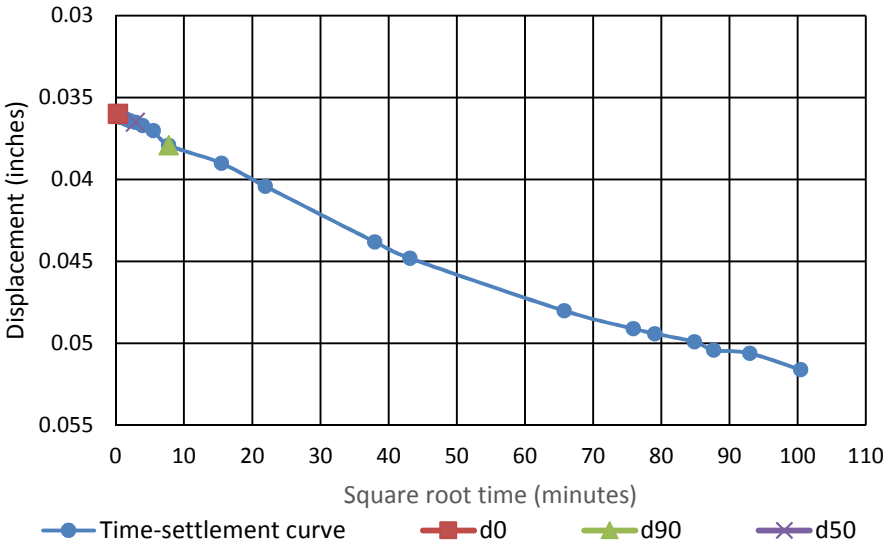

Figure A.11 Consolidation curve (ILT) for 3000 psf ENS on square root time scale at second load increment from 500 psf to 1500 psf.

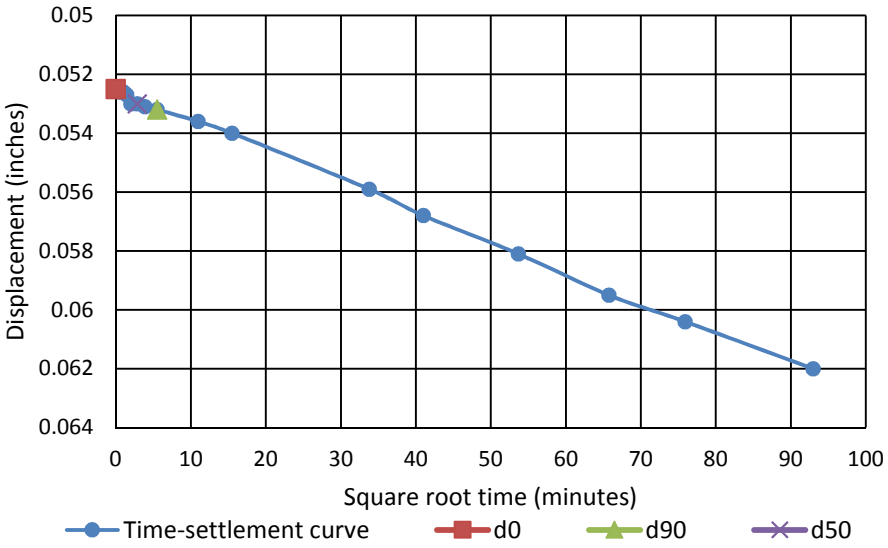

Figure A.12 Consolidation curve (ILT) for 3000 psf ENS on square root time scale at last load increment from 1500 psf to 3000 psf.

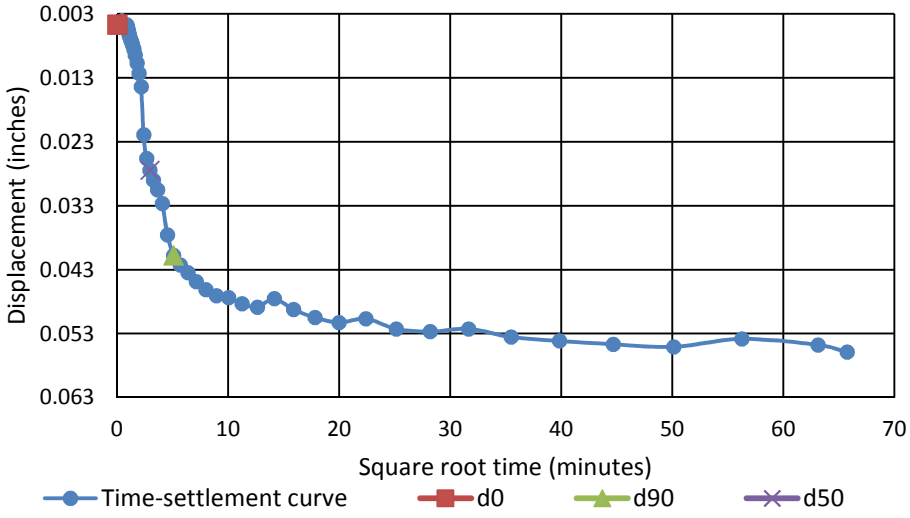

Figure A.13 Consolidation curve (Automated direct shear machine) for 3000 psf ENS on square root time scale at first load increment from 0 to 500 psf.

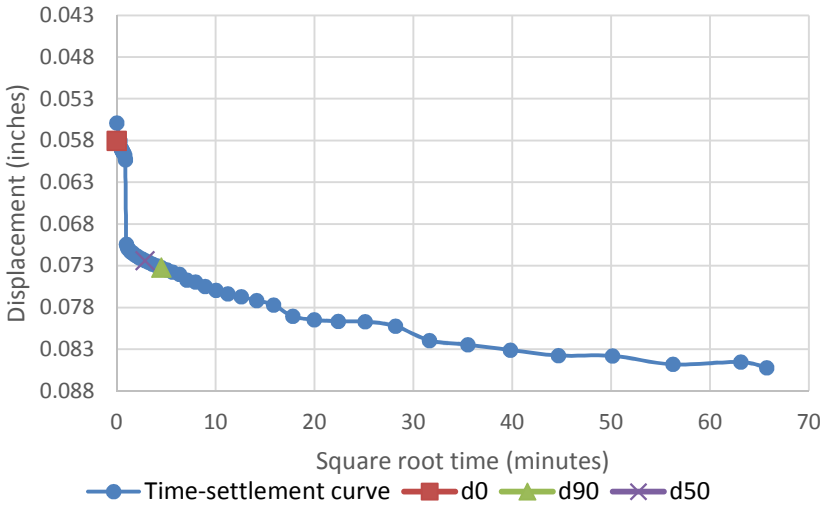

Figure A.14 Consolidation curve (Automated direct shear machine) for 3000 psf ENS on square root time scale at second load increment from 500 psf to 1500 psf.

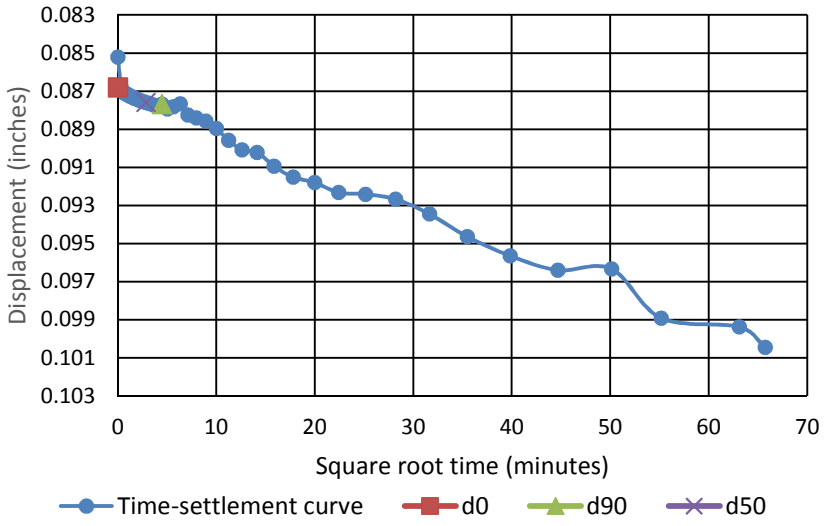

Figure A.15 Consolidation curve (Automated direct shear machine) for 3000 psf ENS on square root time scale at last load increment from 1500 psf to 3000 psf.

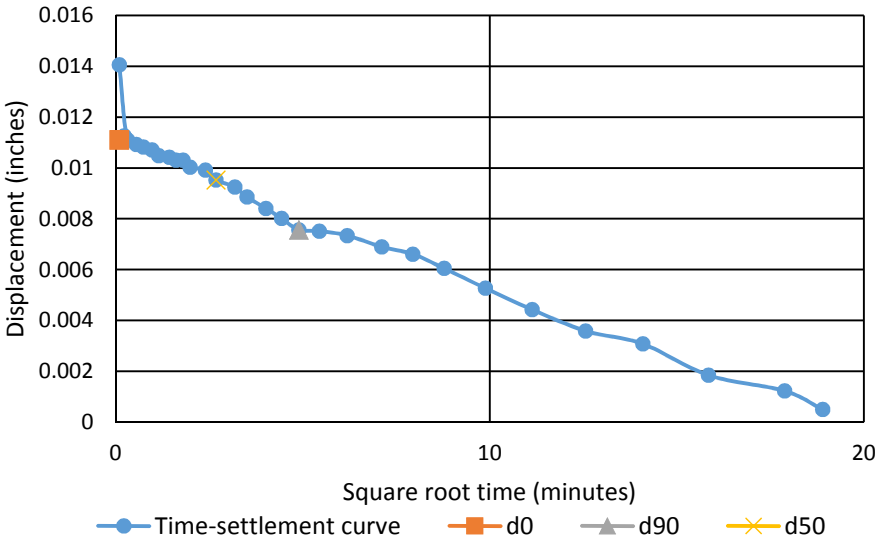

Figure A.16 Consolidation curve for 4000 psf ENS on square root time scale (Zhang, 2013)

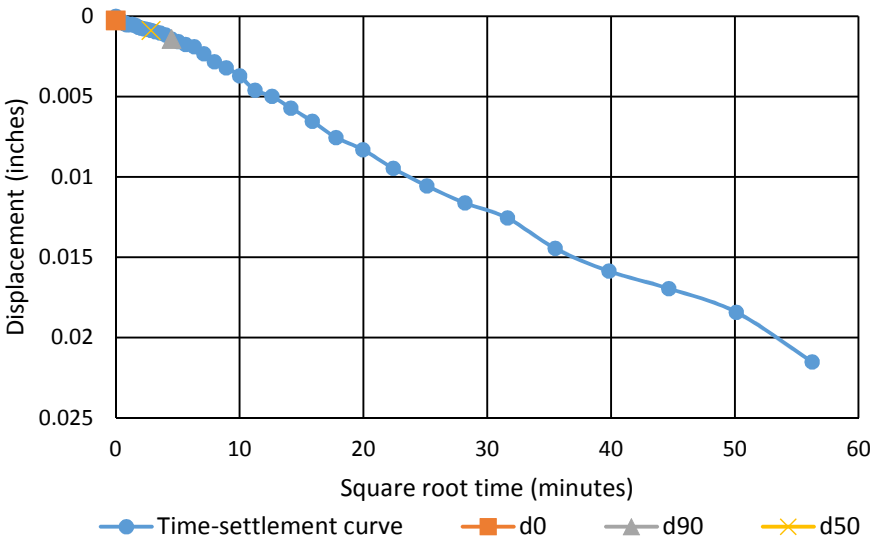

Figure A.17 Consolidation curve for 6000 psf ENS on log time scale (Zhang, 2013)

3. STRESS-DISPLACEMENT GRAPH WITH PEAK POINT AND VOLUME CHANGE CURVES FOR FGD SLUDGE WITH DIFFERENT EFFECTIVE NORMAL STRESSES AT NDR, NDRI AND NDRD.

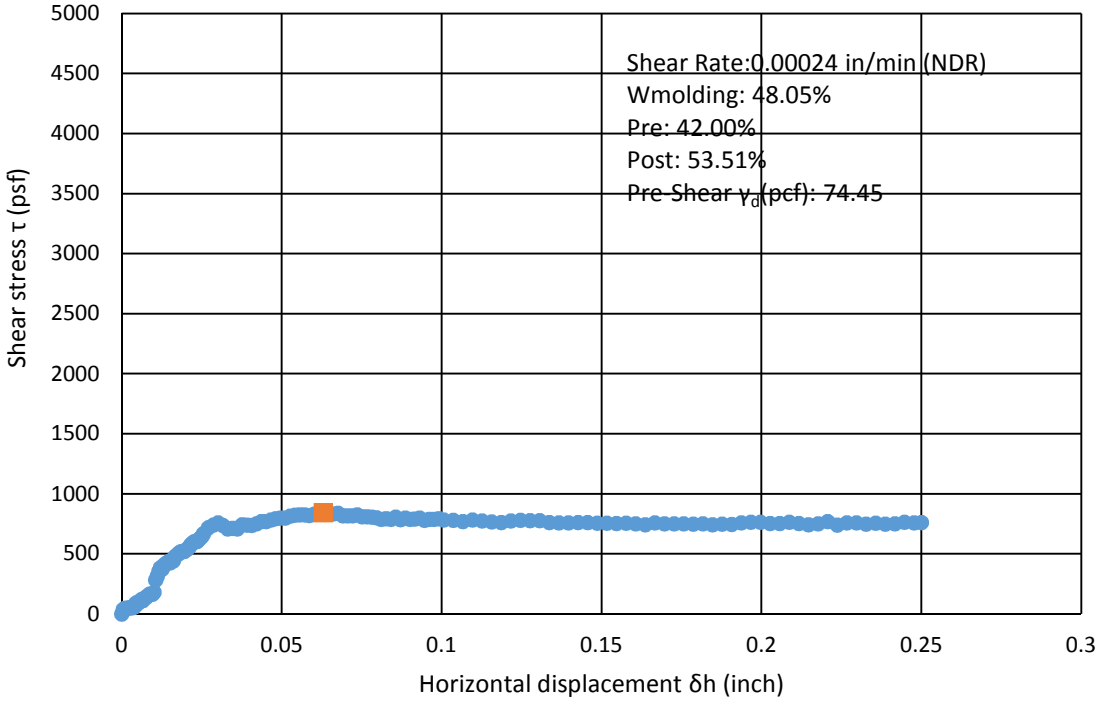

Figure A.18 (a) Stress-displacement for FGD sludge and peak point with 500 psf effective normal stress at NDR.

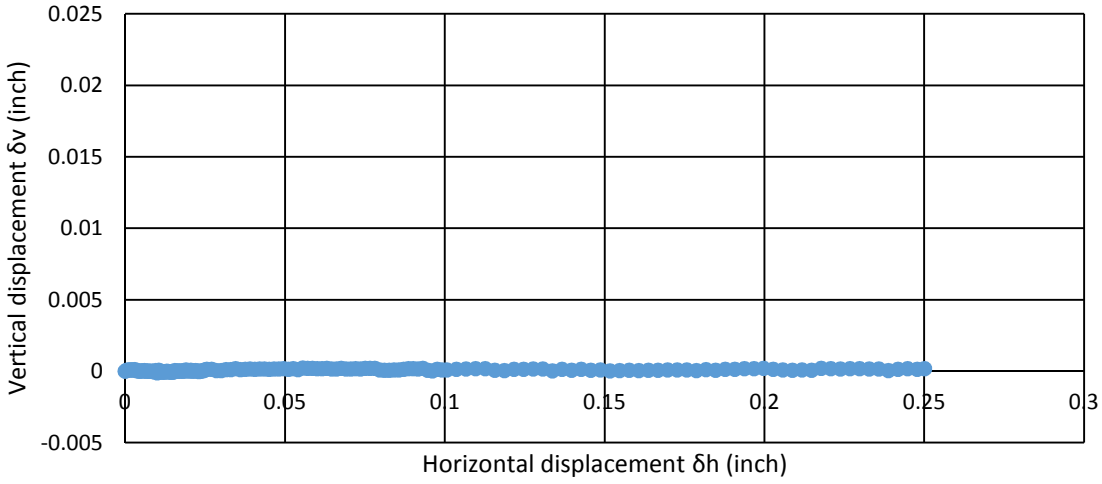

Figure A.18 (b) Volume change curves for NDR on FGD sludge at 500 psf effective normal stress.

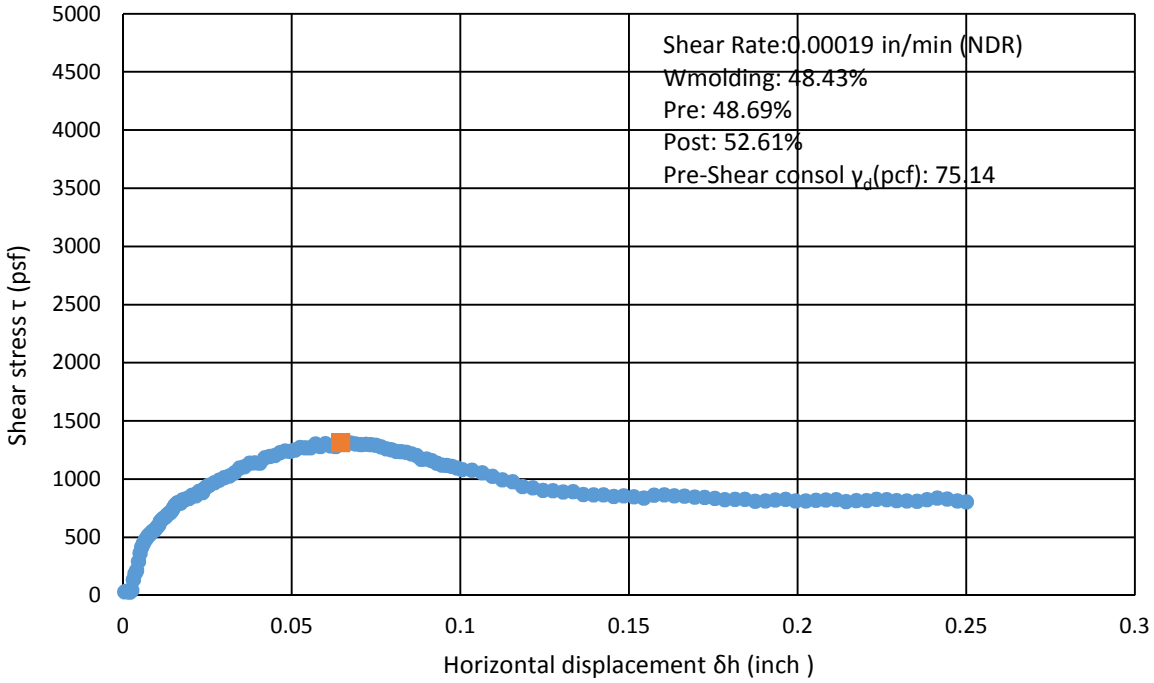

Figure A.19 (a) Stress versus displacement for FGD sludge and peak point with 1000 psf effective normal stress at NDR.

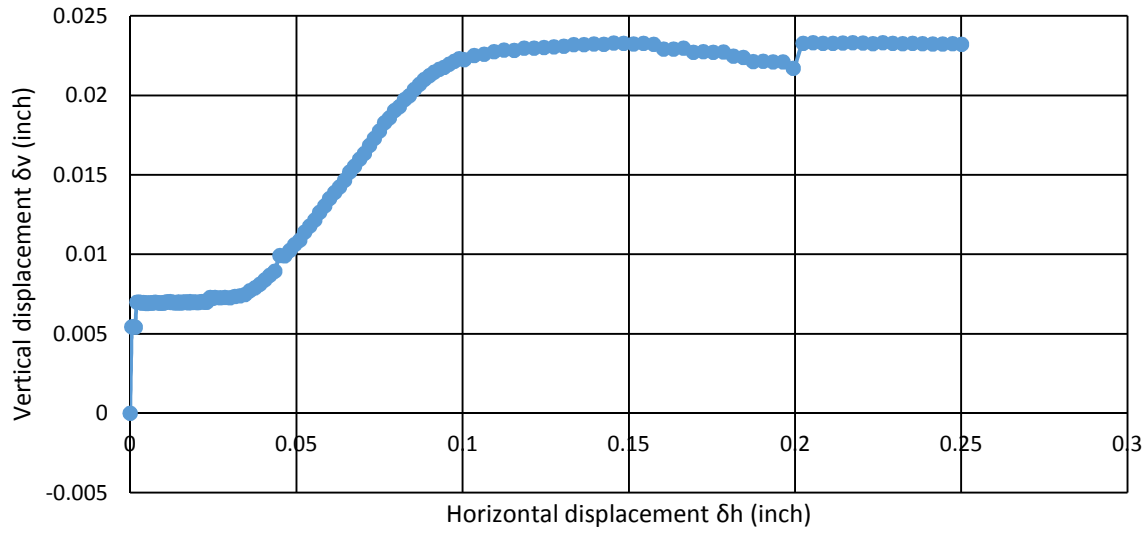

Figure A.19 (b) Volume change curves for NDR on FGD sludge at 1000 psf effective normal stress.

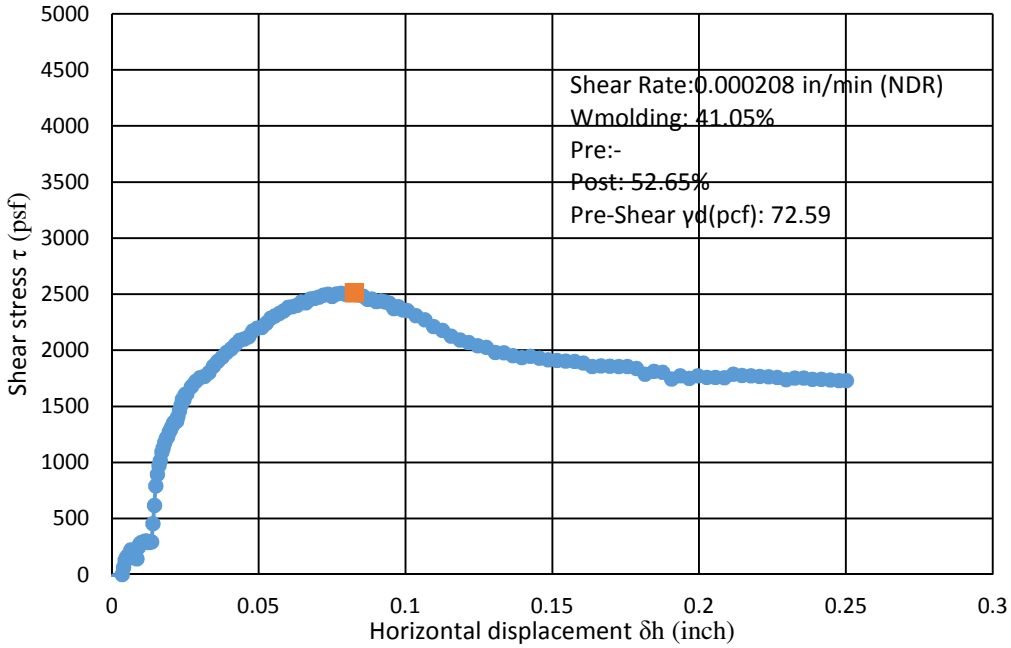

Figure A.20 (a) Stress-displacement for FGD sludge and peak point with 2000 psf effective normal stress at NDR.

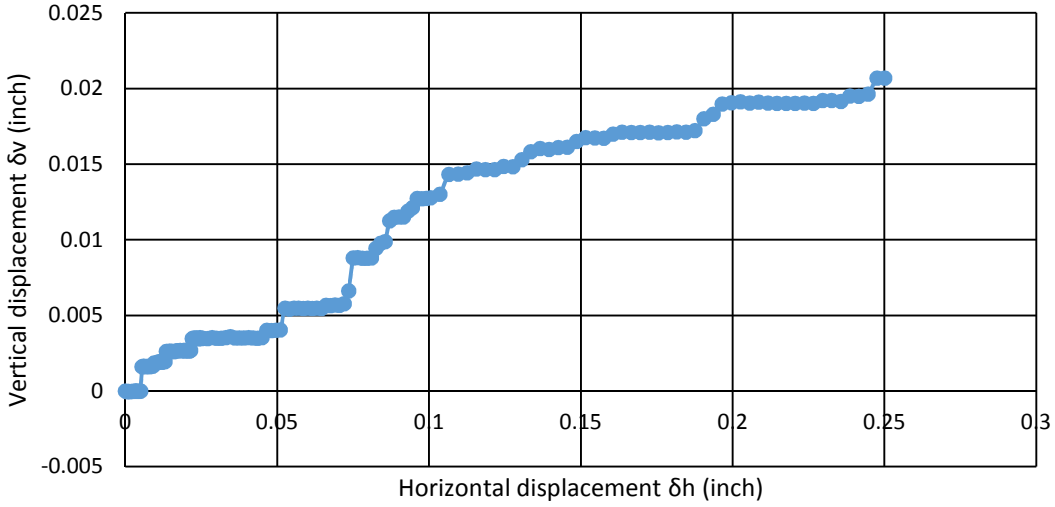

Figure A.20 (b) Volume change curves for NDR on FGD sludge at 2000 psf effective normal stress.

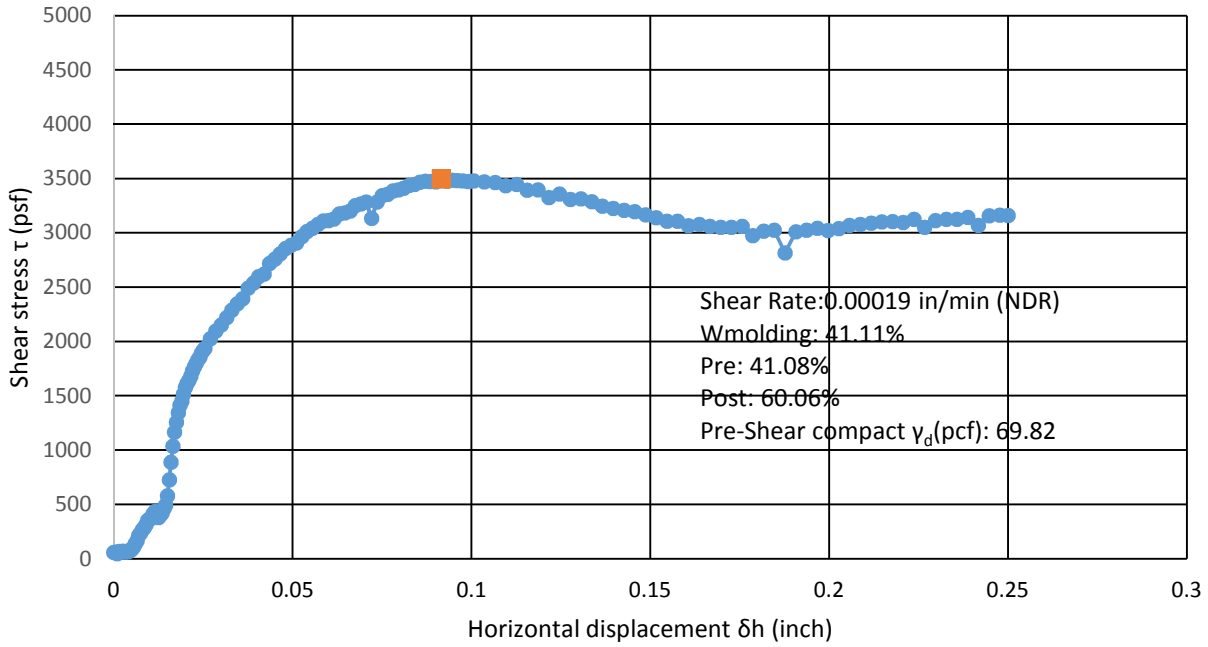

Figure A.21 (a) Stress-displacement for FGD sludge and peak points with 3000 psf effective normal stress at NDR.

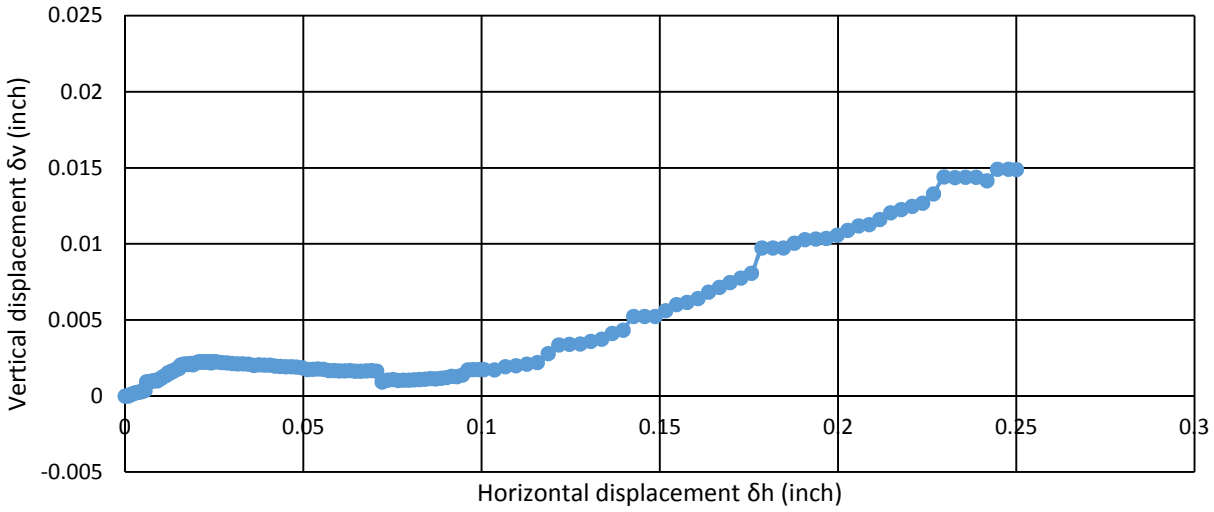

Figure A.21 (b) Volume change curves for NDR on FGD sludge at 3000 psf effective normal stress.

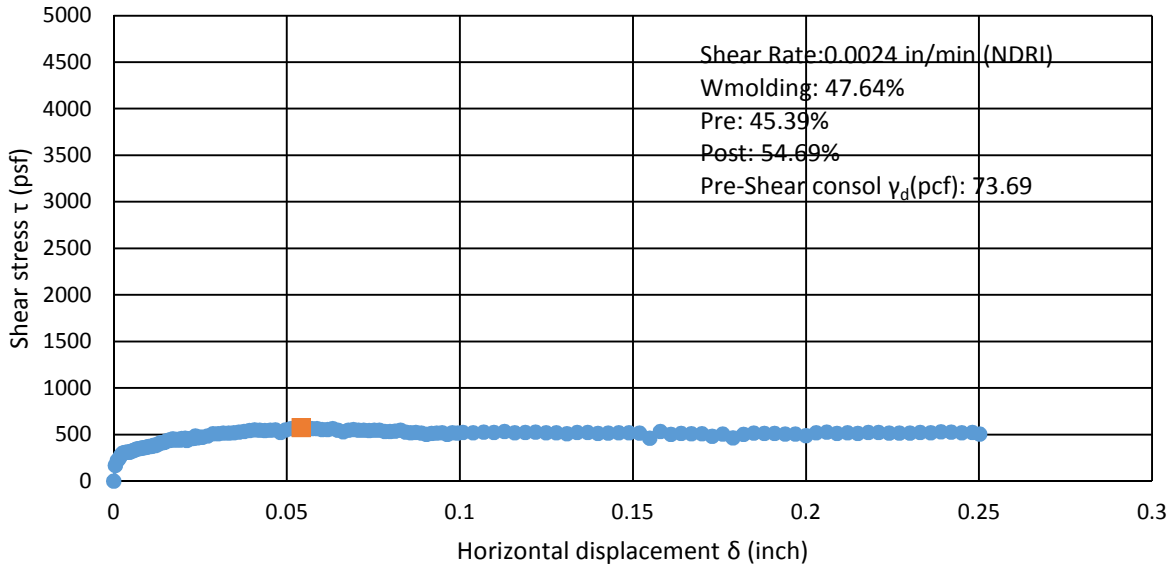

Figure A.22 (a) Stress-displacement for FGD sludge and peak points with 500 psf effective normal stress at NDRI.

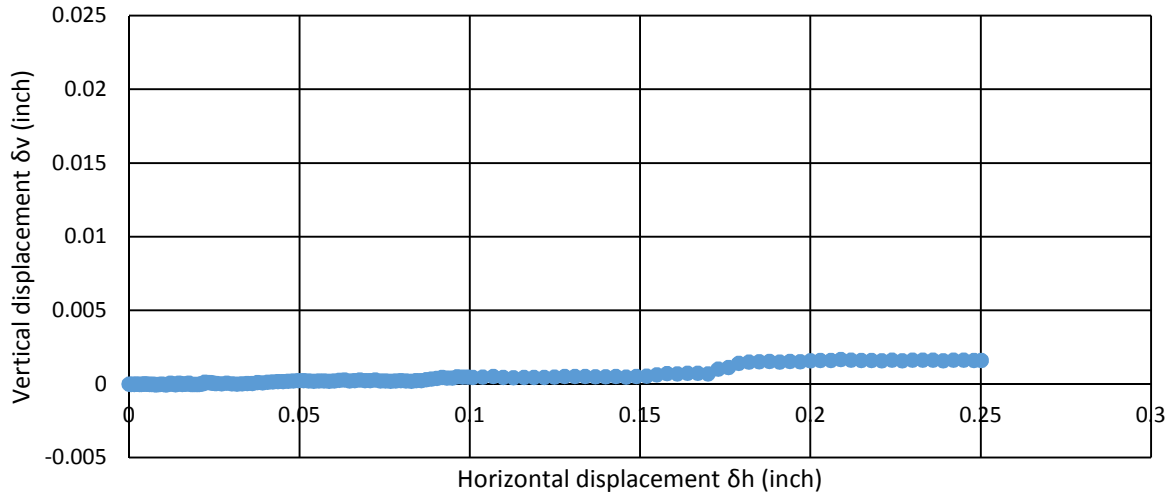

Figure A.22 (b) Volume change curves for NDRI on FGD sludge at 500 psf effective normal stress.

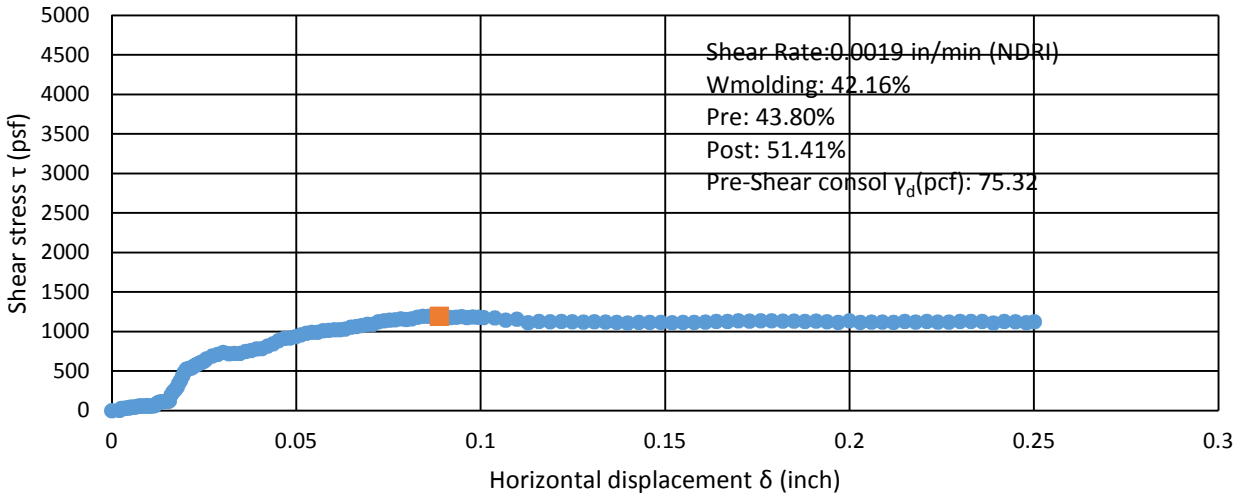

Figure A.23 (a) Stress-displacement for FGD sludge and peak points with 1000 psf effective normal stress at NDRI.

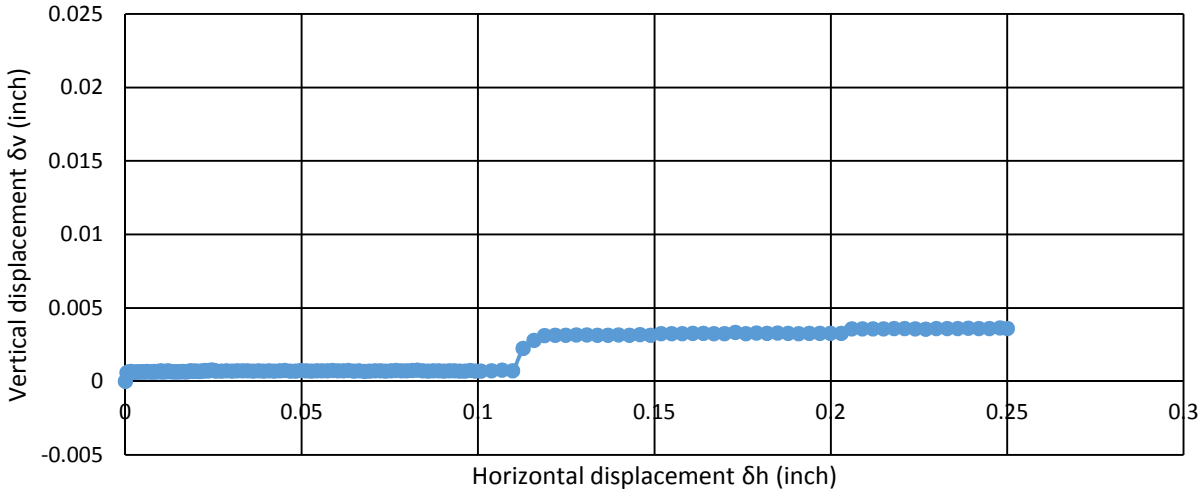

Figure A.23 (b) Volume change curves for NDRI on FGD sludge at 1000 psf effective normal stress.

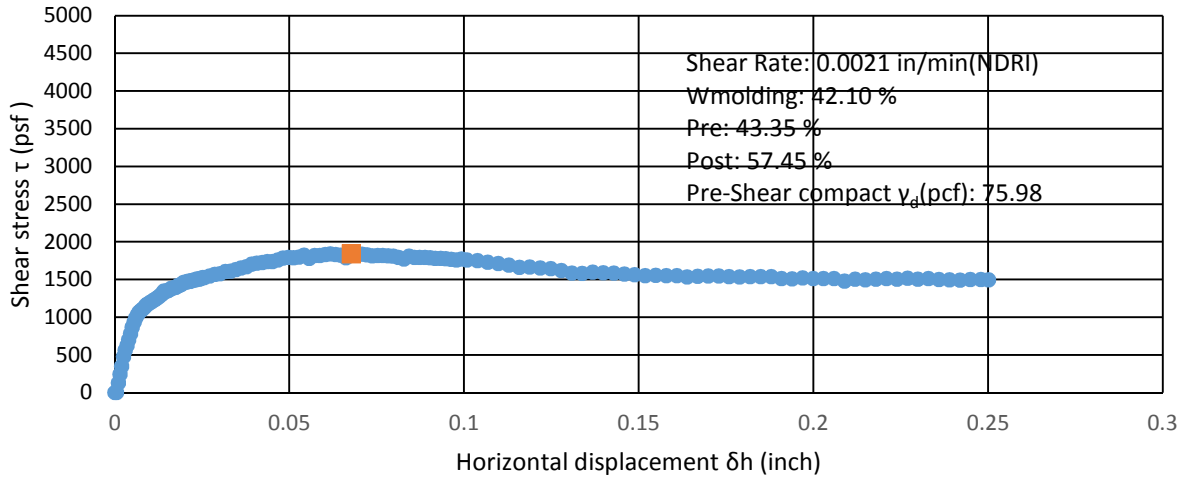

Figure A.24 (a) Stress-displacement for FGD sludge and peak points with 2000 psf effective normal stress at NDRI.

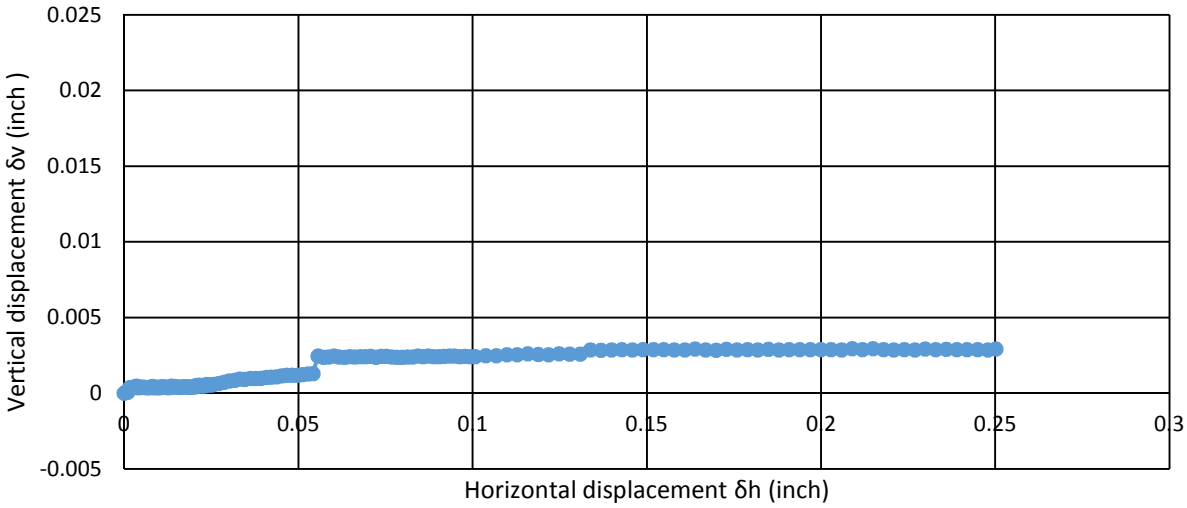

Figure A.24 (b) Volume change curves for NDRI on FGD sludge at 2000 psf effective normal stress.

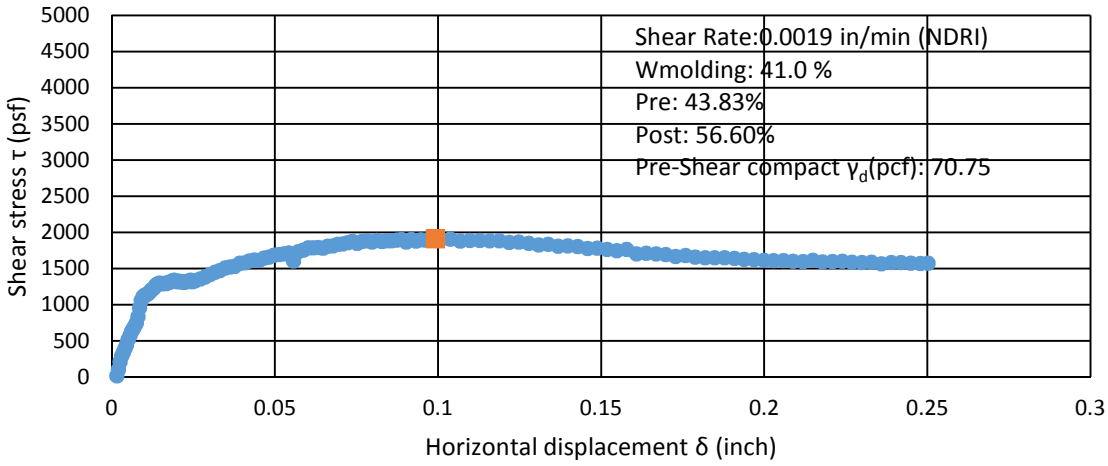

Figure A.25 (a) Stress-displacement for FGD sludge and peak points with 3000 psf effective normal stress at NDRI.

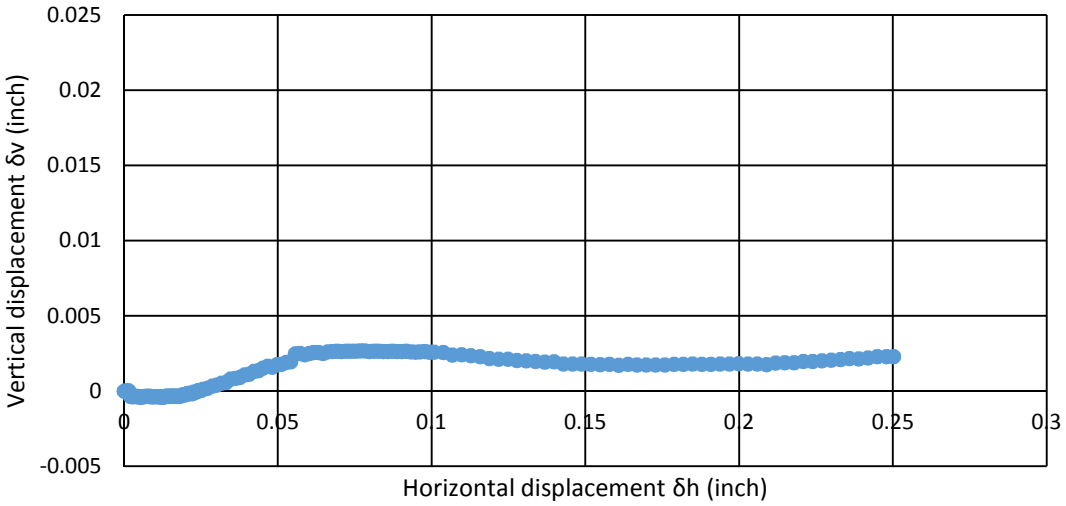

Figure A.25 (b) Volume change curves for NDRI on FGD sludge at 3000 psf effective normal stress.

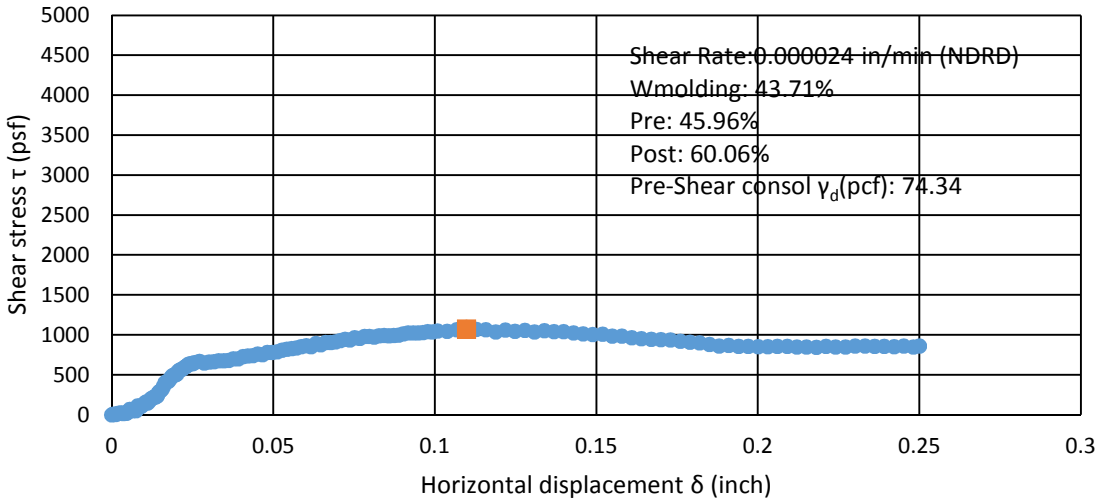

Figure A.26 (a) Stress-displacement for FGD sludge and peak points with 500 psf effective normal stress at NDRD.

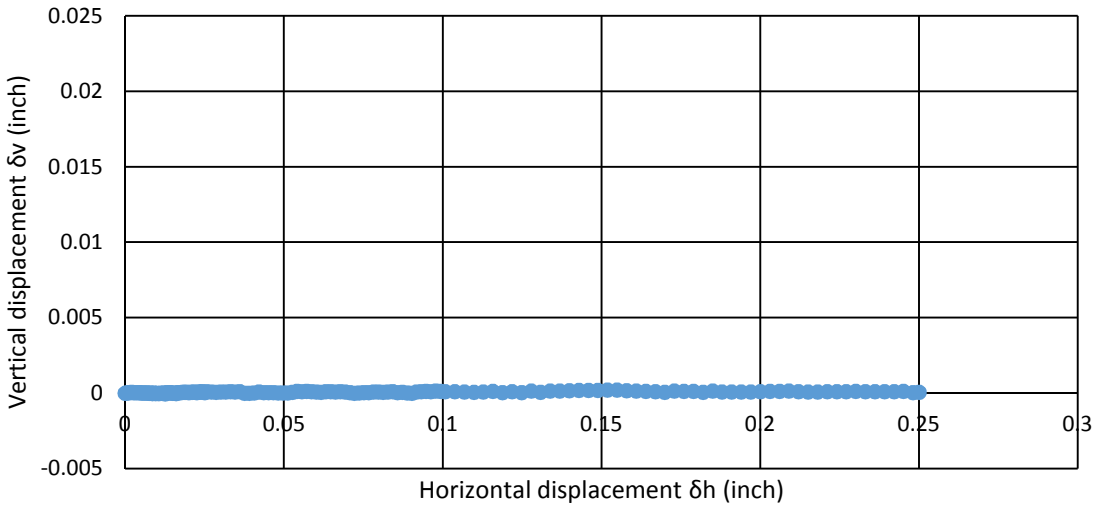

Figure A.26 (b) Volume change curves for NDRD on FGD sludge at 500 psf effective normal stress.

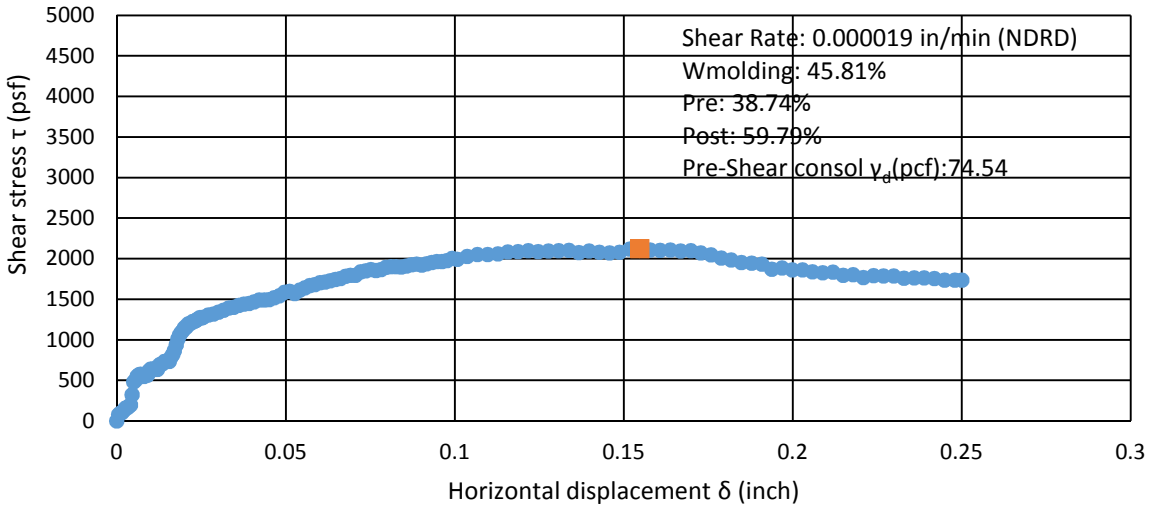

Figure A.27 (a) Stress-displacement for FGD sludge and peak points with 1000 psf effective normal stress at NDRD.

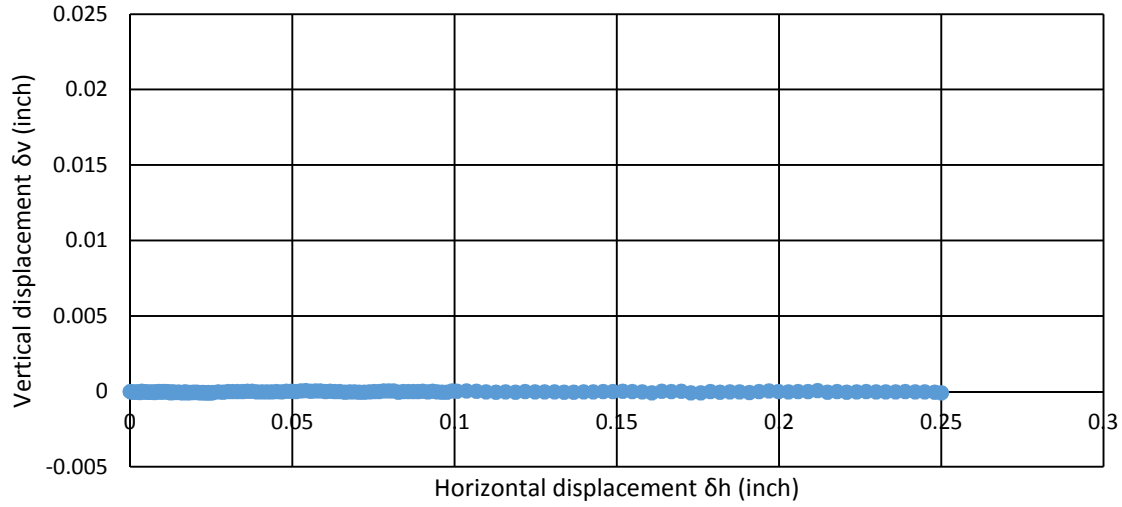

Figure A.27 (b) Volume change curves for NDRD on FGD sludge at 1000 psf effective normal stress.

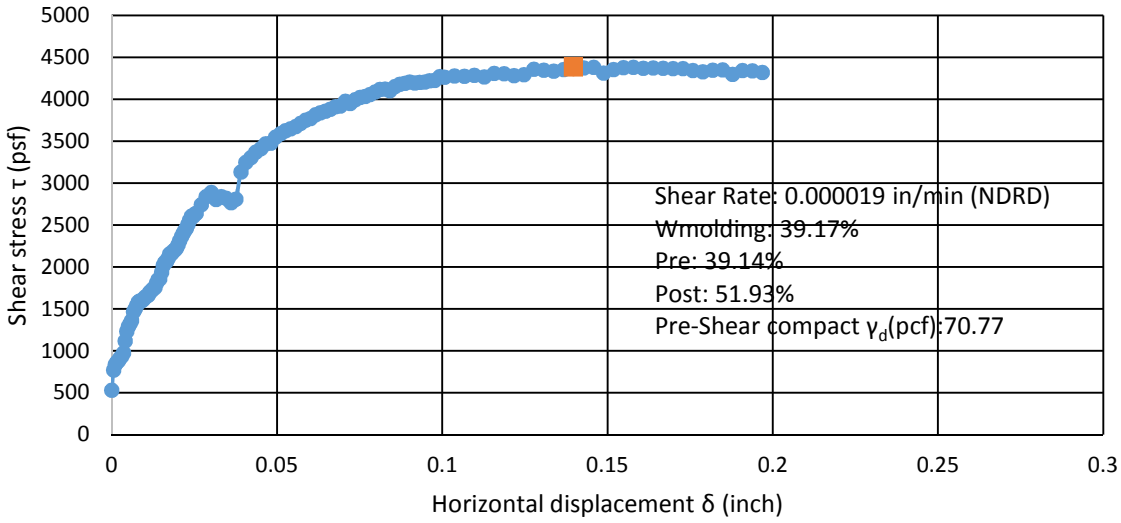

Figure A.28 (a) Stress-displacement for FGD sludge and peak points with 3000 psf effective normal stress at NDRD.

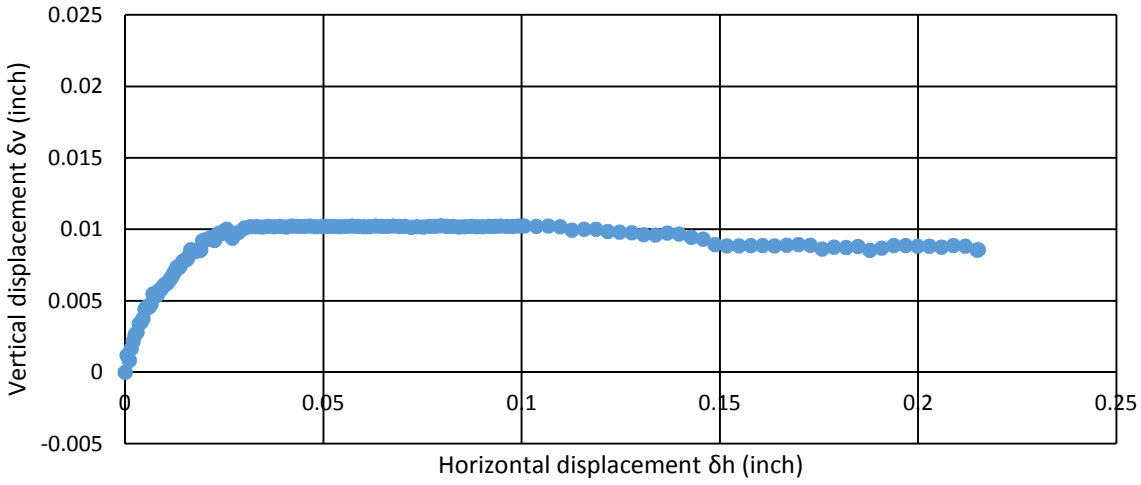

Figure A.28 (b) Volume change curves for NDRD on FGD sludge at 3000 psf effective normal stress.

4. PERMEABILITY TESTS

Table A.7 Hydraulic conductivity of FGD sludge from 0 to 28 days under constant effective confining stress (500 psf), Specimen A.

Average effective confining stress σ' in specimen (psf)/(psi)	Cell pressure σ(psi)	a (cm^2)	L (cm)	Δt (s)	Head Water (cm)		h bottom of sample (cm)	Tail Water (cm)		h top of sample (cm)	Δh_1 (cm)	Δh_2 (cm)	$\Delta h_1/\Delta h_2$	$\ln(\Delta h_1/\Delta h_2)$	K (cm/s)
500/3.5	5.5	5.5	2.54	480	ht_1	21.3	231.3	ht_1	5.8	75.8	155.5		1.05	0.049	2.27E-05
					ht_2	17.5	227.5	ht_2	9.5	79.5		148			
500/3.5	5.5	1	2.54	480	ht_1	21.5	231.5	ht_1	3	73	158.5		1.08	0.081	6.81E-06
					ht_2	15.3	225.3	ht_2	9.2	79.2		146.1			
500/3.5	5.5	1	2.54	960	ht_1	16.9	226.9	ht_1	6.5	76.5	150.4		1.06	0.064	2.7E-06
					ht_2	12.2	222.2	ht_2	11.2	81.2		141			
500/3.5	5.5	1	2.54	960	ht_1	22	232	ht_1	2	72	160		1.26	0.232	9.72E-06
					ht_2	5.5	215.5	ht_2	18.7	88.7		126.8			
500/3.5	5.5	1	2.54	480	ht_1	24	234	ht_1	2	72	162		1.11	0.112	9.38E-06
					ht_2	15.4	225.4	ht_2	10.6	80.6		144.8			

a = area of the reservoirs containing either influent/inflow or effluent/outflow liquid (in the specimen B pipette and annulus have been used, area of pipette = 1 cm^2 and area of annulus is 4.5 cm^2), L = length of specimen, cm

Δt = interval of time, s, over which the flow ΔQ occurs ($t_2 - t_1$), t_1 = time at the start of permeation trial, date: hr: min: sec, t_2 = time at the end of permeation trial, date: hr:min:sec,

ht_1 = head loss across the specimen at t_1, cm of water, ht_2 = head loss across the specimen at t_2, cm of water, Head water, pore pressure u = 3 psi = 210 cm water, Tail water, pore pressure u = 1 psi = 70 cm water, throughout the test for all average effective confining stresses the pore pressures are maintained constant.

K = hydraulic conductivity, cm/s

Table A.8 Hydraulic conductivity test for different average effective confining stress in Specimen B

Average effective confining stress σ' in specimen (psf)/(psi)	Cell pressure σ(psi)	a (cm^2)	L (cm)	Δt (s)	Head Water (cm)		h bottom of sample (cm)	Tail Water (cm)		h top of sample (cm)	Δh_1 (cm)	Δh_2 (cm)	$\Delta h_1/\Delta h_2$	$\ln(\Delta h_1/\Delta h_2)$	K (cm/s)
500/3.5	5.5	5.5	2.54	480	ht_1	21.5	231.5	ht_1	2.8	72.8	158.7		1.044	0.0437	2.01E-05
					ht_2	17.8	227.8	ht_2	5.9	75.9		151.9			
1000/7	9	5.5	2.54	240	ht_1	23.5	233.5	ht_1	3.9	73.9	159.6		1.023	0.0228	2.1E-05
					ht_2	21.7	231.7	ht_2	5.7	75.7		156			
2000/14	16	5.5	2.54	960	ht_1	21.7	231.7	ht_1	5.8	75.8	155.9		1.078	0.0752	1.73E-05
					ht_2	16	226	ht_2	11.4	81.4		144.6			
3000/21	23	5.5	2.54	240	ht_1	24.7	234.7	ht_1	6	76	158.7		1.018	0.0184	1.7E-05
					ht_2	23.2	233.2	ht_2	7.4	77.4		155.8			
4000/28	30	5.5	2.54	480	ht_1	23	233	ht_1	7.8	77.8	155.2		1.023	0.0234	1.08E-05
					ht_2	21.2	231.2	ht_2	9.6	79.6		151.6			
6000/42	44	5.5	2.54	960	ht_1	21	231	ht_1	9.7	79.7	151.3		1.037	0.0370	8.51E-06
					ht_2	18.4	228.4	ht_2	12.6	82.6		145.8			

a = area of the reservoirs containing either influent/inflow or effluent/outflow liquid (in the specimen B pipette and annulus have been used, area of pipette = 1 cm^2 and area of annulus is 4.5 cm^2), L = length of specimen, cm

Δt = interval of time, s, over which the flow ΔQ occurs ($t_2 - t_1$), t_1 = time at the start of permeation trial, date: hr: min: sec, t_2 = time at the end of permeation trial, date: hr:min:sec,

ht_1 = head loss across the specimen at t_1, cm of water, ht_2 = head loss across the specimen at t_2, cm of water, Head water, pore pressure u = 3 psi = 210 cm water, Tail water, pore pressure u = 1 psi = 70 cm water, throughout the test for all average effective confining stresses the pore pressures are maintained constant.

K = hydraulic conductivity, cm/s

5. EQUATIONS USED FOR DATA REDUCTION FOR THE DIRECT SHEAR TEST

A. Horizontal Load (lbs) = (Value – Zero Value) * Cal.Factor / Excitation……(A.1)
B. Vertical Load (lbs) = (Value – Zero Value) * Cal.Factor / Excitation……..(A.2)
C. Vertical Displacement (inch) = (DCDT Value – Initial DCDT Value) * Cal.Factor / Excitation……(A.3)
D. Horizontal Displacement (inch) = (Horizontal Actuator Value – Initial Horizontal Actuator Value) / Cal.Factor……(A.4)
E. Normalized Displacement (%) = (Horizontal Displacement Value – Initial Horizontal Displacement Value) / Diameter……(A.5)
F. Corrected Area (in^2) = ($Diameter^2$ / 4 *π) * (1 – Original Horizontal Displacement * SIN {.ACOS [(Horizontal Displacement / (2* Diameter)]} / (2π* Diameter)..(A.6)
G. Horizontal Stress (psf) = Horizontal Load Value / Corrected Area *144…….(A.7)
H. Vertical Stress (psf) = Vertical Load Value / Corrected Area *144……...(A.8)
I. Strain (%) = Normalized Displacement Value - Initial Normalized Displacement Value. (Begin with the value in which the Horizontal Load has positive value).....(A.9)
J. Shear Stress (psf) = Original Horizontal Stress Value - Initial Horizontal Stress Value. (Begin with the value in which the Horizontal Load has positive value)……...(A.10)
K. Normal stress (Begin with the value in which the Horizontal Load has positive value)…….. (A.11)

6. FIGURES

This part of appendix provides photographs of the testing methods.

Figure A.29 The direct shear testing mold with interior components.

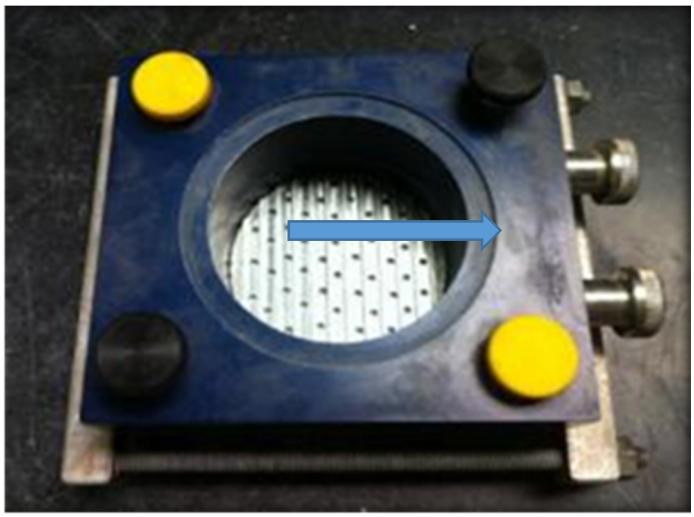

Figure A.30 Gripper plates are oriented such that the groves are perpendicular to the shearing motion.

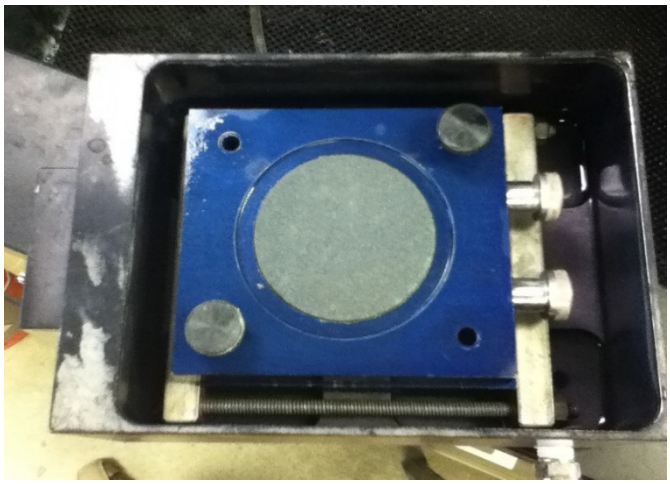

Figure A.31 The direct shear testing mold in the shearing device box.

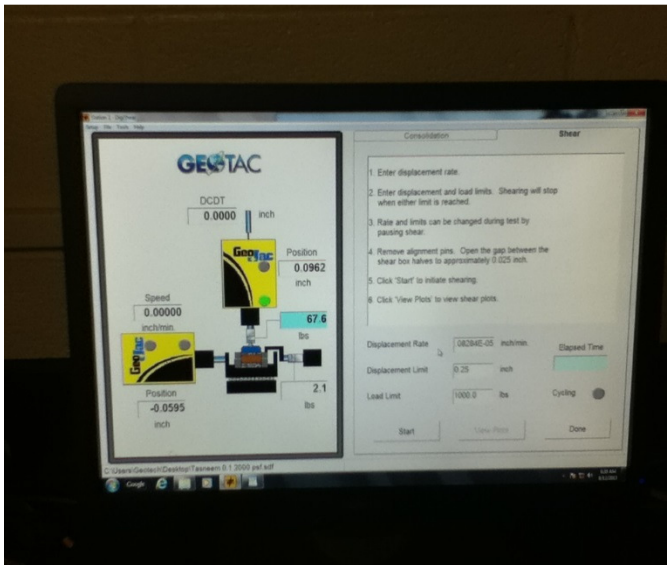

Figure A.32 The S2220 DigiShear TM Automated Direct Shear System computer ready to begin the shearing stage after the completion of consolidation stage.

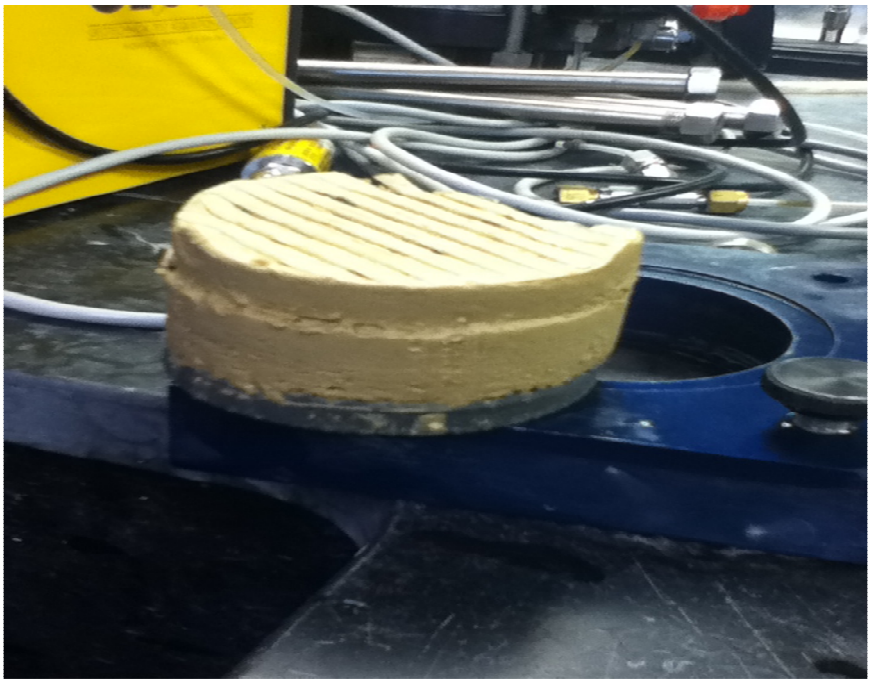

Figure A.33 Elevation view of failed compacted FGD specimen after test.

Figure A.34 Plan view of failed compacted FGD specimen after test.

Figure A.35 Extractor device used for extracting specimen from Proctor mold.

Figure A.36 Incremental load test apparatus.

Figure A.37 Trimming tools used for preparing FGD sludge specimen.